Free Radical Polymerization studies of vinyl ester monomers using Pulsed-Lased Polymerization with Size Exclusion Chromatography (PLP-SEC)

By

OTLAATLA MONYATSI

A thesis submitted to the Department of Chemical Engineering

in conformity with the requirements for the

Degree of Masters of Applied Science

Queen's University

Kingston, Ontario, Canada

(November, 2015)

Abstract

Polyvinyl acetate and other polyvinyl esters, and their copolymers are used in coatings, adhesives and plastics, and hence fundamental understanding of the mechanisms and polymerization kinetics is vital for process development, and production of existing and new polymer grades in an effective and safe manner. The propagation kinetics of radical homopolymerization (bulk) of vinyl acetate (VAc), vinyl pivalate (VPi) and vinyl benzoate (VBz) was studied using Pulsed-Laser Polymerization coupled with Size Exclusion Chromatography (PLP-SEC) at laser pulse repetition rate (prr) between 2 and 500 Hz, and the temperature range of 25 - 90 °C. The propagation rate coefficient, k_p, determined for VAc and VPi increases significantly with prr (20 % between 200 and 500 Hz prr), with the k_p value for VPi ~50 % higher than that of VAc. This significant increase in k_p with prr has been explained by the head-to-head addition defects that occur during vinyl ester polymerizations. For VBz, no k_p value was reported due to lack of PLP-structure, likely due to resonance stabilization of the radical. Solution polymerization of VAc and VPi was also studied by PLP-SEC using ethyl acetate (EAc) and heptane (50 % by volume) at 50 °C, with the k_p values having no substantial solvent effect. The polymerization kinetics of these vinyl ester monomers were also investigated using small-scale batch polymerization at 60 °C both in bulk and in solution (using EAc). The monomer conversion profiles obtained showed the same pattern in both bulk and solution, with the rate of conversion faster for VAc than VBz, and VPi even faster, trends consistent with the k_p values determined using PLP-SEC. Kinetic models were implemented in the Predici software package, and are shown to fit the experimental batch polymerization data reasonably well.

Acknowledgments

I would like to express my deepest appreciation to all those who provided contribution to complete my research project. A special thank you and gratitude goes to Dr. Robin Hutchinson, for his help, guidance and encouragement throughout my research project. In addition, for his continual support and for all the opportunities I had through my research thesis, including going to the international Polymer Reaction Engineering conference. Furthermore, I would like to thank and appreciate one of our collaborators, Dr. A. Nikitin (Russia) for his discussion and contribution with the simulation work for VAc polymerization studies. Last but not least, I will also thank E.I DuPont, NSERC and Queen's University for the financial support of this project. Finally, many thanks go to my research group members for all the help and support they gave working in the lab and dealing with some issues I had with my project since day one especially Jan and Thomas.

Table of Contents

List of Tables

List of Figures

Nomenclature

Symbol	Units	Definition
A	$L \cdot mol^{-1} \cdot s^{-1}$	Preexponential factor (2^{nd} order reaction)
AIBN		2,2′-Azobis(2-methylpropionitrile)
C_{tr}		Chain transfer constant
C_M		Chain transfer to monomer constant
C_S		Chain transfer to solvent constant
$CDCl_3$		Chloroform-d
CRP		Controlled radical polymerization
CSTR		Continuous Stirred Tank Reactor
DCP		Dicumyl peroxide
D_n		Dead polymer chain of length n
d*n*/d*c*		Specific refractive index increment
DMPA		2,2-Dimethoxy-2-phenylacetophenone
DP_0		Number-average degree of polymerization
DRI/RI		Differential refractometer detector
E_a	$kJ \cdot mol^{-1}$	Activation Energy
EAc		Ethyl acetate
EPR		Electron Paramagnetic Resonance
Expt'l		Experimental
f		Initiator decomposition efficiency
FRP		Free radical polymerization
HT		Head-to-tail addition
HH		Head-to-head addition
[I]	$mol \cdot L^{-1}$	Initiator concentration
IUPAC		International Union of Pure and Applied Chemistry
IV		Intrinsic Viscosity detector

K, a		Mark-Houwink Parameters
k_d	s^{-1}	Initiator decomposition rate constant
k_p	$L \cdot mol^{-1} \cdot s^{-1}$	Propagation rate coefficient
k_p^{av}	$L \cdot mol^{-1} \cdot s^{-1}$	Average propagation rate coefficient
k_p^{app}	$L \cdot mol^{-1} \cdot s^{-1}$	Apparent propagation rate coefficient
k_t	$L \cdot mol^{-1} \cdot s^{-1}$	Overall termination rate coefficient
k_{tc}	$L \cdot mol^{-1} \cdot s^{-1}$	Termination rate coefficient by Combination
k_{td}	$L \cdot mol^{-1} \cdot s^{-1}$	Termination rate coefficient by disproportionation
k_t^{11}	$L \cdot mol^{-1} \cdot s^{-1}$	Chain length dependent termination
k_{tr_sol}	$L \cdot mol^{-1} \cdot s^{-1}$	Transfer rate coefficient to solvent
k_{tr_mon}	$L \cdot mol^{-1} \cdot s^{-1}$	Transfer rate coefficient to monomer
k_{p11}	$L \cdot mol^{-1} \cdot s^{-1}$	Head-to-tail addition individual propagation rate coefficient
k_{p12}	$L \cdot mol^{-1} \cdot s^{-1}$	Head-to-head addition individual propagation rate coefficient
k_{p21}	$L \cdot mol^{-1} \cdot s^{-1}$	Tail-to-tail addition individual propagation rate coefficient
k_{p22}	$L \cdot mol^{-1} \cdot s^{-1}$	Tail-to-head addition individual propagation rate coefficient
L_i		Characteristic chain length of PLP-generated chains
LCB		Long chain branching
MALS/LS		Multi Angle Light Scattering detector
[M]	$mol \cdot L^{-1}$	Monomer concentration
M_i		Monomer i (i=1, 2, …)
MMA		Methyl methacrylate
MeOH		Methanol
M_w		Weight averaged molecular weight
MW		Polymer molecular weight
MMD		Molar Mass distribution
n, m		Chain-length indices (subscripts)
PDI		Polymer polydispersity Index
$(PhCOO)_2$		Benzyl peroxide

PLP		Pulsed-laser polymerization
prr		Pulse repetition rate
P_n		Polymeric radical of length n
R*		Initiator-derived primary radical species
R_{poly}		Rate of polymerization
R_{tr}		Rate of chain transfer to polymer
[S]	$mol \cdot L^{-1}$	Solvent concentration
SCB		Short chain branching
SEC		Size Exclusion Chromatography
T	K, ° C	Temperature
TD		Triple detector
TH		Tail-to-head addition
THF		Tetrahydrofuran
TT		Tail-to-tail addition
t_d	s	Thermal radical initiator half life
t_0	s	Time between laser flashes
^{t}BuOOBu^t		Di-*tert*-butyl peroxide
VAc		Vinyl acetate
VPi		Vinyl pivalate
VBz		Vinyl benzoate
V67		2,2-azobis(2-methylbutane-nitrile)
X_p		Monomer conversion
ρ	$g \cdot L^{-1}$	Density
Φ		Monomer volume fraction

Chapter 1: Introduction

Close to half of all synthetic polymers are formed via radical polymerization, with a wide variety of industrial and consumer applications in diverse areas such as automotive coatings, biomedical and adhesives. With the introduction of new technologies, the industries continue to strive to reduce the operating costs and the environmental impact associated with producing these polymers. However, in order to achieve these targets, the fundamental polymerization behavior has to be well understood, knowledge sometimes lacking due the complex kinetics and difficulty in characterizing polymeric structure. With knowledge of radical polymerization mechanisms and the accurate determination of kinetic rate coefficients such as the chain growth rate coefficient of radical polymerization, k_p, it becomes possible to construct models to enhance understanding of the polymerization systems. The introduction of a novel experimental method, Pulsed-Laser Polymerization combined with Size Exclusion Chromatography (PLP-SEC), in 1987 by Olaj and coworkers has been a major advance in polymerization studies as it can directly estimate the propagation rate coefficient, k_p from the molar mass distribution (MMDs) analysis of the resulting polymer of interest.[1]

Vinyl acetate (VAc) is one of the main monomer systems of interest to the industry (such as DuPont Company) for its use in coatings, adhesives and other commercial applications.[2] It is also a significant monomer used in ethylene copolymerization, yielding resins with flexible, toughness and clear properties and used in seafood and meat packaging systems.[3] Even though this monomer (VAc) is widely used, characterization of its propagation kinetics by the PLP-SEC method has proven to be difficult. Early studies suggested that this difficulty is due to high transfer and termination rates.[4] Junkers et al.[5] found a significant increase of k_p with laser pulse repetition rate (prr) and suggested that

the result was due to the intramolecular transfer to polymer (commonly known as backbiting), which disrupts the relation between prr and chain length as in acrylate systems.[1,6-7] However, this side reaction (i.e. backbiting) in VAc homo-polymerization and copolymerization with ethylene systems has been found to be negligible or low compared to acrylate systems.[8-10] Another potential explanation for this behavior can be the effect of chain transfer to monomer followed by slow reinitiation of radical chains which can affect the PLP-generated MMD-structure of polyvinyl acetate. In addition, the inverted monomer insertion which is important to vinyl ester monomer reactions and known to occur during VAc polymerization, results in the formation of a second, possibly less reactive, propagating radical structure that affects the chain growth kinetics may be a cause of the significant increase in k_p values with prr.[10] As part of this study, the unusual behavior of the notable change in k_p with prr will be thoroughly investigated.

1.1 Research project Objective

The aim of the research is to provide a better understanding of the polymerization kinetics of VAc using the PLP-SEC technique to aid in product and process development efforts applied in polymer industry, including a reduction of process costs and environmental footprints.

The principal goals of this research project include:

- To use the PLP-SEC method to measure the propagation rate coefficient of VAc and assess the unusual behavior observed.
- Apply the PLP-SEC technique further to other vinyl ester monomers, vinyl benzoate (VBz) and vinyl pivalate (VPi). (See Figure 1.1 for monomer structures.)

In addition, some efforts have been done to:

- Develop a small-scale batch polymerization experimental method and study the polymerization kinetics both in bulk and solution for vinyl ester monomers.
- Develop a simple model using PREDICI software to interpret the polymerization kinetics of VAc and VPi.

Vinyl acetate (VAc) Vinyl pivalate (VPi) Vinyl benzoate (VBz)

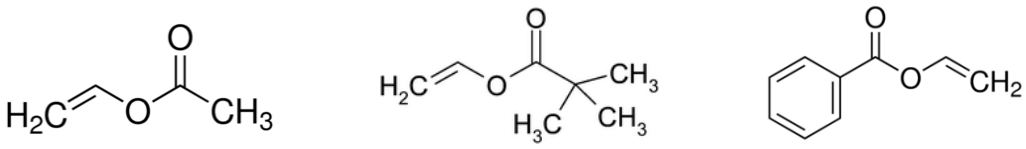

Figure 1.1: Vinyl ester monomer structures.

References

1. O. F. Olaj, I. Bitai, F. Hinkelmann, *Makromol. Chem.* **1987**, *188*, 1689.
2. http://www.britannica.com/science/polyvinyl-acetate, **2014**.
3. http://www.dupont.ca/en/products-and-services/plastics-polymers-resins/ethylene-copolymers/brands/elvax-ethylene-vinyl-acetate.html, **2015**.
4. R. A. Hutchinson, J. R. Richards, M. T. Aronson, *Macromolecules* **1994**, *27*, 4530.
5. T. Junkers, D. Voll, C. Barner-Kowollik, *e-Polymers* **2009**, *no 076*.
6. A. N. Nikitin, R. A. Hutchinson, M. Buback, P. Hesse, *Macromolecules* **2007**, *40*, 863.
7. K. Liang, R. A. Hutchinson, *Macromol. Rapid Commun.* **2011**, *32*, 1090.
8. J. C. Randall, C. J. Ruff, M. Kelchtermans, B. H. Gregory, *Macromolecules* **1992**, *25*, 2624.
9. E. F. McCord, W. H. Shaw Jr., R. A. Hutchinson, *Macromolecules* **1997**, *30*, 246.
10. D. Britton, F. Heatley, P. A. Lovell, *Macromolecules* **1998**, *31*, 2828.

Chapter 2: Literature Review

2.1 Free Radical Polymerization

Polyvinyl esters are produced via free radical polymerization (FRP). Therefore kinetic understanding of FRP processes is essential to provide a fundamental path for ease and effective production of new and existing grades of these polymers. FRP is simple, versatile, compatible with various functional groups, and tolerant to impurities. The FRP mechanism consists of the following distinctive reactions; initiation, propagation, termination and chain transfer to small molecules, as shown below:

Initiation

$$I \xrightarrow{k_d} 2fR^* \qquad [2.1]$$

$$R^* + M \xrightarrow{k_p} P_1 \qquad [2.2]$$

Propagation

$$P_n + M \xrightarrow{k_p} P_{n+1} \qquad [2.3]$$

Transfer Chain to Monomer

$$P_n + M \xrightarrow{k_{tr\_mon}} D_n + P_1 \qquad [2.4]$$

Chain transfer to Solvent

$$P_n + S \xrightarrow{k_{tr\_sol}} D_n + P_1 \qquad [2.5]$$

Termination by Combination

$$P_n + P_m \xrightarrow{k_{tc}} D_{n+m} \qquad [2.6]$$

Termination by Disproportionation

$$P_n + P_m \xrightarrow{k_{td}} D_n + D_m \qquad [2.7]$$

Where:

I : Initiator

R*: Initiator radical

M : Monomer of interest

P : Propagating Chain radical

S : Solvent

D : Dead polymer chain

k_d : Initiator decomposition rate coefficient

k_p : Propagation rate coefficient

k_{tr_mon} : Transfer to monomer rate coefficient

k_{tr_sol} : Transfer to solvent rate coefficient

k_{tc} : Termination by combination rate coefficient

k_{td} : Termination by disproportionation rate coefficient

f : Initiator efficiency

n and m : Chain length of the polymerizing chains

2.1.1 Initiation

Initiation is the first step in polymerization, with most radical initiators molecules with weak-covalent bonds, low dissociation energies and easy to break.[1] The bond cleavage produces two radical species via thermal, photochemical or redox process (Equation 2.1). In some rare cases auto-initiation can occur as seen for styrene at higher temperatures (>100°C).[2-3] Most commonly used thermal initiators are azo-compounds such as 2,2-azobis(2-methylbutane-nitrile) (V-67) and 2,2′-Azobis(2-methylpropionitrile) (AIBN), and peroxides such as di-*tert*-butyl peroxide (^{t}BuOOBu^{t}) and benzyl peroxide ((PhCOO)$_2$), and photoinitiators used to generate radicals in the PLP-SEC technique include 2,2-Dimethoxy-2-phenylacetophenone (DMPA), benzoin and dicumyl peroxide (DCP) (also a thermal initiator for higher temperatures). Each thermal radical initiator is characterized by its decomposition rate (k_d), half-life (t_d) and initiator efficiency (f). The latter is considered to be proportional to the generation rate of primary radicals (R*) and is typically in the range $0.4 < f < 0.9$.[4] Initiator decomposition generally has an associated activation energy, E_a of 100-150 kJ·mol^{-1},[1] with the radical generation rate thus heavily depends on the temperature compared to other steps (i.e. propagation and termination).

2.1.2 Propagation

Radical propagation comprises a sequence of radical additions to monomer double bonds, with the reactive radical functionality remaining at the end of the growing chain radical (equation 2.3). This step will continue until a termination or transfer reaction occurs, with the continuous addition of monomer not changing the number of free radicals nor the stability of the growing chain radical once the structure is originally transformed from the primary initiator-derived radical by the first monomer addition.[5] The propagation of radical polymerization is chemically controlled, with the chain being initiated, propagating to final chain-length and terminating with a chain-lifetime of less than second. In order to understand kinetics of polymerization, accurate and reliable measurements of the propagation rate

coefficient, k_p, has to be made. Various methods for k_p measurement such as Electron Paramagnetic Resonance (EPR), Pulsed-Laser Polymerization (PLP) has been previously used and reviewed.[6-8] k_p is assumed to be independent of chain length but dependent of the nature of the substituents. Compared to initiator decomposition, it has a lower E_a of typically 15-30 kJ·mol^{-1}.[1]

If all the sub-steps during propagation are considered, there are four possible routes for monomer addition to the growing chain radical during polymerization. These monomer addition sequences are: head-to-tail (HT), head-to-head (HH), tail-to-head (TH) and tail-to-tail (TT) addition as illustrated in Figure 2.1. During polymerization, HT is the dominant route and is preferred for both steric and resonance reasons. The other monomer addition orientations (i.e. HH, TH and TT) can be neglected for most monomer systems, as structural analysis of polymers formed from 'simple' monomers such as styrene, acrylates and methacrylates indicate none of the chain defects that results from head-to-head addition.[9-11] However, for the family of vinyl ester monomers including vinyl acetate (VAc) and vinyl benzoate (VBz), head-to-head addition cannot be neglected.[12-13]

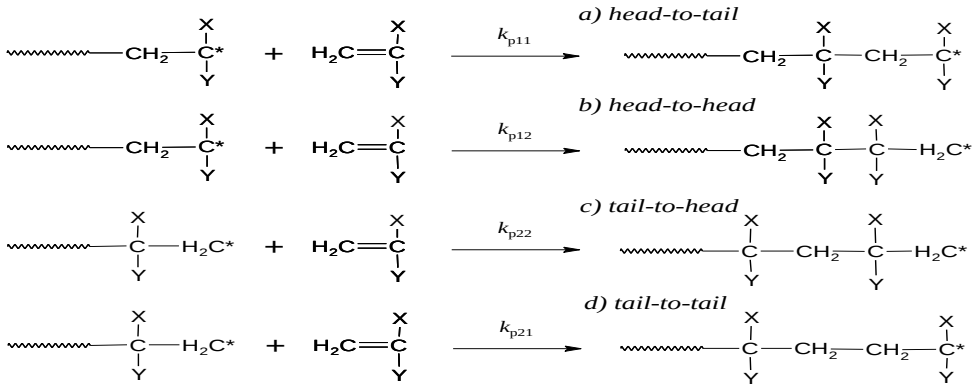

Figure 2.1: Possible routes for monomer addition during radical polymerization.

2.1.3 Termination

In FRP, two propagating radicals are terminated either through combination or disproportion, forming the final "dead" polymer product (equation 2.6-2.7). Termination by combination involves two radicals

combining together to form a single chain while disproportionation involves transfer of a β-hydrogen atom from one radical chain-end to another yielding two polymer chains (one with a carbon-carbon double bond). The rate coefficients of termination by combination and disproportionation are defined as k_{tc} and k_{td} respectively, and there are often summed up to give an overall termination rate coefficient, k_t. These rate coefficients are essential for describing polymerization kinetics and are affected by pressure, temperature, viscosity of the system and molecular weight (MW) of the reacting radicals.[5] There have been difficulties in measuring rate coefficient of termination, k_t, with discrepancies of the reported values due to the different methods used and quantifications used.[14] However, there has been a major advance in the development and knowledge of termination kinetics with the introduction of pulsed laser methods.[8] The activation energy of termination is between 10-15 kJ·mol^{-1}, lower than that for initiation and propagation.[1] For VAc polymerization system, termination occurs mostly by disproportion and combination is normally not included with the kinetic analysis.

2.1.4 Chain Transfer to Small Molecules

Chain transfer reactions with small molecules can also occur during radical polymerization, with the growing chain radical abstracting a weakly bonded hydrogen atom from a small molecule to form a dead polymer chain (D_n) and a new radical reactive enough to reinitiate polymerization (see equation 2.4 and 2.5).[15] These small molecules can either be an initiator, solvent, monomer, or a transfer agent added separately to control polymer molecular weight. The chain transfer rate coefficients (i.e k_{tr_mon}, $k_{tr\text{-}sol}$) are most often expressed in terms of a chain transfer constant, C_{tr}, in relation with the propagation rate coefficient (i.e. $C_{tr} = \frac{k_{tr}}{k_p}$).

2.2 Polymerization of VAc system

2.2.1 Head-to-head Addition (HH)

As described, there are four possible propagation steps by which VAc monomer can add to the growing radical chain (see Figure 2.1). These monomer additions dictate the structural arrangement of the growing polymer chain units. Head-to-head addition is an important side reaction for the vinyl ester family of monomers as well as fluorine and chlorine substituted α-olefins,[12,16-19] that not only affects the properties of the final polymer but also possibly the overall rate of chain growth kinetics. The occurrence of 1-2% head-to-head addition during VAc polymerization was first reported in the late 1940s by Flory et al., based upon structural analysis of the polymer formed, with the level of defects increasing with polymerization temperature.[12] Even though the occurrence of HH during VAc polymerization is relatively small, it can have a significant influence on the propagation kinetics of VAc. Moreover, in the late 1960s Hayashi and Otsu[13] examined the presence of HH during polymerization of various vinyl ester monomers including VAc, vinyl benzoate, vinyl valerate and vinyl butyrate; the levels in all cases 1-2%, similar to what Flory et al. reported. Most recently controlled radical polymerization of VAc was conducted by Morin and coworkers[20] reported 1.23% HH addition occurred during VAc polymerization at 40 °C. Even though some controlled radical polymerization was achieved, HH addition had an impact on the final polymer formed.

2.2.2 Long chain branching (LCB)

A branched polymer is defined as a polymer with points along the chain (either atoms or a group of atoms) from which more than two polymer segments originate.[21] Branching occurs either by chain transfer to polymer or/ and reaction of terminal double bonds during polymerization. There are two types of branching: short chain branching (SCB) and long chain branching (LCB), with LCB arising from intermolecular reactions such that branches have length similar to that of the main chain of the

polymer. First reported as far back as the 1930s, the mechanism has a significant impact on polymer properties and thus the material applications.[21] Specifically, LCB affects the melt rheological properties of the polymer by reducing the size of the polymer chains relative to linear systems.[22-24] The Size Exclusion Chromatography (SEC) technique with multiple detectors including Multi-Angle Light Scattering (MALS) and Intrinsic Viscometric (IV), has been used to predict/detect LCB for various polymers including poly(VAc). [25-26]

Different numerical modeling methods have been used to represent LCB in poly(VAc) including studies by Teymour,[27] Nie,[28] Kumar,[29] and Kallis.[30] However there are still some uncertainties as to the kinetic mechanisms and associated rate coefficients, with different assumption made developing these models. For example, Chaterjee[23] and Graessley[24] report that chain-termination is dominated by chain transfer such that the molecular weight distribution is independent of termination and initiation rates; while this provided a reasonable representation of polymer formed in batch reactor, it could not successfully describe VAc polymerization in a Continuous Stirred Tank Reactor (CSTR). In addition, as discussed by Taylor and Reichert this assumption cannot hold for higher initiator concentration.[32] Most models assume that each polymer chain possess a maximum of one radical center as well as one terminal double bond,[23,31-33] to avoid more complex equations even though there are chances of polyradicals (from high MW polymer chains with high rate of branching). As part of this study, further investigations will be conducted to examine LCB in VAc polymerization.

2.2.3 Degradative chain transfer on VAc Solution Polymerization

Solvent choice has been shown to significantly effect on VAc homo and copolymerization kinetics in previous studies. Wisotsky and Kober[34] investigated the solvent effects on the rate of polymerization on copolymerization of ethylene with VAc using aliphatic and aromatic solvents. They hypothesized

that the rate of polymerization was higher for aliphatic solvents, as the hydrogen abstraction chain-transfer to solvent reaction results in reactive alkyl radicals, which are able to readily reinitiate chain growth. The situation is different, however, for aromatic solvents, which slowed down the rate of polymerization. As benzene (one of the aromatic solvents used), does not readily undergo hydrogen abstraction, it was hypothesized that the lowered polymerization rate may be due to complex formation of the aromatic ring with the radical species. Toluene, on the other hand, readily undergoes hydrogen abstraction reaction, but the resulting benzyl radical species is resonance stabilized and thus postulated to be inefficient at reinitiating chain growth, as both monomers (VAc and ethylene) have low reactivity. This scenario is called retardation and it has been observed by others for VAc homopolymerization using toluene and other aromatic solvents.[35-37]Allen et al.[38] proposed that this retardation mechanism can be considered as degradative chain transfer, as no or very slow reinitiation of the resonance-stabilized solvent-derived radical occurs due to the low reactivity of VAc monomer, which leads to no or very slow reinitiation of benzyl radical species. In addition, Londsale et al.[39] showed through a combination of experiment and modeling, that for VAc polymerization in toluene this mechanism is dominant. The reluctance of VAc monomer to react with certain radicals must also be considered when selecting a photoinitiator for PLP experiments, as discussed in the next chapter.

2.3 Pulsed-Laser Polymerization-Size Exclusion Chromatography

A major advance in polymerization kinetics studies has been the introduction of the pulsed-laser polymerization coupled with Size Exclusion Chromatography (PLP-SEC) method, which determines the propagation rate coefficient, k_p from the molar mass distribution (MMD) of the resulting polymer.[40] This method is reliable and easy to use and has been recommended as the method of choice to determine k_p by the IUPAC subcommittee on Modeling of Polymerization Kinetics and Processes.[8] This

technique has been applied to measure k_p of common monomers such as styrene, acrylates and methacrylates at a wide temperature range and in multiple laboratories, and a series of benchmarks papers have been published to provide the best-fit Arrhenius parameters for these monomer systems.[41-46]

For PLP experiments, low monomer conversion is generated by exposing a monomer-photoinitiator mixture (sometimes with a solvent for solution polymerization) controlled at the desired temperature to the laser light (UV wavelength) at a constant pulse rate (prr), normally between 10 and 500 Hz. A population of new radicals is formed at each flash, initiating radical chain growth of new chains via propagation as well as terminating existing chains that have been growing during the dark period since the last laser pulse. During the time between the laser pulses, there is a continuous decrease in radical concentration and thus the rate of termination with time. A burst of termination occurs with the next flash, with the radicals that have survived to that point having a much great probability of termination at that instant. However, some radicals do survive two or more pulse cycles, with the probability of their termination at the next laser light, where new chain radicals are also formed. Polymer observed by SEC analysis show distinct features arising from the product terminated by the action of the laser light, with the number of propagation steps between the laser pulses reflected by the average chain length of the polymer produced.[47] The chain length, L_i of the dead polymer chain formed is related to time between laser pulses (t_o), by equation (2.18), where [M] is the monomer concentration. For known [M] and t_o, k_p can be easily evaluated with no any other kinetic parameter involved. As some growing radicals escape termination at a flash and continue growth, the resulting polymer molar mass distribution will contain an observable increased fraction of chains that will have specific chain length L_i (i= 1, 2, 3, 4, …) which is proportional to the number of pulses that they have survived. To define a

good PLP structure, both the 1st and 2nd inflection points of the 1st derivative plot of the corresponding molar mass distribution (MMD) have to be present and clearly seen, with the 2nd inflection point at approximately twice the M_o value.[8,40]

$$L_i = ik_p[M]t_o \qquad [2.18]$$

Theoretical studies on the analysis of molar mass distributions yielded from periodic pulsed initiation have been previously conducted.[48] In 1987, Olaj and coworkers were the first group to apply the PLP technique experimentally, showing that best measure of L_1 is the low molar mass inflection point of the 1st peak in the number or weight distribution.[40] By rearranging equation 2.18, the 1st inflection point from the 1st derivative curve of the corresponding MMDs is used to evaluate k_p (equation 2.19).

$$k_p = \frac{M_o}{\rho_{mon}\emptyset_{mix}t_o} \qquad [2.19]$$

M_o is the polymer MW corresponding to the 1st inflection point (maxima) of the 1st derivative curve of the polymer MMDs, ρ_{mon} is the monomer density and Φ is the monomer volume fraction in mixture (equal to 1 in bulk systems).

As PLP is temperature dependent, the Arrhenius equation (2.20) relates the propagation rate coefficient with temperature in terms of the pre-exponential factor A and activation energy E_a, with the values estimated using experimental data determined over a range of temperature.

$$k_p = Aexp(-\frac{E_a}{RT}) \qquad [2.20]$$

Even though this method (PLP-SEC) has been used to study a wide range of monomers, there is little data available for vinyl ester family of monomers, other than vinyl acetate[47,49] and an early study of vinyl decanoate.[50] The study of VAc and other vinyl ester monomers have proven to be difficult and

it was originally believed to be due to high chain transfer and termination rates.[49] Recently VAc studies via PLP technique by Junkers[44] utilized high frequency of up to 500 Hz, and surprisingly found out that there is a significant increase in k_p as the repetition rate increases (with 33% increase from 100 to 500 Hz). For this work, this method will be further utilized to provide a better understanding and improved knowledge of vinyl esters polymerization kinetics.

References

1. H. Kattner, MAsc Thesis, University of Gottingen (Gottingen) **2012.**
2. Mayo, F. R. *J. Am. Chem. Soc.* **1953**, *75*, 6133.
3. Mayo, F. R. *J. Am. Chem. Soc.* **1968**, *90*, 1289.
4. R. A. Hutchinson, *Handb. Polym. React. Eng.* **2005**, 153.
5. L. Kun, PhD Thesis, Queen's University (Kingston) **2013**.
6. M. Stickler, *In Comprehensive Polymer Science*; G. C. Eastmond, A. Ledwith, S. Russo, P. Sigwalt, Eds.; Pergamon: London, **1989**, *3*, 59.
7. A. M. Van Herk, *J. Macromol. Sci., Rev. Macromol. Chem. Phys.* **1997**, *37*, 633.
8. S. Beuermann, M. Buback, *Prog. Polym. Sci*. **2002**, *27*, 191.
9. D. R. Hensley, S. D. Goodrich, A. Y. Huckstep, H. J. Harwood, R. L. Rinaldi, *Macromolecules* **1995**, *28*, 1586.
10. T. Kashawagi, A. Inaba, J. E. Brown, K. Hatada, T. Kitayama, E. Masuda, *Macromolecules* **1986**, *19*, 2160.
11. L. E. Manring, D. Y. Sogah, G. M. Cohen, *Macromolecules* **1989**, *22*, 4654.
12. P. E. Flory, F. S. Leutner, *J. Polym. Sci.* **1948**, *3*, 880.
13. K. Hayashi, T. Ostu, *Makromol. Chem.* **1969**, *127*, 54.
14. J. Brandrup, E. H. Immergut, E. A. Grulke, (Eds.); *Polymer Handbook 4th Edition*, John Wiley & Sons, Inc., New York, **1999**.
15. R. J. Young, P. A. Lovell, Introduction to Polymers, *Technology and Engineering*, 3rd edition, CRC Press, Boca Raten, **2011**.
16. D. Britton, F. Heatley, P. A. Lovell, *Macromolecules* **1998**, *31*, 2828.

17. O. Vogl, M. F. Qin, A. Zilkha, *Prog. Polym. Sci.* **1999**, *24*, 1481.

18. J. Guiot, B. Ameduri, B. Boutevin, *Macromolecules* **2002**, *35*, 8694.

19. D. W. Ovenall, R. E. Uschold, *Macromolecules* **1991**, *24*, 3235.

20. A. N. Morin, C. Detrembleur, C. Jérôme, P. De Tullio, R. Poli, A. Debuigne, *Macromolecules* **2013**, *46*, 4303.

21. S. Thomas, McMaster University (Hamilton) **1998**.

22. G. D. Verros, D. S. Achilias, *J. Appl. Polym. Sci.* **2009**, *111*, 2171.

23. A. Chaterjee, W. S. Park, W. W. Graessley, *Chem. Eng. Sci.* **1977**, *32*, 167.

24. W. W. Graessley, R. D. Hartung, W. C. Uy, *J. Polym. Sci.: Part A-2* **1969**, *7*, 1919.

25. S. Grcev, P. Schoenmakers, P. Iedema, *Polymer* **2004**, *45*, 39.

26. D. Goedhart , A. Opschoor, *J. Polym. Sci.: Part A-2* **1970**, *8*, 1227.

27. F. Teymour , J. D. Campbell, *Macromolecules* **1994**, *27*, 2460.

28. L. Nie, W. Yang, H. Zhang, S. Fu, *Polymer* **2005**, *46*, 3175.

29. S. Kumar, Ramkrishna, *Chem. Eng. Sc.*, **1996**, *51*, 1311.

30. A. Krallis, C. Kiparissides, *Chem. Eng. Sci.* **2007**, *62*, 5304.

31. T. W. Taylor and K. H. Reichert, *J. Appl. Polym. Sci* **1985**, *30*, 227.

32. H. Tobita, *J. Polym. Sci. Part B: Polym. Phys.* **1994**, *32*, 901.

33. H. Tobita, *J. Polym. Sci. Part B: Polym. Phys.* **1994**, *32*, 911.

34. M. J. Wisotsky, A. E. Kober, *J. Appl. Polym. Sci.* **1972**, *16*, 849.

35. T. F. McKenna, A. Villanueva, *J. Polym. Sci. Part A: Polym. Chem.* **1999**, *37*, 589.

36. R. Jovanovic, M. A. Dube, *J. Appl. Polym. Sci.* **2001**, *82*, 2958.

37. K. Hatada, Y. Terawaki, T. Kitayama, M. Kamachi, M. Tamaki, *Polym. Bull* **1981**, *4*, 451.

38. P. W. Allen, F. M. Merrett, J. Scanlan, *Trans Faraday Soc.* **1955**, *75*, 95.

39. D. E. Lonsdale, G. Johnston-Hall, A. Fawcett, C. A. Bell, C. N. Urbani, M. R. Whittaker, M. J. Monteiro, *J. Polym. Sci: Part A: Polym. Chem.* **2007**, *45*, 3620.

40. O. F. Olaj, I. Bitai, F. Hinkelmann, *Makromol. Chem.* **1987**, 188, 1689.

41. M. Buback, R. G. Gilbert, R. A. Hutchinson, B. Klumperman, F.-D. Kuchta, B. G. Manders, K. F. O'Driscoll, G. T. Russell, J. Schweer, *Macromol. Chem. Phys.* **1995**, *196*, 3267.

42. S. Beuermann, M. Buback, T. P. Davis, R. G. Gilbert, R. A. Hutchinson, O. F. Olaj, G. T. Russell, J. Schweer, A. M. van Herk, *Macromol. Chem. Phys.* **1997**, *198*, 1545.

43. S. Beuermann, M. Buback, T. P. Davis, R. G. Gilbert, R. A. Hutchinson, A. Kajiwara, B. Klumperman, G. T. Russell, *Macromol. Chem. Phys.* **2000**, *201*, 1355.

44. S. Beuermann, M. Buback, T. P. Davis, N. García, R. G. Gilbert, R. A. Hutchinson, A. Kajiwara, M. Kamachi, I. Lacík, G. T. Russell, *Macromol. Chem. Phys.* **2003**, *204*, 1338.

45. J. M. Asua, S. Beuermann, M. Buback, P. Castignolles, B. Charleux, R. G. Gilbert, R. A. Hutchinson, J. R. Leiza, A. N. Nikitin, J. P. Vairon, A. M. Van Herk, *Macromol. Chem. Phys.* **2004**, *205*, 2151

46. C. Barner-Kowollik, S. Beuermann, M. Buback, P. Castignolles, B. Charleux, M. L. Coote, R. A Hutchinson, T. Junkers, I. Lacik, G. T. Russell, M. Stach, A. M. van Herk, *Polym. Chem.* **2014**, *5*, 204.

47. T. Junkers, D. Voll, C. Barner-Kowollik, *e-Polymers.* **2009**, *076*, 1.

48. V. N. Genkin, V. Sokolov, *Doklady Akademii Nauk SSSR.* **1997**, *234*, 94.

49. R.A. Hutchinson, J. R. Richards, M. T. Aronson, *Macromolecules* **1994**, *27*, 4530.

50. R. Balic, R. G. Gilbert, M. D. Zammit, T. P. Davis, C. M. Miller, *Macromolecules* **1997**, *30,* 3775.

Chapter 3: A study of vinyl acetate propagation kinetics using the PLP-SEC Technique

Preface

As the initial stage of my research project, bulk homopolymerization of vinyl acetate (VAc) was studied using PLP-SEC and three different photoinitiators in order to fully explore the dependence of the measured propagation rate coefficient on pulse repetition rate, and to determine whether the results could be understood in terms of head-to-head addition. This chapter is edited from the resulting publication in Macromolecules (2014, vol. 47, page 8145) that reports the experimental study. As the simulation work was conducted by one of our collaborators, Dr. Anatoly Nikitin in Russia, this portion of the publication has been moved to Appendix 1, with only the key results reported here.

Supporting work for this chapter is contained in additional appendices. Appendices 2 and 3 summarize work done to ensure that the observed variation of k_p with prr is not due to temperature variation during pulsing (Appendix 2) or uncertainty in determining the precise position of the inflection point from the first derivative plot (Appendix 3). Appendix 4 summarizes the Nuclear Magnetic Resonance (NMR) analysis of head-to-head defects in poly(VAc) experiments, while Appendix 5 summarizes the complete set of PLP-SEC experiments performed with bulk VAc.

Summary

The radical propagation kinetics of vinyl acetate (VAc) has been studied by pulsed-laser polymerization coupled with analysis of the resulting polymer molar mass distributions. The significant increase in the apparent propagation rate coefficient, k_p^{app}, observed with increasing pulse repetition rate is explained by the influence of the head-to-head defects formed during chain-growth. Simulations that include head-to-head monomer addition are combined with an analysis of the experimental results to estimate the

subsequent rate coefficients for reaction of the resultant radical as well as the k_p of normal head-to-tail addition. An analytical expression is derived for an averaged rate coefficient, k_p^{av}, for the system, with the best-fit Arrhenius parameters of $\ln(A/\text{L}\cdot\text{mol}^{-1}\cdot\text{s}^{-1}) = 16.56\pm0.35$ and $E/R = 2508\pm108$ K.

3.1 Introduction

Mechanistic understanding of polymerization kinetics is a critical component required to guide the optimization of operating conditions for existing and new polymer grades, to discriminate between kinetic and physical effects during process development, to perform design and safety studies, and to understand and optimize transitions and other dynamics. These process development and modeling efforts are enabled by knowledge of the underlying polymerization mechanisms and accurate values of kinetic rate coefficients. A major advance has been the introduction of the PLP-SEC technique, in which Pulsed-Laser Polymerization (PLP) is combined with analysis of the resulting polymer molecular mass distribution (MMD) to directly estimate k_p, the chain growth rate coefficient for radical polymerization.[1-2] However, the study of vinyl acetate (VAc) propagation kinetics by PLP has proven to be difficult. Originally believed due to high termination and transfer rates,[3] more recent investigations suggest the difficulty arises from other kinetic features of the system. Junkers et al. recently have utilized pulse repetition rates up to 500 Hz laser to study VAc.[4] Surprisingly, the apparent k_p value (hereby referred to as k_p^{app}) increased by 33% as the pulse repetition rate (prr) was increased from 100 to 500 Hz. This behavior, not seen for "simple" monomers such as styrene and methacrylates,[2] is an indicator that side reactions are confounding the kinetic analysis.

Junkers et al. hypothesized that the influence of prr on VAc k_p^{app} was a result of intramolecular transfer to polymer (backbiting) disrupting the relation between repetition rate and chain-length, as has been found for acrylate systems.[5-7] However, backbiting involving VAc during homopolymerization and

copolymerization with ethylene is negligible or very low relative to corresponding acrylate systems.[8-10] In addition, Kattner and Buback[11] have recently shown that no poly(VAc) midchain radicals could be detected using the powerful single-pulse PLP method coupled with time-resolved electron paramagnetic resonance measurement of radical concentrations (the SP-PLP-EPR technique).

Kattner and Buback also highlighted another difficulty of using PLP to study VAc kinetics: while VAc radicals are very reactive, addition to the double bond of VAc monomer is slow. Ample evidence of the reduced reactivity of VAc (relative to acrylate or methacrylate monomers) to radical addition is found in the literature. In the 1940s Mayo et al. investigated the copolymerization of VAc with eight representative monomers and found that the monomer is one of the least reactive of any common monomers toward radical attack.[12] This low reactivity has been studied computationally, and is attributed to the increased partial negative charge on the CH_2 group resulting from the influence of the adjoining ester group that inhibits radical attack relative to other monomers.[13] Additionally, the rate of VAc (co)polymerization is retarded in aromatic solvents such as toluene due to slow addition of monomer to the toluene radical formed after transfer to solvent.[14-16] For effective PLP experimentation, the radicals formed by decomposition of the photoinitiator must be sufficiently active to attack the VAc double bond; if not, the efficiency of initiation suffers greatly, with some of the primary radicals formed only able to terminate existing growing chains rather than initiate new ones.[11] As part of the current study, the influence of ineffective primary radicals is considered through simulation. Although photoinitiator choice has some influence on the structure of PLP-generated poly(VAc) MMDs (and thus determination of k_p^{app}), it is not sufficient to fully explain the apparent prr effect. Herein we present a plausible explanation based on a long-known feature of VAc systems, head-to-head monomer addition.

The influence of head-to-head addition confounds the analysis of chain-growth kinetics, as shown by considering the possible modes of radical propagation associated with monomer structure shown in Scheme 3.1. For most monomers, the microstructure of the polymer chains produced indicates that head-to-tail propagation occurs exclusively, as this addition is favored on both steric and resonance grounds. The presence of head-to-head linkages in polymer chains are known to cause a lowering of the onset temperature for polymer thermal degradation,[17-18] and thus have been intensively searched for in polymers such as poly(methyl methacrylate)[17-18] and poly(styrene).[19] These studies ruled out the possibility of head-to-head monomer addition, with any head-to-head linkages that were found attributed to termination by combination. Thus, the rate coefficient for head-to-tail propagation (k_{p11} in Scheme 3.1) can be considered as the sole rate coefficient for homopropagation for most monomers, and the other three addition mechanisms can be neglected.

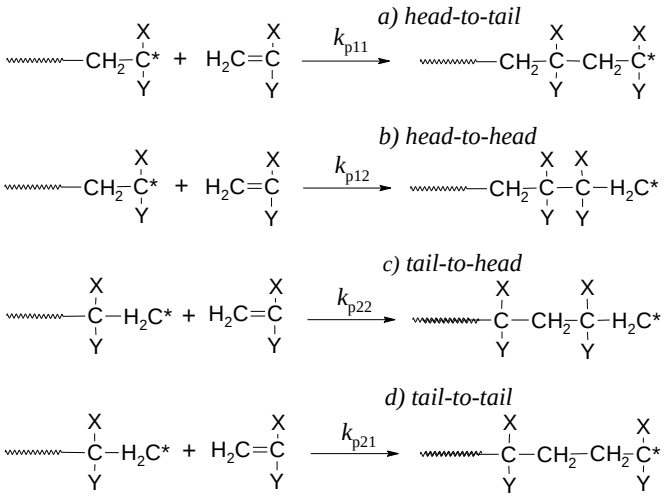

Scheme 3.1: The propagation reactions in free radical homopolymerization, accounting for the possibility of inverted monomer addition.

However, the situation is different for VAc: dating back to the study by Flory and Leutner[20] it was found that poly(VAc) chains contain defects resulting from inverted monomer insertion at a level of 1-2% (on average every 50 to 100 monomer units).[10,20-22] The head-to-head addition that leads to the observed —$COC(O)CH_3$-CH_2-CH_2-$COC(O)CH_3$— defect is a result of the low reactivity of VAc monomer towards attack, such that radicals occasionally add across the VAc monomer $COC(O)CH_3$ "head" rather than the less sterically-hindered CH_2 "tail" of the monomer. Recently Morin et al. show that low MW poly(VAc) (average DP of 78 units as produced by controlled-radical polymerization) have a lower concentration of defects than high MW material, and attribute the difficulty in conducting controlled radical polymerization of VAc to the loss of reactivity caused by the increased stability of the CH_2 radical complexed to the controlling agent in the system.[21]

The influence of head-to-head additions during PLP-SEC experiments should vary with the target chain-length controlled by the laser prr, and thus may explain the reported k_p dependency.[4] Assuming a defect level of 1%, head-to-head addition can influence the value of k_p^{app} at lower repetition rates where DP_0 of the poly(VAc) is longer than 100 units but not for PLP experiments conducted at high repetition rates. Thus we report here a systematic PLP-SEC investigation of the effect of prr on k_p^{app} for bulk VAc between 25 and 65 °C. Three different photoinitiators are used to examine the possible confounding effect of ineffective initiation on the structure of the resulting MMD and k_p^{app} estimates. The experimental study is accompanied by simulations that account for head-to-head addition as well as the reduced reactivity of the resulting inverted radical structure, with a comparison of simulation and experiment used to provide estimates for the VAc addition rate coefficients. Finally, an expression for an averaged propagation rate coefficient is derived that can be used to consider the influence of head-to-head insertion on continuously-initiated polymerization systems.

3.2 Experimental Section

Vinyl acetate (VAc, Aldrich 99+ %), methyl methacrylate (MMA, Aldrich), 2, 2-dimethoxy acetophenone (DMPA, Aldrich 99%), dicumyl peroxide (DCP, Aldrich 98%), and benzoin (Aldrich ≥99.5%) was used as received. The experimental set up and procedure is similar to previous work.[3,23-24] Bulk monomer solution of VAc (or MMA) with 5 mmol·L^{-1} DMPA or benzoin photoinitiator were prepared; experiments with DCP were conducted with 90 mmol·L^{-1} DCP, as suggested by previous literature.[11] Samples were transferred into cuvettes and allowed to equilibrate to the desired temperature (±0.5°C) before being exposed to the laser light generated by a Xantos XS-500 laser operating at wavelength 351nm, 3-15 ns pulse duration and pulse energy of 3-8 mJ/pulse. The experiments were run to low monomer conversion (< 2%) at a constant pulse repetition rate (prr) controlled between 20 and 300 Hz for MMA at 50 °C, and between 100 and 500 Hz for VAc in a temperature range of 25 to 65 °C. The samples were precipitated in cold hydroquinone/methanol solution. After allowing the heterogeneous mixture to settle overnight in a freezer, the liquid was decanted and the polymer dried under vacuum.

The molar mass distributions (MMD) of the samples were analyzed by size exclusion chromatography (SEC) at 30 °C using tetrahydrofuran (THF) as an eluent with a flow rate of 0.3 mL·min^{-1}. The SEC system consists of a Waters 2960 separation module, auto injector, four Styragel® THF columns (HR 0.5, 1, 3, 4), a Waters 410 differential refractometer (DRI) and a Dawn EOS 690 nm Laser Photometer. The poly(MMA) PLP samples were analyzed using direct calibration against narrow poly(MMA) standards, while the MMD of the poly(VAc) PLP samples were estimated using the principle of universal calibration against a polystyrene calibration established using narrow molar mass standards in the range of 370 – 860 000 Da; the Mark-Houwink parameters utilized are summarized in Table 3.1.

The experimental MMDs were smoothed and differentiated using OriginLab software, with k_p^{app} estimated from the position of the first inflection point (M_o), known monomer density (ρ_{mon}) calculated as a function of temperature,[3] and the time between pulses (t_o), according to equation (3.1).[1-2]

$$k_p = \frac{M_o}{1000 \rho_{mon} t_o} \quad (3.1)$$

The accuracy of the position of the inflection points was checked for some samples using output from the LS detector analyzed using known d*n*/d*c* values (Table 3.1) for the polymer in THF, as described in previous work.[24]

Table 3.1: Calibration parameters required for determination of k_p values from SEC analysis of PLP-generated molar mass distributions.

	Poly(St)[23]	Poly(VAc)[23]
Mark-Houwink parameters		
K (dL·g^{-1})×10^4	1.14	1.56
a	0.716	0.708
d*n*/d*c* (mL·g^{-1})	0.183	0.058

3.3 Results and Discussion

3.3.1 PLP-SEC Experimental Results

Well-structured MMDs were obtained for poly(MMA) and poly(VAc) samples generated by PLP experiments at 50 °C with DMPA and benzoin photoinitiator respectively, as shown in Figure 3.1. Primary and secondary inflection points were observed in the first-derivative plots for MMA pulsed between 20 Hz (the lowest prr employed) up to 300 Hz, with the position of the secondary inflection point at approximately twice the value of M_o, as expected.[2,3] (Detailed results for all PLP experiments are shown in Appendix 5.) The position of the primary inflection point shifts from 3×10^4 to 2×10^3 Da for poly(MMA) as prr is increased from 20 to 300 Hz. The resulting value of k_p^{app}, however, is independent of prr; as shown in Figure 3.2, the value fluctuates between 650 and 710 L·mol^{-1}·s^{-1}, in

reasonable agreement with the value of 650 $L \cdot mol^{-1} \cdot s^{-1}$ estimated from the benchmark data set published for MMA.[25]

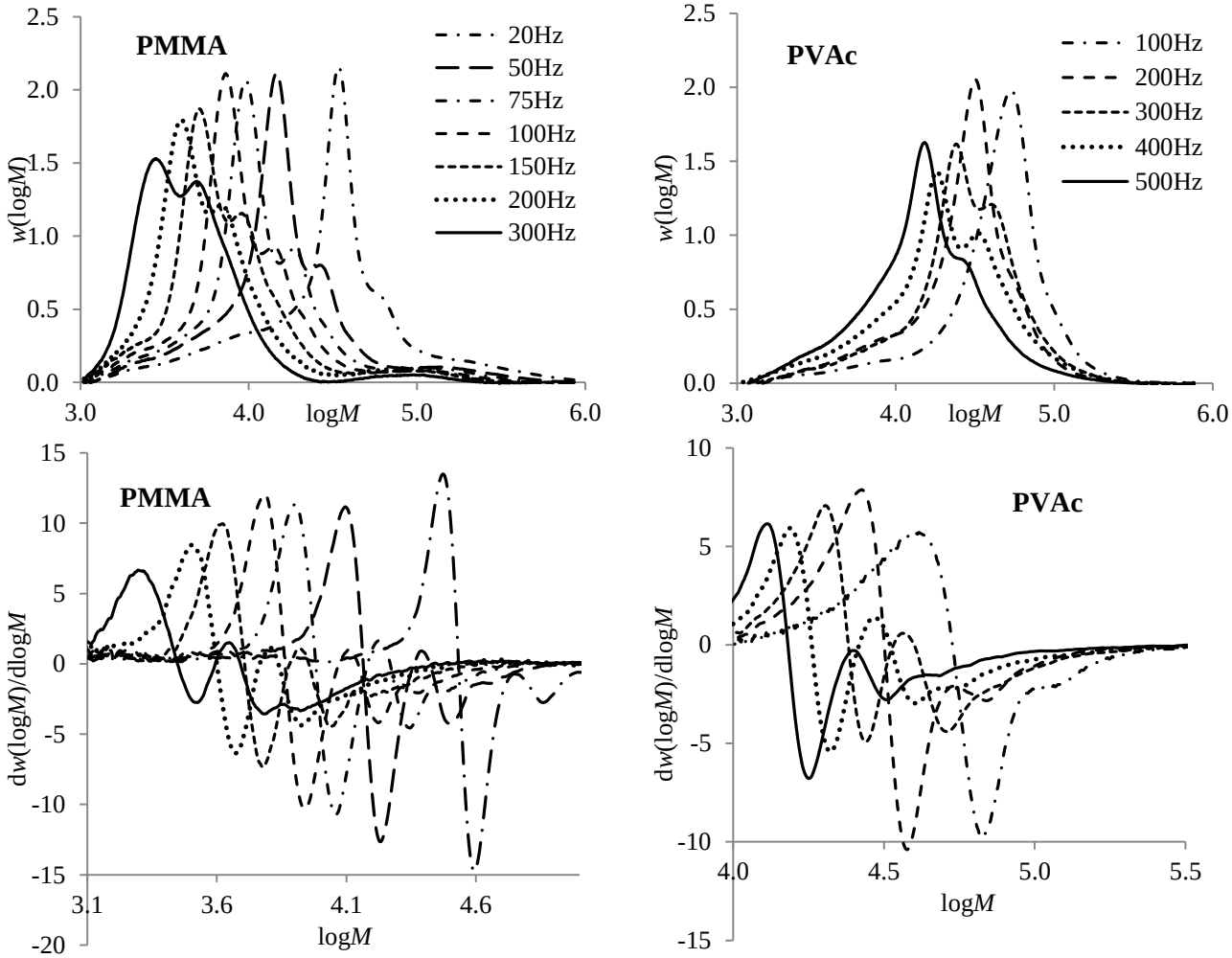

Figure 3.1: Molar mass distributions (top) and corresponding first-derivative plots (bottom) for poly(MMA) (left) and poly(VAc) (right) produced by PLP at various pulse repetition rates at 50°C.

A similar series of experiments were conducted with VAc at 50 °C using benzoin photoinitiator, with prr varied between 100 and 500 Hz; as described in previous work,[4,23] the higher prr is required because of the faster propagation rate of VAc and to achieve PLP-structured MMDs. At 100 Hz the secondary inflection point is barely observable on the corresponding derivative plot, with structure improving as prr is increased to 500 Hz (Figure 3.1), the maximum value possible with the laser setup used. As shown

in Figure 3.2 and as in agreement with Junkers et al.,[4] there is a significant increase in k_p^{app} for VAc, with the value increasing from 5500 to 7550 L·mol^{-1}·s^{-1} as prr is increased from 100 to 500 Hz.

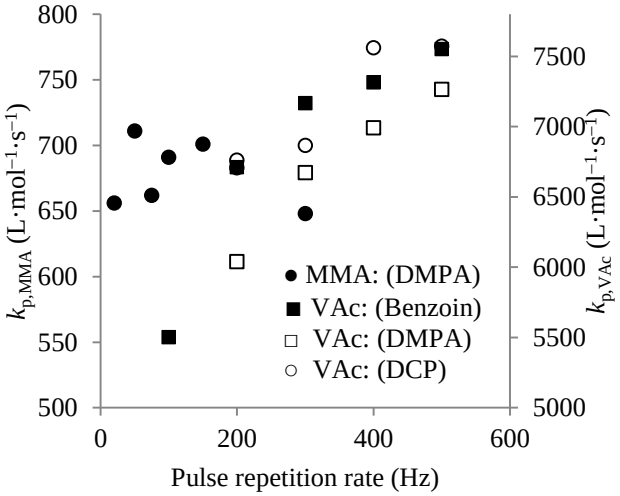

Figure 3.2: Values for k_p as a function of pulse repetition rate obtained from PLP experiments at 50 °C for bulk VAc with benzoin, DMPA and DCP photoinitiators and for bulk MMA with DMPA photoinitiator.

The systematic variation in k_p^{app} for VAc is also found (Figure 3.2) for experiments with DMPA (as used by Junkers et al.[4]) and DCP (as used by Kattner and Buback[11]) photoinitiators. As shown in Figure 3.3, the photoinitiator choice has a significant effect on the shape of the PLP-generated MMD, an influence that results not only from the concentration of primary radicals generated from the photoinitiator by the laser pulse but also from the efficiency of those radicals in initiating VAc chain growth.[11] For DMPA and DCP, PLP structure is lost at 100 Hz (Figure 3.3); thus the majority of the experiments in this study were done using benzoin as photoinitiator. As long as good PLP structure is achieved, however, the position of the inflection point is not influenced by photoinitiator choice, and the increase of k_p^{app} with prr is seen for all three photoinitiators studied (Figure 3.2).

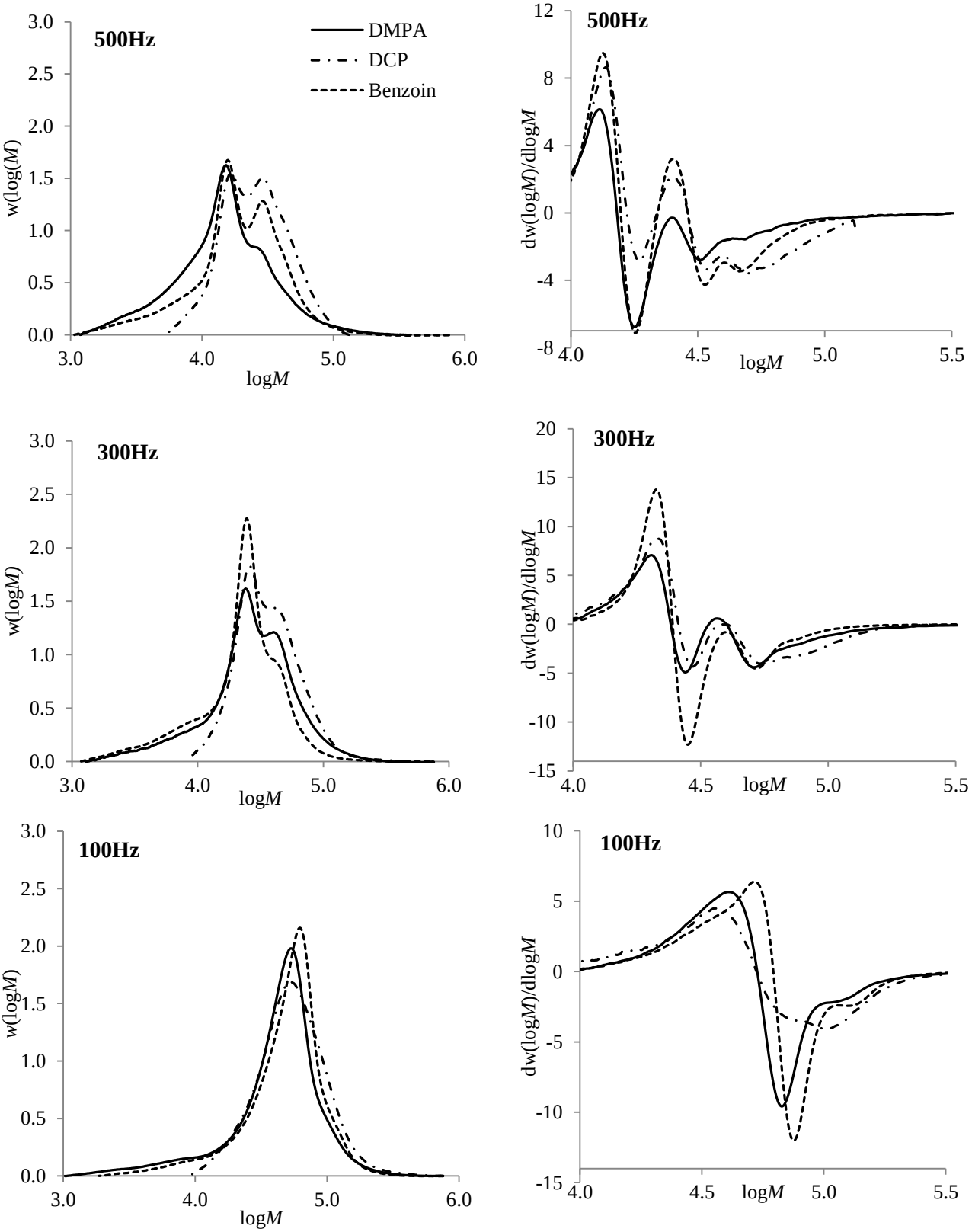

Figure 3.3: MMDs and corresponding first-derivative plots for poly(VAc) produced by PLP at 50°C with three photoinitiators at 500 (top), 300 (middle) and 100 (bottom) Hz.

Further experiments were conducted between 25 and 65 °C at prr of 100 to 500 Hz, with the complete set of data tabulated in Appendix 5. The data and the Arrhenius fits are shown in Figure 3.4, with the Arrhenius parameters summarized in Table 3.2. The curves are separated into two plots so that it is easier to distinguish between the data sets. There is a significant shift to higher k_p^{app} values as prr is increased from 100 to 500 Hz, with the best-fit value at 50 °C increasing by 25% from 5771 to 7388 $L \cdot mol^{-1} \cdot s^{-1}$, as summarized in Table 3.2. Moreover, the estimated activation energy systematically increases from 18.6 to 23.2 $kJ \cdot mol^{-1}$ with increasing prr.

Table 3.2: Arrhenius parameters obtained from linear fitting of ln(k_p) values estimated from PLP-SEC experiments for bulk VAc conducted between 25 and 65 ºC. Separate fits were conducted at each pulse repetition rate.

Repetition rate, Hz	ln (A/L·mol^{-1}·s^{-1})	(E/R), K	k_p at 50 °C (L·mol^{-1}·s^{-1})
100	15.58 ± 0.34	2236 ± 109	5771
200	16.11 ± 0.35	2346 ± 110	6976
300	16.43 ± 0.26	2449 ± 84	6985
400	16.92 ± 0.29	2603 ± 92	7079
500	17.56 ± 0.22	2796 ± 67	7388
Hutchinson et al.[23]	16.50 ± 0.14	2485 ± 41	6701
Junkers et al.[4]	17.12 ± 0.16	2621 ± 50	8178

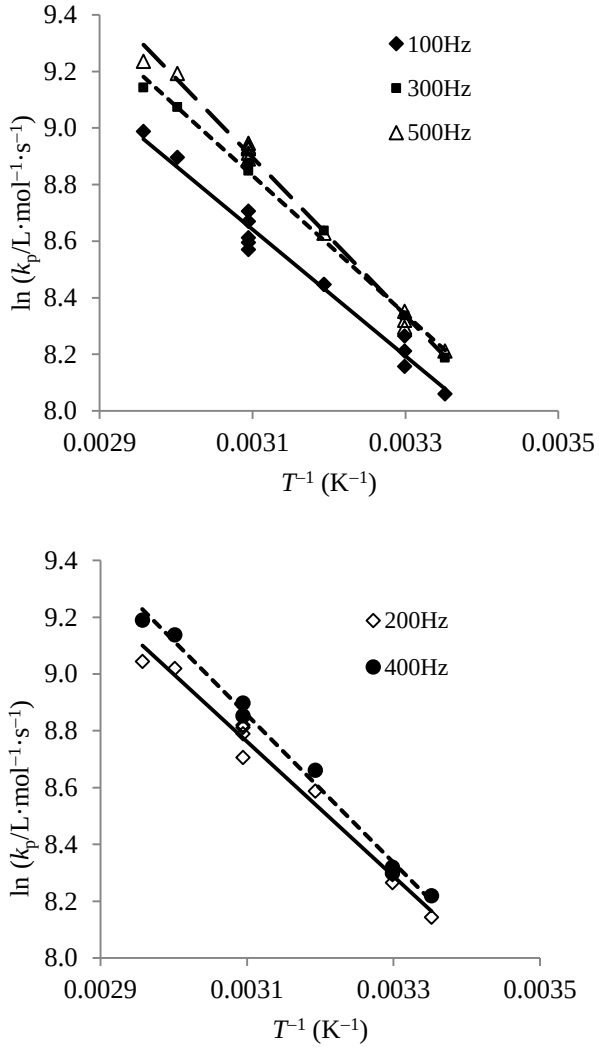

Figure 3.4: Arrhenius plots of VAc apparent propagation rate coefficients for experiments conducted at 100, 300 and 500 Hz (top) and 200 and 400 Hz (bottom). Best-fit Arrhenius parameters are summarized in Table 3.2.

It is instructive to compare these data and Arrhenius fits to the previous studies of VAc propagation kinetics. The activation energy of 21.8 kJ·mol^{-1} reported by Junkers et al. from experiments conducted at 500 Hz [4] is higher than the 20.7 kJ·mol^{-1} value from Hutchinson et al. from experiments conducted at 50-100 Hz,[23] in agreement with the systematic increase in activation energy with prr observed in the current study. As shown in Figure 3.5, the values of k_p^{app} measured in this study at 100 Hz are 10-15% lower than calculated using the Arrhenius parameters from Hutchinson et al., while the k_p^{app} values measured at 500 Hz are more in line (but still approximately 10% lower) with the predictions from the

fit to the Junkers et al. data set. Despite this 10% offset (within the acceptable error limits of k_p values estimated by PLP[6,25]), it is clear that the difference between the k_p estimates (and corresponding Arrhenius plots) from the two previous studies of VAc is indeed due to the systematic increase in k_p^{app} with prr, as reported by Junkers et al.[4] As described below, an explanation for this behavior is the head-to-head addition that occurs during VAc polymerization.

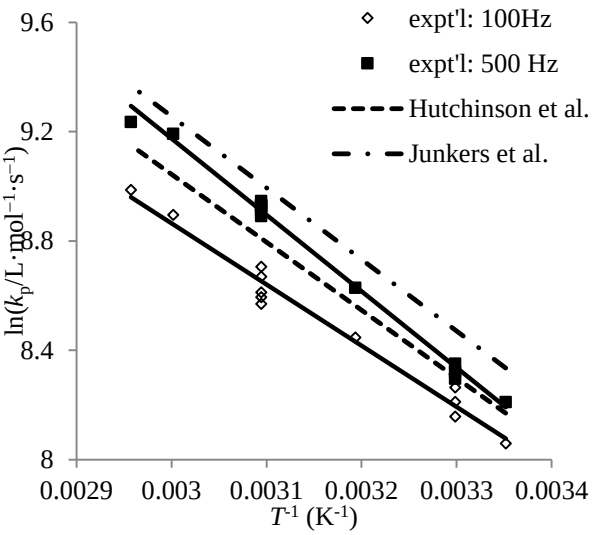

Figure 3.5: A comparison of VAc apparent propagation rate coefficients obtained from experiments conducted at 100 and 500 Hz to predictions from Arrhenius fits taken from literature.[4,23]

3.3.2 Theoretical Considerations and Simulation Results

As mentioned, simulation work was conducted to support the experimental results, with detailed information of the model developed by Dr. A. Nikitin presented in Appendix 1. Herein is presented a summary of the model predictions and the comparison with the experimental work.

3.3.2.1 The average propagation rate coefficient, k_p^{av}

The 1-2 % of head-to-head defects found in poly(VAc)[10,20-21] and other poly(vinyl esters)[22] is relatively unique among non-halogenated polymers.[26-27] However, head-to-head addition is quite important in the polymerization of the fluorine substituted α-olefins poly(trifluoroethylene), poly(vinyl fluoride) and poly(vinylidene fluoride), with the fraction of defect linkages between 5 and 15 %,

depending on the degree of fluorine substitution.[26-30] Head-to-head addition also occurs during the polymerization of vinyl chloride, leading to the formation of internal allylic chloride groups through an intramolecular hydrogen atom shift, and lowering the stability of the polymer.[31-32]

Inverted additions not only impact polymer properties, but may also considerably influence chain-growth kinetics. As detailed in Appendix 1 and using the four propagation rate coefficients defined in Scheme 3.1, Dr. Anatoly Nikitin has derived an equation for the averaged propagation rate coefficient, k_p^{av} value, shown here as Equation 3.2.

$$k_p^{av} = k_{p11} - \frac{k_{p11} - k_{p22} - 2k_{p21}}{1 + \frac{k_{p21}}{k_{p12}}} \qquad [3.2]$$

This equation is based upon the set of mechanism shown as Scheme 3.1, and provides a limiting value for k_p^{app} as prr is lowered. The experimental results were used to guide estimates of the individual kinetic rate coefficients in the system by comparison of simulated MMDs (obtained using the Predici software package) with experiment. The major results are summarized in Figure 3.6, a plot of simulated and experimental k_p^{app} values plotted against prr.

For both sets of simulation results shown in Figure 3.6, variation in k_p^{app} with pulse repetition rate is observed, with the value estimated by differentiating the simulated MMDs using the model and kinetic coefficient described in Appendix 1. At low prr the limiting value is slightly (<10%) below k_p^{av}, a behavior that has been attributed to the influence of peak broadening on the value estimated from the inflection point on the low-molecular-weight side of the first PLP-induced peak[33] and by the fact that the system is approaching the high termination rate regime.[34] As prr is increased, both sets of the simulated dependencies show a corresponding increase in k_p^{app}. For the simulations conducted without

head-to-head addition, however, k_p^{app} increases above k_p^{av} only slightly and only when prr is increased well above 500 Hz; this feature of PLP experiments conducted at the low termination rate limit has been discussed before[35] and is the reason why PLP conducted in this regime (very high prr) is not recommended for k_p determination.[36] (Note that our experimental MMDs, even at 500 Hz, have an easily-observed secondary inflection point, indicating that these distributions were not measured at the high termination rate limit.[37]) For the simulations conducted with the head-to-head addition reaction included, the crossover point where k_p^{app} is equal to k_p^{av} occurs at about 200 Hz, and k_p^{app} continues to increase towards the k_{p11} value, as the majority of radicals are not subjected to a head-to-head propagation event before the next pulse arrives.

On the basis of these simulations, we conclude that the consideration of head-to-head addition is required to capture the extent of the variation in k_p^{app} seen experimentally in both our data and that published by Junkers et al.[4] We were only to match the experimental variation by setting k_{p11} (9400 $L \cdot mol^{-1} \cdot s^{-1}$ at 50 °C) to a much higher value than k_p^{av} (6750 $L \cdot mol^{-1} \cdot s^{-1}$), with the PLP-determined k_p^{app} values much closer to the latter value than the former. In addition and as presented (see Table 3.3), the model does not capture the extent of the increase in activation energy of k_p^{app} with the increase of pulse repetition rate observed experimentally (Table 3.2). Thus, the PLP-SEC data cannot be used to provide a reliable estimate of the true chain-end head-to-tail propagation rate coefficient (k_{p11}) for VAc.

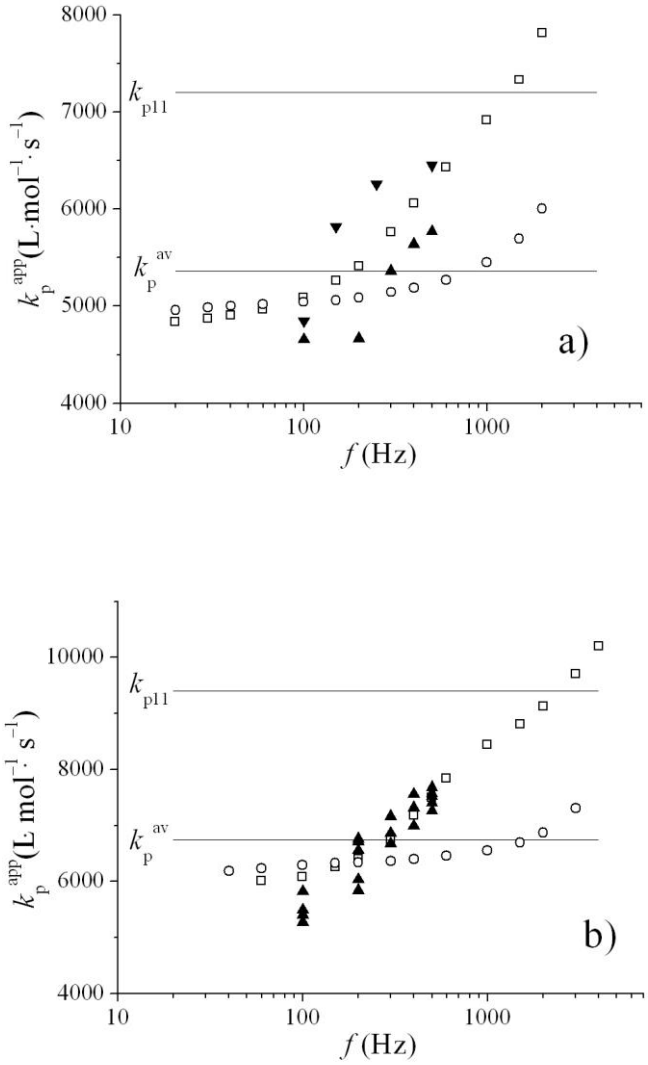

Figure 3.6: Experimental (triangles) and simulated (squares when head-to-head addition is considered; circles with only head-to-tail addition) prr dependencies of apparent propagation rate coefficients obtained from molar mass distributions for vinyl acetate pulsed laser polymerization at 40.5 (a) and 50 °C (b). For calculations kinetic parameters (given in Appendix 1) are chosen with σ =0.04 and ρ = 3×10^{-7} (a) and 6×10^{-7} mol·L^{-1} (b).

Table 3.3: Arrhenius parameters obtained from linear fitting of k_p^{app} values estimated from simulations of PLP-SEC experiments for VAc polymerization at 50 °C. Separate fits were conducted at each pulse repetition rate.

Repetition rate, Hz	ln (A)	(E/R), K
100	16.01	2349
200	15.74	2245
300	15.67	2207
400	15.99	2294
500	16.37	2399

3.3.3 Further considerations

The results of this analysis have several implications. A recommended self-consistency check for the determination of reliable k_p data by the PLP-SEC technique is that the measured k_p^{app} values should be independent of laser-pulse repetition rate.[36] It is clear that this check is not entirely valid for monomers such as VAc that exhibit head-to-head propagation, as the k_p^{app} value determined from PLP varying between the two limiting values of k_{p11} and k_p^{av}. This dependency would be even stronger for a monomer such as vinylidene fluoride (VDF), for which PLP-determined k_p values (determined at a prr of 500 Hz) have recently been reported.[37] Recent *ab initio* calculations suggest that VDF head-to-head addition and the subsequent reactivity of the less reactive "tail" radical have a significant impact on overall propagation kinetics.[38] Further analysis is required to determine whether the recent PLP data obtained for VDF provide a better estimate of k_p^{av} or k_{p11} of the system. This may be difficult, as the VDF system is further complicated by the occurrence of backbiting.[37-38]

Note that under steady-state conditions, the fraction of radicals that are in the inverted "tail" state V (see Appendix 1) can be estimated as:

$$\frac{[V]}{[V]+[R]} = \frac{k_{p12}}{k_{p12}+k_{p21}} \tag{3.8}$$

Using the parameters shown in appendix 1, this fraction is roughly 30%. However, in the EPR study by Kattner and Buback[11] only a single type of radical attributed to the expected "head" structure was observed. This result may partially be explained by the non-stationary nature of the SP-PLP-EPR experiment, but may also indicate that our estimate for k_{p21} is too low. Thus, while we have shown that head-to-head addition explains the strong influence of prr on k_p^{app}, the simulations indicate that k_p^{app} is much closer to k_p^{av} than k_{p11} for the VAc system, making it difficult to use the PLP-SEC data to obtain precise estimates of k_{p11} and k_{p21}.

We consider that the possibility to determine k_p^{av} by the PLP-SEC technique for monomers with marked head-to-head propagation is an important advantage of this technique. For these monomers, the propagation of continuously-initiated polymerizations can be described by this single rate coefficient at normal conditions of polymerization for which number-average degree of polymerization is higher than k_{p11}/ k_{p12}. While the situation has some similarities to the case of acrylate polymerization, in which propagation kinetics are affected by intramolecular chain transfer that forms a more stable mid-chain radical structure, there is an important distinction. For simulation of acrylate polymerization, it is necessary to explicitly model the presence of the two radical structures, as their relative population varies with monomer concentration and conversion.[5-7] The situation arising from head-to-head addition is different, as k_p^{av} is independent of monomer concentration (see Appendix 1), and as it is unlikely that the radical structure has a significant influence on radical termination kinetics. Thus, while k_{p11} can be considered as the true head-to-tail propagation rate coefficient for VAc, it is recommended that k_p^{av} be used to simulate continuously-initiated radical polymerization of VAc. The exception to this recommendation is when the model is written to explicitly consider the production of head-to-head linkages in the polymer. Another exception is the case of controlled radical polymerization (CRP): as

shown by Morin et al.,[21] for many CRP systems VAc radicals reactivate at a much slower rate following a head-to-head addition, significantly decreasing the overall polymerization rate.

The simulations results summarized in Figure 3.6 suggest we are able to determine only the value of k_p^{av} for VAc using our experimental data, as the accessible prr regime for k_p^{app} is far from the limiting value of k_{p11}. While the k_p^{app} values determined at 500 Hz overestimate k_p^{av} by 13%, the values determined at low repetition rate underestimate the value by 9% due to the broadening of the PLP-controlled peak (see Figure 3.6). Therefore the mean value from all of the experimental k_p^{app} values could be considered as a good estimation of k_p^{av}. An Arrhenius fit of the complete data set yields $\ln(A/\text{L}\cdot\text{mol}^{-1}\cdot\text{s}^{-1}) = 16.56\pm0.35$ and $E/R = 2508\pm108$ K , in reasonable agreement with previous studies.[3-4]

3.4 Conclusions

An extensive set of experiments confirms that the apparent rate coefficient, k_p^{app}, measured for VAc propagation by the PLP-SEC technique varies by more than 25% when laser pulse repetition rate is increased from 100 to 500 Hz. This behavior is attributed to the influence of head-to-head additions on the rate of VAc chain growth, with the probability of defect insertions affecting k_p^{app} decreasing as the time between pulses decreases. An expression for an averaged rate coefficient, k_p^{av}, is derived to capture the influence of head-to-head addition as well as the reactivity of the resulting "tail" radical. Simulations indicate that, while the repetition rate dependence is explained by the presence of head-to-head propagation in the system, the data set could not be used to estimate the individual rate coefficients. Indeed, the mean value from all of the experimental k_p^{app} values is considered as a reasonable estimation of k_p^{av}. Further experiments are being performed with vinyl pivalate to examine the generality of this behavior for the vinyl ester family of monomers.

References

1. O. F. Olaj, I. Bitai, F. Hinkelmann, *Makromol. Chem.* **1987**, *188*, 1689.
2. S. Beuermann, M. Buback, *Prog. Polym. Sci.* **2002**, *27*, 191.
3. R. A. Hutchinson, J. R. Richards, M.T. Aronson, *Macromolecules* **1994**, *27*, 4530.
4. T. Junkers, D. Voll, C. Barner-Kowollik, *e-Polymers* **2009**, *no 076*.
5. C. Plessis, G. Arzamendi, J. R. Leiza, H. Schoonbrood, D. Charmot, J. M. Asua, *Macromolecules* **2000**, *33*, 4.
6. J.M. Asua, S. Beuermann, M. Buback, P. Castignolles, B. Charleux, R. G. Gilbert, R.A. Hutchinson, J. R. Leiza, A. N. Nikitin, J. –P. Vairon, A. M. van Herk, *Macromol. Chem. Phys.* **2004**, *205*, 2151.
7. A. N. Nikitin, R. A. Hutchinson, M. Buback, P. Hesse, *Macromolecules* **2007**, *40*, 8631.
8. J. C. Randall, C. J. Ruff, M. Kelchtermans, B. H. Gregory, *Macromolecules* **1992**, *25*, 2624.
9. E. F. McCord, W. H. Shaw Jr., R. A. Hutchinson, *Macromolecules* **1997**, *30*, 246.
10. D. Britton, F. Heatley, P. A. Lovell, *Macromolecules* **1998**, *31*, 2828.
11. H. Kattner, M. Buback, *Macromol. Chem. Phys.* **2014**, *215*, 1180.
12. F. R. Mayo, C. Walling, F. M. Lewis, W.F. Hulse, *J. Am. Chem. Soc*. **1948**, *70*, 1523.
13. M. Dossi, K. Liang, R. A. Hutchinson, D. Moscatelli, *J. Phys. Chem. B* **2010**, *114*, 4213.
14. M.J. Wisotsky, A. E. Kober, *J. Appl. Polym. Sci.* **1972**, *16*, 849.
15. T. F. McKenna A. Villanueva, *J. Polym. Sci. Polym. Chem.* **1999**, *37*, 589.
16. D. E. Lonsdale, G. Johnston-Hall, A. Fawcett, C. A. Bell, C. N. Urbani, M. R. Whittaker, M. J. Monteiro, *J. Polym. Sci: Part A: Polym. Chem.* 2007, 45, 3620.

17. T. Kashawagi, A. Inaba, J. E. Brown, K. Hatada, T. Kitayama, E. Masuda, *Macromolecules* **1986**, *19*, 2160.

18. L. E. Manring, D. Y. Sogah, G. M. Cohen, *Macromolecules* **1989**, *22*, 4654.

19. D. R. Hensley, S. D. Goodrich, A. Y. Huckstep, H. J. Harwood, R. L. Rinaldi, *Macromolecules* **1995**, *28*, 1586.

20. P. E. Flory, F. S. Leutner, *J. Polym. Sci.* **1948**, *3*, 880.

21. A. N. Morin, C. Detrembleur, C. Jérôme, P. De Tullio, R. Poli, A. Debuigne, *Macromolecules* **2013**, *46*, 4303.

22. K. Hayashi, T. Ostu, *Makromol. Chem.* **1969**, *127*, 54.

23. R. A. Hutchinson, D. A. Paquet, J. H. McMinn, S. Beuermann, R. E. Fuller, E. I. Jackson, *Dechema Monographs* **1995**, *131*, 467.

24. K. Liang, M. Dossi, D. Moscatelli, R. A. Hutchinson, *Macromolecules* **2009**, *42*, 7736.

25. S. Beuermann, M. Buback, T. P. Davis, R. G. Gilbert, R. A. Hutchinson, O. F. Olaj, G. T. Russell, J. Schweer, A. M. van Herk, *Macromol. Chem. Phys.* **1997**, *198*, 1545.

26. O. Vogl, M. F. Qin, A. Zilkha, *Prog. Polym. Sci.* **1999**, *24*, 1481.

27. O. Vogl, *J. Polym. Sci. Polym. Chem. Ed.* **2000**, *38*, 4013.

28. R. E. Cais, J. M. Kometani, *Macromolecules* **1984**, *17*, 1932.

29. D. W. Ovenall, R. E. Uschold, *Macromolecules* **1991**, *24*, 3235.

30. J. Guiot, B. Ameduri, B. Boutevin, *Macromolecules* **2002,** *35*, 8694.

31. W. H. Starnes, Jr., *Prog. Polym. Sci.* **2002**, *27*, 2133.

32. W.H. Starnes, Jr., *Proc. Chem.* **2012**, *4*, 1.

33. M. Buback, M. Busch, R. A. Lämmel, *Macromol. Theory Simul.* **1996,** *5*, 845.

34. J. Sarnecki, J. Schweer, *Macromolecules* **1995**, *35*, 4080.

35. S. Beuermann, *Macromolecules* **2002**, *35*, 9300.

36. M. Buback, R. G. Gilbert, R. A. Hutchinson, B. Klumperman, F. –D. Kuchta, B. G. Manders, K. F. O'Driscoll, G. T. Russell, J. Schweer, *Macromol. Chem. Phys.* **1995**, *196*, 3267.

37. R. Siegmann, M. Drache, S. Beuermann, *Macromolecule*s **2013**, *46*, 9507.

38. E. Mavroudakis, D. Cuccato, M. Dossi, G. Comino, D. Moscatelli D. *J. Phys. Chem. A* **2014**, *118*, 238.

Chapter 4: A study of vinyl pivalate and vinyl benzoate propagation kinetics using the PLP-SEC Technique

Preface

In this chapter, the study of vinyl acetate (VAc) propagation kinetics using the PLP-SEC technique is extended to vinyl pivalate (VPi) and vinyl benzoate (VBz) in order to generalize the kinetic behavior of the vinyl ester monomer family. The work in this chapter is part of the manuscript recently accepted for publication by Macromolecular Chemistry and Physics. Appendix 4 includes the Nuclear Magnetic Resonance (NMR) analysis of VPi, with a detailed summary of the PLP experiments described in this chapter contained in Appendix 6.

Abstract

Radical propagation kinetics of the bulk homopolymerizations of vinyl pivalate (VPi) and vinyl benzoate (VBz) have been studied using pulsed-laser polymerization (PLP) combined with size exclusion chromatography (SEC). As part of the study, the Mark-Houwink parameters of poly(VPi) and poly(VBz) in tetrahydrofuran were determined using a triple detector SEC. The observed significant increase (by approximately 20 %) of the bulk VPi propagation rate coefficient (k_p) as pulse repetition rate is increased from 200 to 500 Hz is similar to that reported for vinyl acetate (VAc). Data collected in the temperature range of 25 to 85 °C for VPi is well fit by the Arrhenius relation $\ln(k_p/\mathrm{L\cdot mol^{-1}\cdot s^{-1}}) = 15.73 - 2093(T/\mathrm{K})$. The activation energy is similar to that found for vinyl acetate (VAc), with k_p values higher by ~50%. PLP studies in ethyl acetate and in heptane found no substantial solvent effect on VPi or VAc k_p values. Attempts to measure the propagation kinetics of VBz by PLP were not successful, suggesting that significant radical stabilization occurs for the system. Small-scale batch polymerization

experiments demonstrated relative polymerization rates of these vinyl ester monomers that were consistent with the PLP results.

4.1 Introduction

Production of existing and new polymer grades requires well-detailed understanding of polymerization kinetics and mechanisms, to aid process development and the optimization of product properties and operating conditions. The determination of individual kinetic coefficient such as the chain growth rate coefficient of radical polymerization, k_p, is required to enable modeling of these systems.

In 1987 Olaj and co-workers introduced a novel experimental method, Pulsed-Laser Polymerization coupled with Size Exclusion Chromatography (PLP-SEC), to directly estimate k_p, from the molar mass distribution (MMD) analysis of the resulting polymer.[1] This technique has been recommended as the method of choice for determination of k_p by the IUPAC sub-committee on Modeling of Polymerization Kinetics and Process for its reliability and ease of use.[2] Since its introduction, a series of benchmark papers have been published providing best-fit Arrhenius parameters to data collected in multiple labs over a broad temperature range for styrene, methacrylates and acrylates.[3-8] However, there is less data available for the vinyl ester family of monomers, other than vinyl acetate (VAc)[9-11] and an early study of vinyl deaconate.[12] Kubota et al. determined the k_p of vinyl pivalate (VPi, IUPAC: ethenyl 2,2-dimethylpropanoate) in heptane using Electron Paramagnetic Resonance (EPR)[13] to quantify the radical concentration, reporting estimated Arrhenius parameters of $A = 1.39\times10^7$ L·mol^{-1}·s^{-1} and E_a = 20.5 kJ·mol^{-1} for data collected between 9 and 93°C; the k_p value of 6750 L·mol^{-1}·s^{-1} at 50°C is similar to that reported for VAc (6600 - 8000 L·mol^{-1}·s^{-1} at 50 °C), as is the activation energy (20.9 – 21.8 kJ·mol^{-1}).[10-11] This finding is perhaps a bit surprising, as the k_p values of alkyl acrylates and methacrylates increase with increasing size of the ester group in bulk.[5] The difference may perhaps be

related to the use of heptane in the EPR study, as small but significant solvent effects on propagation kinetics are reported.[14]

A complicating factor in the propagation kinetics of vinyl esters is the occurrence of head-to-head additions, on the order of 1-2%, as first reported by Flory et al. for VAc.[15] Indeed, the increased stability of the CH_2 adduct resulting from the inverted addition leads to a reduced rate of reaction when conducting controlled radical polymerization (CRP) of VAc.[16] Recently, CRP of VPi has been studied by Islam et al.;[17] although some control was achieved, difficulty in narrowing the polymer dispersity was attributed to the lack of a conjugating substituent found in styrene and methacrylates, with the high reactivity of the VPi radicals hypothesized to increase the importance of termination and chain transfer reactions.[17] Similar factors were initially believed to be the main difficulty in the study of propagation studies of VAc by PLP-SEC.[18] Junkers et al. suggested that the influence of intramolecular chain transfer (backbiting) in the VAc system led to an increase in measured (apparent) k_p values by 33% as pulse repetition rate (prr) increased from 100 to 500 Hz. However, an EPR study by Kattner and Buback conclusively showed that VAc does not undergo backbiting, as proven by the lack of midchain radicals in the system.[19] Most recently, Monyatsi et al. conducted an experimental PLP study of VAc combined with simulation;[10] the same increase in k_p with prr was found (as seen by Junkers) with an alternative explanation for the behavior proposed, the effect of head-to-head addition.

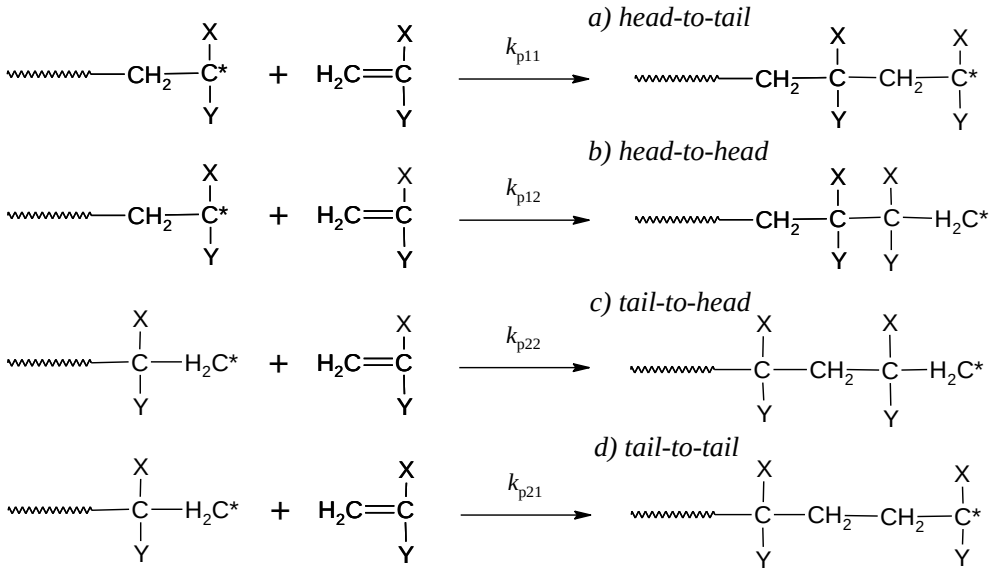

Figure 4.1: Possible routes for monomer addition during radical polymerization of vinyl esters[10]

Head-to-head addition is one of the four possible routes for monomer addition during polymerization, as illustrated in Figure 4.1. Equation (4.1) has been derived for the average chain growth propagation rate coefficient, k_P^{av}, using the individual propagation rate coefficient for all the possible routes for monomer addition shown, with subscripts 1 and 2 referring to tail and head radicals, respectively.[10] Depending upon the value of k_{p21} (tail-to-tail addition), the occurrence of 1-2% of head-to-head additions (k_{p12}/k_{p11} = 0.01-0.02) is sufficient to cause the PLP-determined value to show a dependence of prr not seen for most monomers, such as methacrylates, which only propagate by head-to-tail addition.

$$k_p^{av} = k_{p11} - \frac{k_{p11} - k_{p22} - 2k_{p21}}{1 + \frac{k_{p21}}{k_{p12}}} \qquad (4.1)$$

There is some evidence that head-to-head addition also influences the propagation kinetics of other vinyl esters. In the late 1960s, Otsu and coworkers investigated and found approximately 1-2% head-to-head addition occurs during polymerization of many vinyl ester monomers including VAc, vinyl

valerate, vinyl butyrate, and vinyl benzoate.[20] Thus, it is possible that the study of chain growth kinetics of these monomers by the PLP-SEC technique will also be influenced. In this work, we present a comprehensive study of free radical polymerization kinetics of VPi using PLP-SEC, investigating the effect of pulse repetition rate on k_p between 25-85 °C. As part of the study, the Mark-Houwink (M-H) parameters and the polymer d*n*/d*c* value required for SEC analysis for polyvinyl pivalate (PVPi) and polyvinyl benzoate (PVBz) were also determined.

4.2 Experimental Section

Vinyl pivalate (VPi, Aldrich 99%), vinyl benzoate (VBz, Aldrich ≥99%), vinyl acetate (VAc, Aldrich, 99+%), benzoin (Aldrich ≥99.5%), methanol (MeoH, reagent grade, ACP Chemicals Inc.), acetone (reagent grade, ACP Chemicals Inc.), heptane (Aldrich 99%) and ethyl acetate (EAc, Caledon Labs) was used as received. The experimental set up and procedure is similar to previous PLP studies.[9–11,21] Low monomer conversion (<2%) of bulk VPi was generated using a pulsed laser setup consisting of a Xantos XS-500 laser operating at a wavelength of 351nm, 3-15 ns pulse duration and pulse energy of 3-8 mJ/pulse. Bulk monomer VPi solution with 5 mmol·L^{-1} benzoin photo-initiator was prepared, and approximately 3 mL of the monomer mixture was added to a quartz cuvette and allowed to reach the desired temperature (± 0.5°C) before being exposed to the laser light. The experiments were run at a constant pulse repetition rate (prr) monitored between 100 and 500 Hz in a temperature range of 25 to 85 °C. The residual VPi content was reduced from the samples under an air stream and the resulting mixture was precipitated in methanol. The heterogeneous mixture was allowed to settle overnight in a freezer, the liquid was decanted from the mixture and the remaining polymer precipitate dried under vacuum. The same procedure was followed for bulk VBz experiments (with 1, 5 and 20 mmol·L^{-1} of

benzoin photoinitiator, prr between 2 and 500 Hz, and temperature between 25 and 90 °C), and for VAc and VPi experiments conducted in the presence of 50 vol% heptane or ethyl acetate solvent.

The molar mass distribution (MMDs) of the samples produced were analyzed using an SEC system consisting of a Water 2960 separation module, an auto injector, and two detectors: a Waters 410 differential refractometer (DRI) and a Wyatt Dawn EOS 690 nm Laser Photometer (LS). The system used distilled THF as an eluent, programmed at a flow rate of 0.3 mL·min^{-1} through four Styragel® THF columns (HR 0.5, 1, 3, 4) maintained at 35 °C. The DRI detector was calibrated using narrow polystyrene standards with molecular weight ranging from 370–8.6×10^5 Da. The MMDs of the PLP samples were estimated using the principle of universal calibration, with the Mark-Houwink (M-H) parameters summarized in Table 4.1; the poly(VPi) and poly(VBz) values were determined as part of this study. Moreover, the density of VPi monomer was also determined between 25 and 70 °C using a Paar DMA 48 Density Meter, with linear fit parameters also summarized in Table 4.1 and linear fit plots shown in the appendix.

The poly(VPi) MMDs were smoothed and differentiated using OriginLab software, with k_p estimated using the position of the 1st inflection point (M_o) taken as the maximum from the first-derivative plot, monomer density (ρ_{mon}) calculated at reaction temperature, monomer volume fraction (ϕ_{mon}) in the case of solution experiments, and the time between pulses (t_o) as illustrated in equation (4.2).[1]

$$k_p = \frac{M_o}{1000\phi_{mon}p_{mon}t_o} \qquad (4.2)$$

In order to check the validity and accuracy of DRI results, LS detector results for some samples were analyzed using the d*n*/*dc* value of poly(VPi) (Table 5.1), also measured in this work. Several polymer samples produced by PLP at 100-500Hz prr were used to prepare 4-6 polymer solutions with

concentrations between 0.2-15mg·mL^{-1}; these samples were injected sequentially to a Wyatt Optilab DSP refractometer at 690 nm calibrated using sodium chloride to create a curve with slope d*n*/d*c*. The graphs and individual estimates (between 0.051 and 0.058 mL·g^{-1}) are shown in Appendix 6, with the average value of 0.054 mL·g^{-1} used to process the poly(VPi) MMDs measured by light scattering.

The M-H parameters of poly(VPi) (samples also prepared using PLP at 100-500 Hz prr) were estimated using a triple detector Viscotek SEC described by Nerkar et al.[22] The parameters were determined from processing the intrinsic viscosity and light scattering output with the OmniSEC software using the average d*n*/d*c* value of poly(VPi) reported earlier. The M-H plots obtained for the four samples are included in the appendix, with Table 4.1 summarizing the estimated M-H parameters. While there is some scatter in the individual *K* and *a* values due to their high correlation, the calculated values of intrinsic viscosity for polymer with $M=10^5$ Da are in reasonable agreement (0.406–0.435 dL·g^{-1}). Figure 4.2 illustrates the ability of the global fit values, $K=1.75\times10^{-4}$ dL·g^{-1}and $a=0.676$, to represent the individual experiments. M-H parameters for poly(VAc) (prepared using PLP at a prr of 100 Hz) were also measured as part of this study, to check the accuracy of our setup. As summarized in Table 4.1, the parameters for poly(VAc) in THF are close to previous literature, thus validating the methodologies used to estimate the M-H parameters for poly(VPi). It is also interesting to note that the M-H plot for poly(VAc) is parallel (at slightly higher intrinsic viscosity) to that of poly(VPi) (Figure 4.2),.

The same procedures for determining d*n*/d*c* and M-H parameters were used for poly(VBz), with the graphs shown in Appendix 6, and the average d*n*/d*c* value and the M-H parameters reported in Table 4.1 and plotted in Figure 4.2.

Table 4.1: Parameters used to interpret PLP-SEC results for determine of propagation kinetic parameters.

				Mark–Houwink parameters			
Monomer	ρ (g·mL^{-1})	*dn/dc* (mL·g^{-1})	Polymer	*K* (dL·g^{-1}) × 10^{-4}	*a*	[η]=*K*(*M*)^{a**}	Ref.
Styrene	-	0.185		1.14	0.716	0.433	9
VAc	0.9584-0.00133T/°C[18]	0.058	Set 1	1.56	0.708	0.541	9
			Set 2	2.24	0.674	0.525	9
			100Hz	2.72	0.661	0.550	*
VPi	0.8933–0.00111T/°C*	0.054	100Hz	2.45	0.645	0.412	*
			250Hz (i)	1.16	0.715	0.435	*
			250Hz (ii)	1.67	0.682	0.431	*
			500Hz	1.99	0.662	0.406	*
			Global	1.75	0.676	0.421	*
VBz	1.0821-0.0007T/°C[23]	0.1527		1.53	0.648	0.265	*

*parameters estimated in this work, **calculated for equivalent MW of 10^5 Da

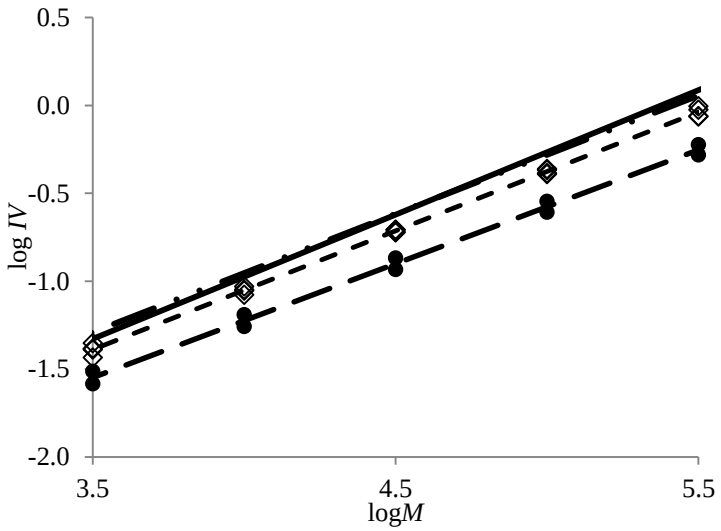

Figure 4.2: log-log plot of intrinsic viscosity vs. *M* for poly(VPi) (◊, - - -) and poly(VBz) (●, ———). Points are exported data, the lines drawn using best-fit Mark-Houwink parameters as reported in Table 4.1. Reference lines for poly(VAc) (**—**, — · · —) plotted using literature M-H parameters (see Table 4.1).

4.3 Results and Discussion

The propagation kinetics of bulk VPi was studied by PLP-SEC between 25 and 85 °C using benzoin photoinitiator with prr between 100 and 500 Hz, with the complete set of experimental data obtained

tabulated in the Appendix 6**.** Representative MMDs and first-derivative plots are shown in Figure 4.3. It can be observed that the MMDs and the corresponding inflection points (as seen on the first-derivative curves) shift to the right as the prr decreases, as expected. Both first and second inflection points are clearly seen for most cases, with the second inflection point at approximately twice the M_o value, as expected.[9,18] As illustrated in Figure 4.3, the poly(VPi) MMDs become more structured as the prr increases. At 100 Hz, the MMD is broader and the 2nd inflection point cannot be identified at 50 °C and higher.

The resulting values of the propagation coefficient, k_p, were determined from equation (4.2) using the measured M_o values. At 50 °C, k_p increased from 9400 to 11300 $L \cdot mol^{-1} \cdot s^{-1}$ as the prr increased from 200 to 500 Hz. This trend, seen at all temperatures, is compared to our previous results for VAc[10] in Figure 4.4. As shown in Figure 4.5, the PLP-generated MMDs of both polymers have a similar shape with clear 1st and 2nd inflection points, with the poly (VPi) inflection points at a higher M_o for the same prr. Two important points can be noted. First, the absolute k_p values determined by PLP-SEC are higher for VPi than VAc, a result to be discussed later. Second, the ~20% increase in apparent k_p values measured with increasing prr for VPi is of similar magnitude as the increase reported for VAc.[10–11]

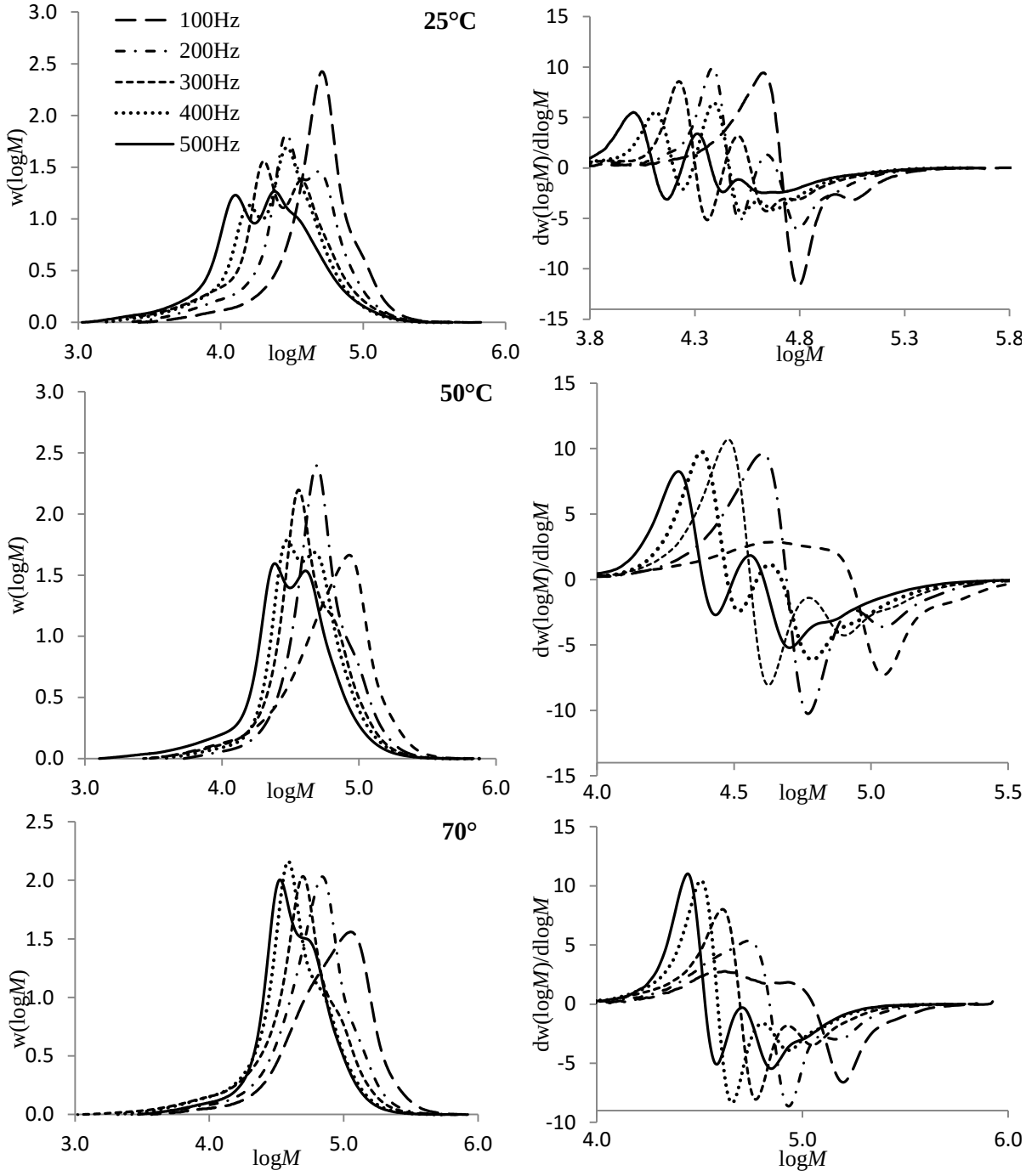

Figure 4.3: MMDs (left) and corresponding first derivative plots (right) for poly(VPi) produced by PLP at 100-500 Hz pulse repetition rate at 25 (top), 50 (middle), and 70 (bottom) °C.

As done for the VAc study, the systematic variation in k_p was further explored by constructing separate Arrhenius fits for the VPi results obtained at each prr, as shown in Figure 4.6 with the corresponding parameters summarized in Table 4.2. There was insufficient data to construct a plot for the prr of 100 Hz, due to the lack of reliable data (no 2nd inflection points) for T ≥50 °C. As well as the increasing k_p

values with prr, the activation energy (E_a) for VPi also increased slightly, from 16.0 to 18.9 kJ·mol^{-1} between 200 and 500 Hz.

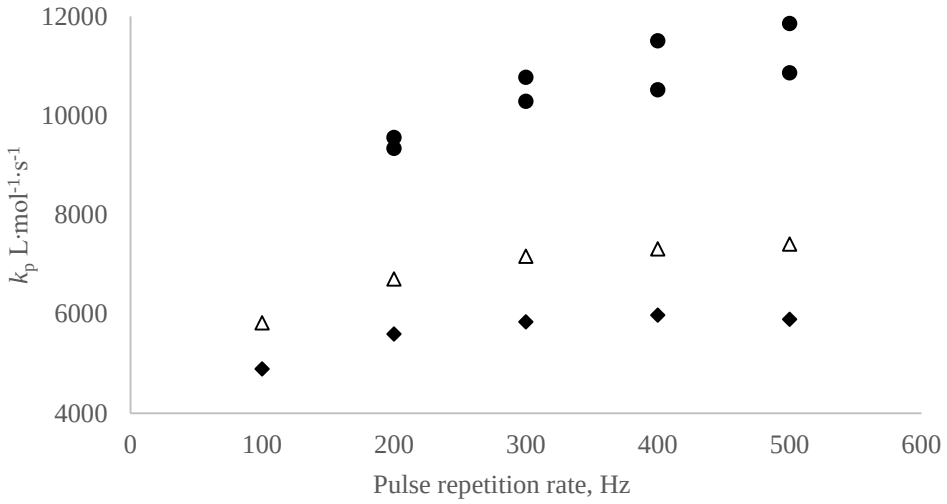

Figure 4.4: k_p vs. pulse repetition rate for VPi PLP-SEC experiments at 25 (♦) and 50 °C (●) and VAc PLP-SEC experiments at 50 °C (Δ)[10] with benzoin photoinitiator.

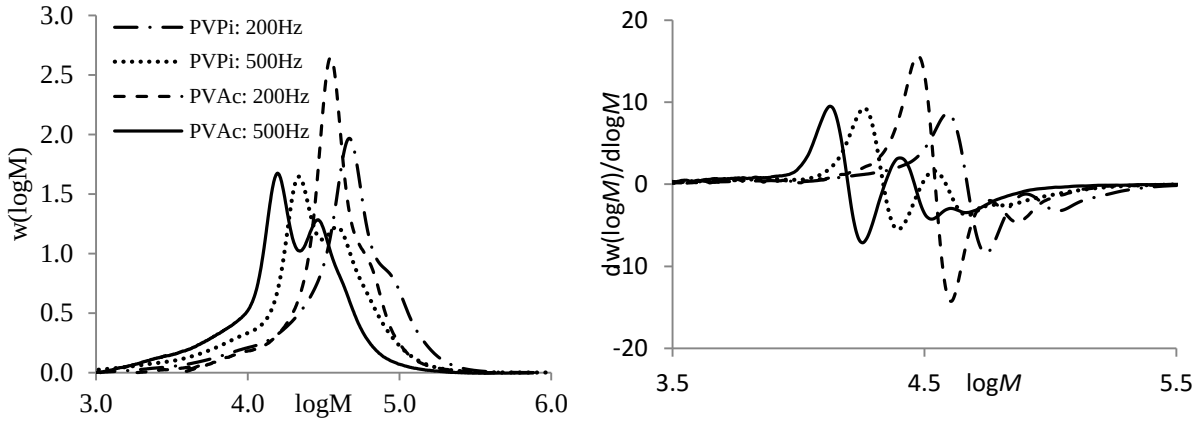

Figure 4.5: MMD and corresponding first derivative plots for poly(VAc) and poly(VPi) produced by PLP at 200 and 500Hz pulse repetition rate at 50 °C.

The trends observed for VPi – a significant increase in PLP-determined k_p values with prr, as well as a corresponding increase in observed activation energy – were also found in our recent study of VAc propagation kinetics.[10] In that paper (see Chapter 3 and Appendix 1), we proposed head-to-head

addition as a possible explanation for the findings, and accompanied the experimental work with a detailed simulation study, with key points summarized below:

- In the absence of head-to-head addition (k_{p12}=k_{p21}=k_{p22}=0), simulations indicated that a small increase in estimated VAc k_p with prr would occur from analysis of the resulting MMDs. This increase, caused by peak broadening and approach to the high termination limit, however was not large enough to explain the 20-25% increase found experimentally.
- The ratio of head-to-head to head-to-tail addition (k_{p12}/k_{p11}, see Figure 4.1 and eq. 4.1) must be set to a value of 0.01-0.02, in order to match the level of head-to-head defects reported in vinyl ester polymers.[15,20]
- The apparent dependence of k_p on prr could be matched only if the rates of addition of monomer to the "tail" radical (k_{p21} and k_{p22}) was reduced by a factor of 50 to 100 compared to the rate of head-to-tail addition. With these parameter values a significant fraction of the radicals (~30%) were predicted to be in the inverted "tail" state. However, this prediction is in conflict with the EPR study of VAc by Kattner and Buback,[19] in which only the "head" radical structure was observed.
- The simulations for VAc were unable to replicate the experimentally-observed increase in activation energy. They did indicate, however, that the PLP-measured k_p values provided a better measure of $\boldsymbol{k_P^{av}}$ than of k_{p11} (see Eq. 4.1).

As the simulation study for VAc did not lead to conclusive results (while head-to-head addition must occur, it is not certain what impact the mechanism has on the PLP-measured k_p values), it has not been repeated for VPi. In addition, although all of the vinyl esters (including vinyl butyrate, vinyl valerate, vinyl caproate and vinyl benzoate) studied by Hayashi and Otsu[20] exhibited the same level of head-to-

head addition as VAc, no literature study of the mechanism specific to VPi could be found. Thus, while head-to-head addition likely occurs, the possible influence of the reaction on the structure of PLP-determined MMDs remains a topic for future study.

Table 4.2: Arrhenius parameters obtained from linear fitting of ln (k_p) values estimated from PLP-SEC experiments for bulk VPi conducted between 25 and 85 ºC. Separate fits were conducted at each pulse repetition rate.

Repetition rate (Hz)	ln (A)	E_a/R (K)	E_a (kJmol^{-1})	k_p (at 50 °C)
200	15.11 ± 0.27	1922 ± 87	16.0	9531
300	15.53 ± 0.23	2034 ± 74	16.9	10257
400	15.91 ± 0.23	2142 ± 74	17.8	10738
500	16.37 ± 0.36	2274 ± 115	18.9	11305
200-500	15.73 ± 0.25	2093 ± 81	17.4	10437
EPR technique[13]	16.45	2466	20.5	6748
50-100[24]	16.29	2321	19.3	9031

Accordingly, a combined fit of the complete data set (200-500Hz) has been performed and compared to the corresponding VAc fit[10] in Figure 4.6. The estimated activation energy for VPi (17.4±0.7 kJ·mol^{-1}) is slightly lower than that for VAc (20.9±0.9 kJ·mol^{-1}).[10] A similar but smaller decrease in activation energy has been found with increasing ester size in the methacrylate family.[5] However, the effect of the *tert*-butyl group is not clear from existing literature; while an early PLP-SEC study reported a value of 27.7 kJ·mol^{-1}[25] for *t*-butyl methacrylate (*t*BMA), a later more systematic examination showed no difference in activation energy (22.1 kJ·mol^{-1})[26] compared to *n*-butyl methacrylate (*n*BMA) (22.9 kJ·mol^{-1})[5] or methyl methacrylate (MMA) (22.4 kJ·mol^{-1}).[4] The 50% increase found between the 50 °C k_p values for bulk VPi vs. VAc (10400 vs. 6600 L·mol^{-1}·s^{-1}) is also higher than that for the corresponding methacrylate analogs: 836[25] and 642[26] for *t*BMA, 756[5] for *n*BMA and 648[4] for MMA (all values in units of L·mol^{-1}·s^{-1}). Finally, it is important to note that these PLP-SEC values for bulk VPi k_p are more than 50% higher than those reported for VPi in heptane measured by the EPR

technique.[13] However, the results are in reasonable agreement with recent values determined at the University of Potsdam using PLP-SEC at 50 and 100 Hz (Table 4.2).[24]

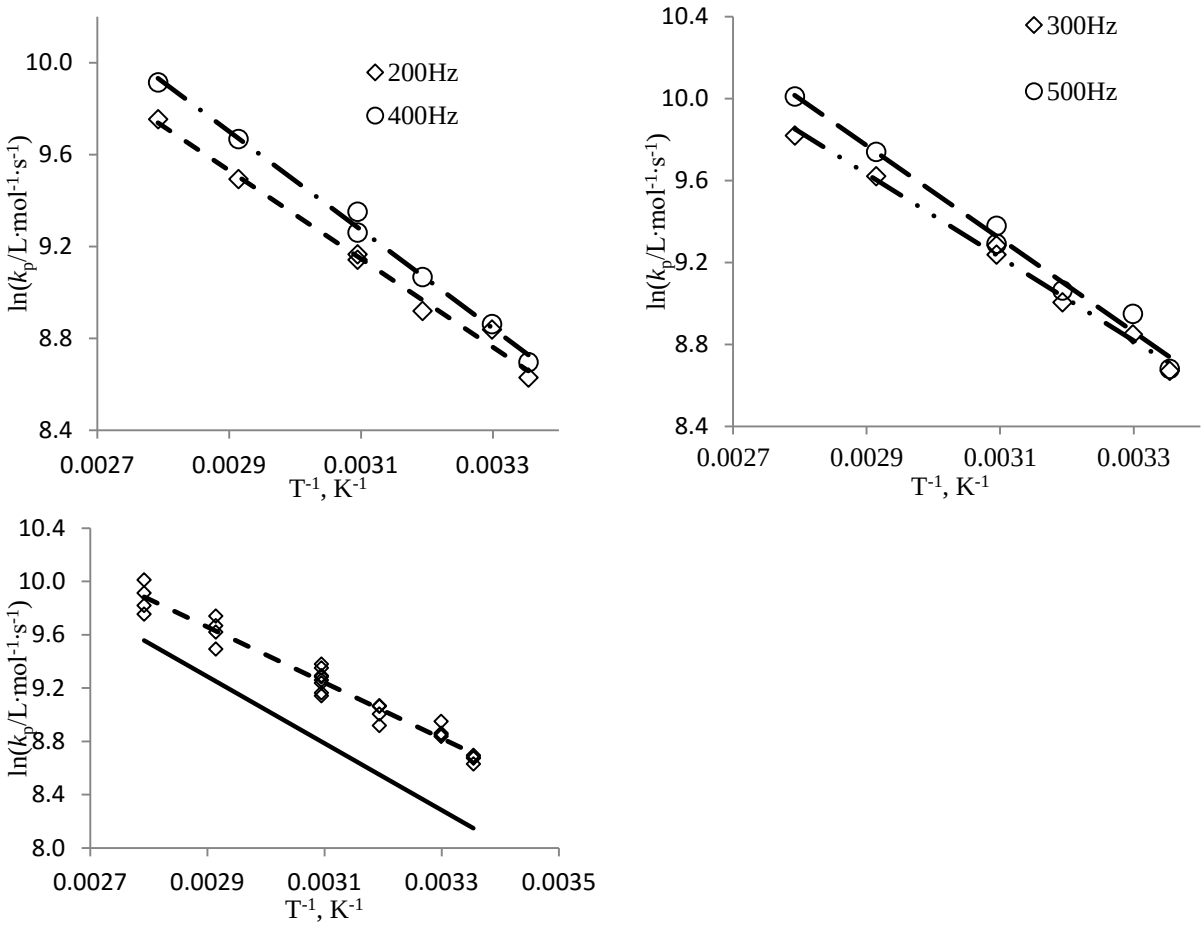

Figure 4.6: Arrhenius plots of VPi apparent propagation rate coefficients for experiments conducted at 200 and 400 Hz (top left), and 300 and 500 Hz (top right). Global fit Arrhenius plot including all data (◊, – – –) in comparison with VAc (—)[10] (bottom). Best-fit Arrhenius parameters are summarized in Table 4.2.

To further investigate the discrepancy with the values determined by EPR, PLP-SEC experiments of both VAc and VPi were conducted in 50 vol% heptane and ethyl acetate (EAc) solvents at 50 °C. Heptane was chosen to match the conditions of the EPR study, while the more polar EAc has been chosen as a solvent for ongoing small-scale batch experiments, as poly(VAc) was observed to precipitate out of heptane at higher conversions. With full experimental details provided in Appendix 6, no major solvent effects on k_p were found. Within the limited data set, the VPi k_p values in solution

were within 20% of that measured in bulk, with values higher in heptane and lower in EAc. Differences in VAc k_p values were also checked, with the value measured for EAc within 10%, and the value in heptane 15 % higher than for bulk VAc. Based upon these k_p determinations by PLP-SEC in solution, we conclude that the k_p values determined by EPR are not of sufficient reliability; although care was taken in that study, the technique is prone to systematic errors caused by calibration.[27-29]

PLP-SEC was also used in an attempt to study the propagation kinetics of VBz, another member of the vinyl ester monomer family. Surprisingly, no PLP structure was observed over a broad range of conditions examined, including significant variations in prr (2 to 500 Hz) and photoinitiator concentrations at 50 and 90 °C (see appendix 6). The low reactivity of VBz has been reported previously in the literature,[30–32] with the cause of the reduced rate still not entirely resolved. Ham and Ringwald[30] first proposed that VBz monomer could copolymerize with itself through radical attack of the aromatic ring to form a more stabilized radical structure. This reaction would lead to a branched structure, discredited by further studies which indicated that addition to the benzene ring does not occur.[33–34] Thus, Santee et al.[34] proposed that the propagating radical can reversibly complex with the aromatic ring, with the resulting adduct radical able to terminate with other radicals but not propagate. However, there is still arguments in literature about whether the aromatic ring is activated through an intramolecular or an intermolecular complex.[34-35] Although the exact mechanism is uncertain, the reduced reactivity of VBz is consistent with results obtained from an ongoing study using small-scale batch experiments.

4.4 Conclusions

The PLP technique has been applied to systematically examine the radical propagation homopolymerization kinetics of VPi and VBz in the temperature range of 25–90 °C and the solution

polymerization of VPi and VAc at 50 °C. The radical propagation rate coefficient, k_p, measured for bulk VPi increases significantly with the laser pulse repetition rate, in a similar trend as seen for VAc, with higher k_p value for VPi than VAc at the same prr. This observation might result from the effect of head-to-head addition that occurs during vinyl ester polymerizations. The k_p values obtained for solution (both in heptane and EAc) polymerization of VPi and VAc were within 20% of that for bulk, with the limited data making it not possible to determine if there was a significant shift. However, it is clear that the difference in VPi k_p between the current PLP study and the values previously determined by EPR[13] cannot be attributed to a solvent effect.

Although the propagation kinetics of VBz could not be determined due to lack of PLP structure in the resulting MMDs, small-scale batch solution polymerizations described in the next chapter confirm a much lower rate of reaction compared to VAc and VPi and demonstrate a consistent trend in rates of conversion with the k_p values determined by PLP.

References

1. O. F. Olaj, I. Bitai, F. Hinkelmann, *Makromol. Chem.* **1987**, *188*, 1689.
2. S. Beuermann, M. Buback, *Prog. Polym. Sci.* **2002**, *27*, 191.
3. M. Buback, R. G. Gilbert, R. A. Hutchinson, B. Klumperman, F.-D. Kuchta, B. G. Manders, K. F. O'Driscoll, G. T. Russell, J. Schweer, *Macromol. Chem. Phys.* **1995**, *196*, 3267.
4. S. Beuermann, M. Buback, T. P. Davis, R. G. Gilbert, R. A. Hutchinson, O. F. Olaj, G. T. Russell, J. Schweer, A. M. van Herk, *Macromol. Chem. Phys.* **1997**, *198*, 1545.
5. S. Beuermann, M. Buback, T. P. Davis, R. G. Gilbert, R. A. Hutchinson, A. Kajiwara, B. Klumperman, G. T. Russell, *Macromol. Chem. Phys.* **2000**, *201*, 1355.
6. S. Beuermann, M. Buback, T. P. Davis, N. García, R. G. Gilbert, R. A. Hutchinson, A. Kajiwara, M. Kamachi, I. Lacík, G. T. Russell, *Macromol. Chem. Phys.* **2003**, *204*, 1338.
7. J. M. Asua, S. Beuermann, M. Buback, P. Castignolles, B. Charleux, R. G. Gilbert, R. A. Hutchinson, J. R. Leiza, A. N. Nikitin, J. P. Vairon, A. M. Van Herk, *Macromol. Chem. Phys.* **2004**, *205*, 2151.
8. C. Barner-Kowollik, S. Beuermann, M. Buback, P. Castignolles, B. Charleux, M. L. Coote, R. A Hutchinson, T. Junkers, I. Lacik, G. T. Russell, M. Stach, A. M. van Herk, *Polym. Chem.* **2014**, *5*, 204.
9. R. A. Hutchinson, D. A. Paquet, J. H. McMinn, S. Beuermann, R. E. Fuller, C. Jackson, *Dechema Monogr.* **1995**, *131*, 467.
10. O. Monyatsi, A. N. Nikitin, R. A. Hutchinson, *Macromolecules* **2014**, *47*, 8145.
11. T. Junkers, D. Voll, C. Barner-Kowollik, *e-Polymers.* **2009**, *076*, 1.

12. R. Balic, R. G. Gilbert, M. D. Zammit, T. P. Davis, C. M. Miller, *Macromolecules* **1997**, *30*, 3775.
13. N. Kubota, A. Kajiwara, P. B. Zetterlund, M. Kamachi, J. Treurnicht, M. P. Tonge, R. G. Gilbert, B. Yamada, *Macromol. Chem. Phys.* **2007**, *208*, 2403.
14. S. Beuermann, *Macromol. Rapid Commun.* **2009**, *30*, 1066.
15. P. J. Flory, F. S. Leutner, *J. Polym. Sci.* **1948**, *3*, 880.
16. A. N. Morin, C. Detrembleur, C. Jérôme, P. De Tullio, R. Poli, A. Debuigne, *Macromolecules* **2013**, *46*, 4303.
17. M. N. Islam, Y. Haldorai, V. H. Nguyen, J.-J. Shim, *Eur. Polym. J.* **2014**, *61*, 93.
18. R.A. Hutchinson, J. R. Richards, M. T. Aronson, *Macromolecules* **1994**, *27*, 4530.
19. H. Kattner, M. Buback, *Macromol. Chem. Phys.* **2014**, *215*, 1180.
20. K. Hayashi, T. Ostu, *Makromol. Chem.* **1969**, *127*, 54.
21. M. Dossi, K. Liang, R. A. Hutchinson, D. Moscatelli, *J. Polym. Sci. Part B Polym. Chem.* **2010**, *114*, 4213.
22. M. Nerkar, J. A. Ramsay, B. A. Ramsay, M. Kontopoulou, R. A. Hutchinson, *J. Polym. Environ.* **2013**, *21*, 24.
23. G. M. Burnett, W. W. Wright, *Trans. Faraday Soc.* **1953**, *49*, 1108.
24. S. Beuermann correspondence. Data from J. Roberg, BSc. Thesis, University of Potsdam (Potsdam), **2010**.
25. P. Pascal, M. A. Winnik, D. H. Napper, R. G. Gilbert, *Makromol. Chem. Rapid Commun*. **1993**, *14*, 213.
26. G. E. Roberts, T. P. Davis, J. P. A. Heuts, G. E. Ball, *Macromolecules* **2002**, *35*, 9954.

27. M. Kamachi, A. Kajiwara, *Macromol. Chem. Phys.* **2000**, *201*, 2160.

28. M. Kamachi, *J. Polym. Sci. Part A: Polym. Chem.* **2002**, *40*, 269.

29. T. Noda, Y. Morishima, M. Kamachi, A. Kajiwara, *Macromolecules* **1998**, *31*, 9078.

30. G. E. Ham, E. L. Ringwald, *J. Poly. Sci.* **1951**, *8*, 91.

31. N. Beredjick, *J. Appl. Poly. Sci.* **1965**, *9*, 439.

32. M. Kamachi, J. Satoh, D. J. Liaw, S.-I. Nozakura, *Macromolecules* **1977**, *10*, 501.

33. G. A. Mortimer, L. C. Arnold, *J. Am. Chem. Soc.* **1962**, *84*, 4987.

34. G. F. Santee, R. H. Marchessault, H. G. Clark, J. J. Kearny, V. Stannett, *Makromol. Chem.* **1964**, *73*, 177.

35. M. Kamachi, J. Satoh, D. J. Liaw, *Poly. Bull.* **1979**, *1*, 581.

Chapter 5: Small-scale batch polymerization of vinyl ester monomers: Experimental and Modeling

Preface

As presented in the previous chapters, VPi has a higher k_p value compared to VAc at the same operating conditions. While the technique did not yield k_p for VBz, it suggest that the monomer polymerizes at a slow rate. This chapter investigates polymerization kinetic behavior of these vinyl ester monomers using small-scale batch polymerization both in bulk and solution. A portion of the work in this chapter is part of the manuscript recently accepted for publication by Macromolecular Chemistry and Physics. As the relevant literature has been elaborated in the previous chapters, the experimental procedure and results will be explained directly. In addition, this chapter also examines modeling of the polymerization kinetics of VAc and VPi using Predici software.

5.1 Experimental Section

5.1.1 Materials

Table 5.1: Chemicals used to conduct experiments in this chapter.

Chemical	Purity (%)
Vinyl acetate (Aldrich, VAc)	99
Vinyl pivalate (Aldrich, VPi)	99
Vinyl benzoate (Aldrich, VBz)	≥ 99
2,2-azobis(2-methylbutane-nitrile)(DuPont, V67)	
Chloroform-d ($CDCl_3$)	
Hydroquinone (Aldrich,)	
Ethyl acetate (Caledon Labs, EAc)	
Methanol (reagent grade, MeOH)	

5.1.2 Procedure

The experimental procedure is similar to previous studies in the literature.[1-2] Monomer-initiator (V-67) stock solution was prepared in a glass vial (with the desired wt. % of V67; i.e. 0.3 – 5 wt. %) and 5 mL of the solution mixture was transferred into the Schlenk tube. A magnetic stir bar was also added to the tube, which was capped with a septa cap. The oil bath was heated to 60 °C and the mixture (in

the tube) was then purged with nitrogen gas for 10 minutes to remove oxygen gas. Once the oil bath reached 60 °C (after 15 minutes), the tube was immersed in the bath with the stirrer turned on to start the reaction (the time at the beginning of the reaction was noted). The reaction was allowed to run until the desired reaction time at which point the tube was immersed in the ice bath to cool the reaction mixture and 2 mg of hydroquinone was added to the mixture. The reaction mixture was transferred into a glass vial and excess monomer was evaporated under air dryer at room temperature (approximately 2 hours). Once the monomer has mostly evaporated, MeOH was introduced into the vial to precipitate the polymer. The heterogeneous mixture was allowed to settle overnight in a freezer and the liquid was decanted. This step was repeated three times to reprecipitate the polymer. The precipitated polymer was dried under the vacuum overnight. The same procedure was followed for solution polymerization (using EAc and $CDCI_3$ solvent) with 50 and 70 % by volume of the solvent respectively. In addition, a few experiments were done in the Nuclear Magnetic Resonance (NMR) instrument with $CDCl_3$ at 60 °C using the same experimental procedure described by Preusser and Hutchinson.[3]

Table 5.2: Experimental conditions for small-scale polymerization conducted at 60°C using V-67 initiator.

	Bulk	Solution (EAc)	Solution ($CDCI_3$)
Initiator wt. %	1, 5	1, 2	0.3, 1
Monomer wt. % (volume)	100	50	30
Reaction time (minutes)	5 - 15	15 - 72	15 - 60

5.1.3 SEC conditions system

The molar mass distributions (MMDs) of the samples produced by small-scale polymerization were analyzed using a triple detector (TD) SEC set up as described by Nerkar et al.[4] The system consists of a 270max separation module, auto injector, two porous Polyanalytik columns in series and three

detectors: differential refractive index (DRI), intrinsic viscosity (IV) and multi-angle light scattering (MALS). The system operates at 40 °C, using distilled tetrahydrofuran (THF) as an eluent programmed at 1mL·min^{-1}. The MMDs of the samples were estimated from processing the DRI, IV and MALS output with the OmniSEC software using the d*n*/d*c* value of these polyvinyl esters (for light scattering) reported in Table 5.3.

Table 5.3: The d*n*/d*c* values for polyvinyl esters used to process MMDs measured by light scattering.

Polyvinyl ester	d*n*/d*c* (mL·g^{-1})
Polyvinyl acetate	0.058
Polyvinyl pivalate	0.054
Polyvinyl benzoate	0.1527

5.1.4 Results and Discussion

5.1.4.1 Data Analysis: Monomer Conversion Profiles

The monomer conversion (X_p) was estimated gravimetrically with the conversion profiles shown in Figure 5.1 constructed from the series of samples run at identical condition to different times. Figure 5.1(a) shows the monomer profiles for VAc experiments (in bulk) conducted at varying initiator concentrations. As expected the rate of monomer conversion is faster for 1 wt. % initiator concentration compared to 0.5 wt. %. It can also be seen that the results are reproducible for the repeated experiments conducted at 10 minutes reaction time. The rate of monomer conversion for the three vinyl ester monomers (i.e. VAc, VPi and VBz) was also examined; as seen from the monomer profiles for 1 wt. % initiator in Figure 5.1(b), VPi is faster followed by VAc and finally VBz (with relatively low conversion). There is less data obtained in bulk, as experiments were not conducted for more than 15 minutes due to the increased viscosity of the reacting solution.

The effect of varying initiator concentration on the rate of monomer conversion was also investigated for solution polymerization. As illustrated in Figure 5.2(a) for the VAc experiments conducted in

chloroform-d, the expected increase in conversion rate with increasing initiator concentration is also observed. The same relative conversion rate for VAc, VPi, VBz experiments in solution (ethyl acetate) were found as observed for bulk as shown in Figure 5.2 (b). In addition, the slight upward curvature of the VPi conversion profiles may perhaps indicates an increased rate due to gel effect, despite the presence of the solvent.

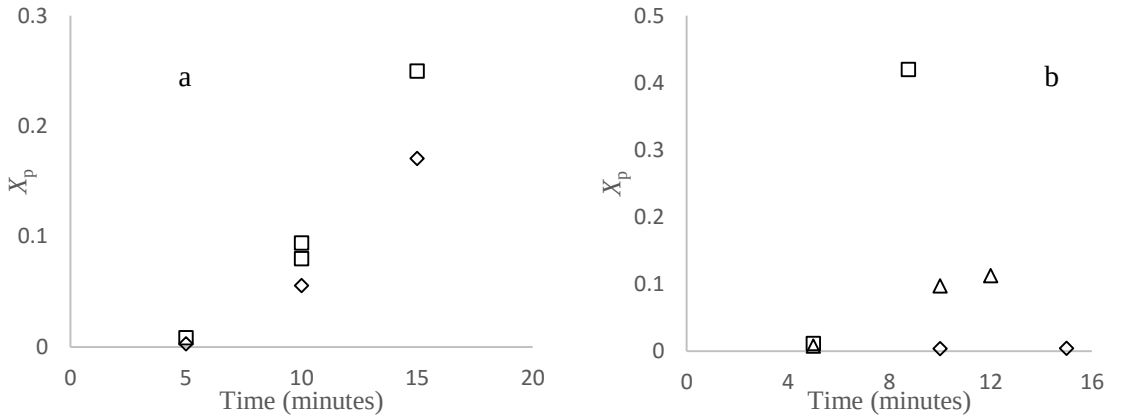

Figure 5.1: Monomer conversion profile obtained by small-scale batch polymerization (bulk) at 60°C: for VAc with 0.5 (◊) and 1.0 (□) wt. % V-67 initiator (left) and for 1.0 wt. % V-67 initiator for VAc (Δ), VPi (□) and VBz (◊) (right).

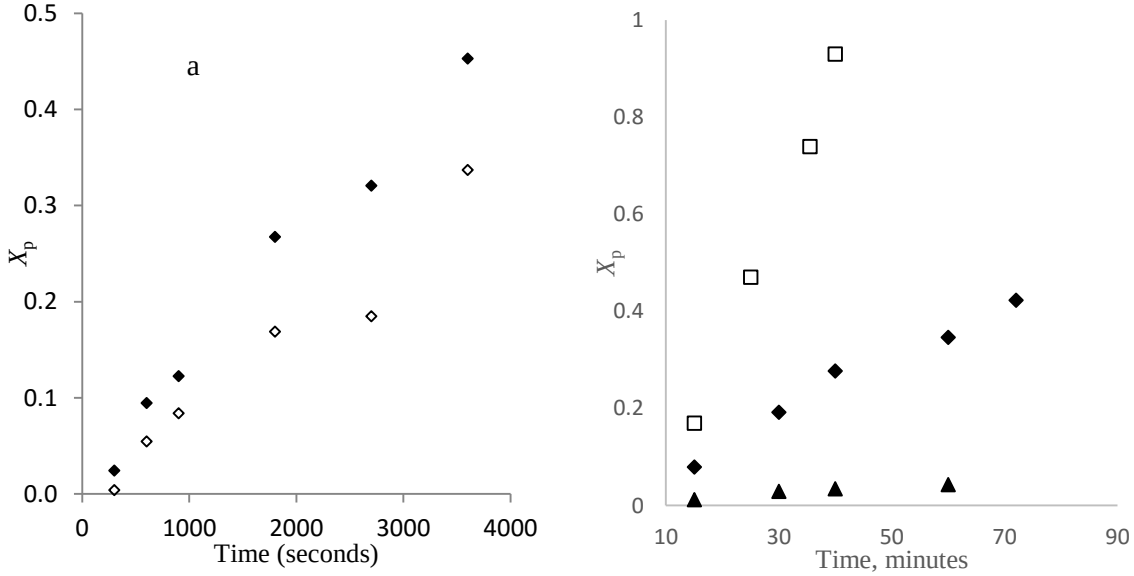

Figure 5.2: Monomer conversion profile obtained by small-scale batch polymerization (solution) at 60 °C: for VAc (in $CDCl_3$) with 0.3 (◊) and 1.0 (♦) wt. % V-67 initiator (left) and 1.0 wt. % V-67 initiator for VPi (□), VAc (♦) and VBz (▲) in EAc (right).

5.1.4.2 SEC Results: Elution volume and MMDs

The polymer samples prepared via small-scale batch polymerizations were analyzed using the triple detector SEC to determine the MMDs and to examine for possible long-chain branching. Figure 5.3(a) shows the log*M* vs. elution volume of poly(VAc) prepared at various reaction times at 60 °C in EAc solution. It can be observed that the curves look similar and have the same *M* at the same elution volume despite the differing conversion of the samples. Figure 5.3(b) shows the corresponding MMDs plots of the same poly(VAc) samples, with the distributions not shifting with conversion. In addition, the weight-average molecular weight (Mw) values of these samples are very similar (Table 5.4), although there is a slight increase in the PDI values with time.

Table 5.4: Operating conditions and SEC results for polyvinyl acetate prepared using small-scale batch polymerization and In-Situ NMR methods using V67 initiator.

Sample #	Initiator wt. %	Solvent used	Solvent wt. %	Reaction time (minutes)	Monomer Conversion, %	Mw	PDI
PLP (100Hz)		N/A	-	0.5	0.21	64600	
PVAc_NMR	0.3	$CDCl_3$	70	120	87	28400	1.982
PVAc_bulk	1.0	N/A	-	10	25	293700	2.407
PVAc_3	2.0	EAc	50	40	38	93800	2.278
PVAc_5	1.0	EAc	50	15	8	133800	2.278
PVAc_6	1.0	EAc	50	30	19	133900	1.521
PVAc_7	1.0	EAc	50	40	28	127200	1.571
PVAc_8/8	1.0	EAc	50	60	34	127800	1.690
PVAc_1.12	1.0	EAc	50	72	41	159000	2.094

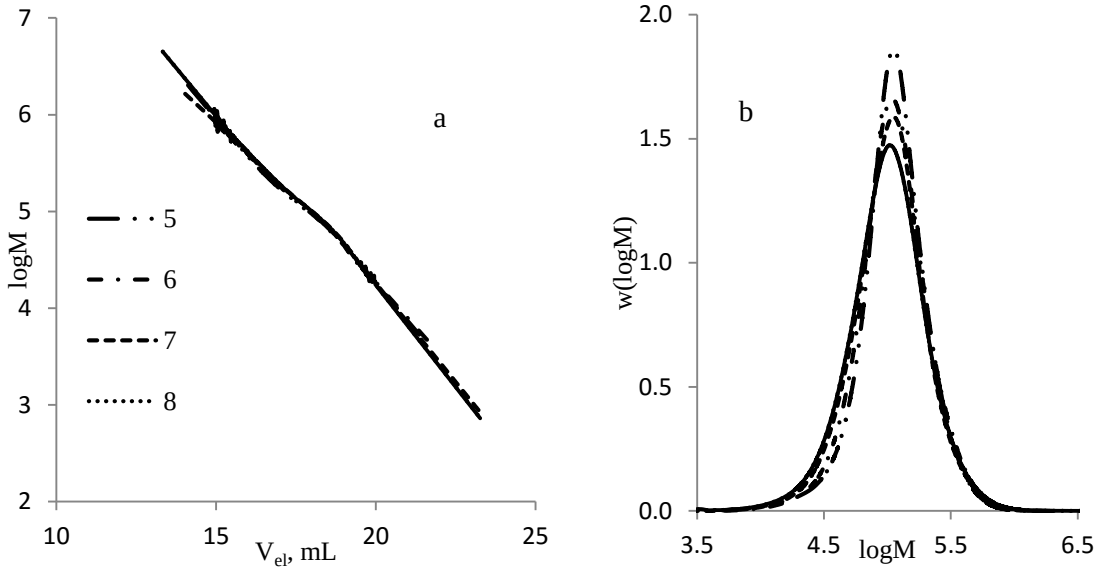

Figure 5.3: SEC results for polyvinyl acetate prepared at 60 °C prepared via small-scale polymerization (solution) technique: log*M*-elution volume (left) and MMDs (right) plots.

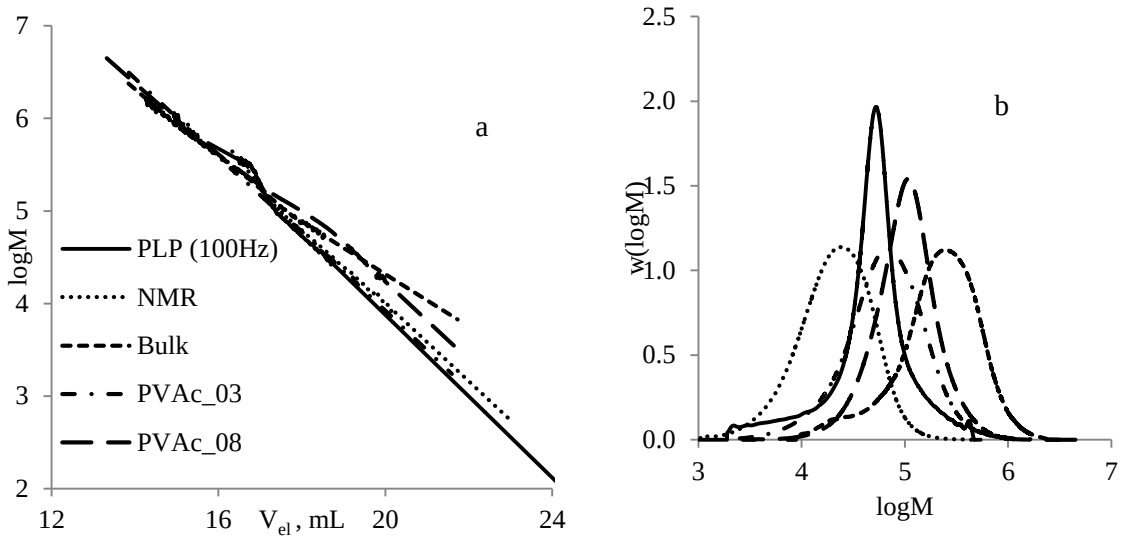

Figure 5.4: SEC results for polyvinyl acetate prepared at 60 °C prepared via small-scale polymerization (both bulk and solution) and In-Situ NMR technique: log*M*-elution volume (left) and MMDs (right) plots. PLP (100Hz) sample was prepared at 50 °C.

SEC analysis was also conducted for various poly(VAc) samples prepared in bulk (small-scale and PLP) and different solvents (small-scale and in-situ NMR) to examine for differences in branching levels, with results summarized in Table 5.4 and Figure 5.4. The samples show a wide variation in MW due to the differences in sample preparation. Since branching results from chain transfer to polymer,

the number of branching points (in a polymer) is related to the rate of polymerization and /or conversion (X_p) as follows:

$$\#\ of\ branched\ points = \frac{R_{br}}{R_{poly}} = \frac{k_{tr}^{poly} X_p}{k_p(1-X_p)} \qquad [5.1]$$

From equation (5.1) we expect the number of branched points to increase with conversion. Thus, the very-low conversion PLP-generated sample should have negligible branching, and can serve as a reference to the other samples. Since higher molecular weight (and branched) polymeric material is eluted first from the columns, we expect to see a variation between the samples at lower elution volume. However, as shown in Figure 5.4(a) this is not the case, as the differences in the curves occur at later elution volumes, and are likely related to the lower polymer concentrations that occur in this MW region for the higher-MW samples. Thus, we conclude that the TD-SEC setup is not sensitive enough to detect branching for the samples produced in our experiments. Figure 5.4(b) shows the corresponding MMDs, with the lowest MWs produced by the solution polymerization in $CDCl_3$ due to higher levels of chain transfer to solvent, and the highest MWs produced in bulk, with slightly broadened distribution (PDI = 2.4). SEC analyses were also conducted for VPi and VBz with similar findings, as shown in Appendix 7.

5.2 Modeling Section

The kinetic models for VAc and VPi were developed using Predici software to describe the batch experiments and to gather insights on the polymerization kinetic behavior of these vinyl ester monomers. The model includes the normal free radical polymerization mechanisms: initiation, propagation, transfer to monomer, transfer to solvent (for solution polymerization) and termination by disproportionation (as shown in Table 5.5). In order to have a good model and able to understand polymerization kinetics, accurate kinetic rate coefficients are needed. Hence the propagation rate

coefficients used to develop these models are those reported in Chapters 3 and 4. As capturing the extent of head-to-head additions was not important for this work, a single propagation step and rate coefficient, is used. Moreover, both the chain-length independent and chain-length dependent termination representation implemented by Nikitin and described in Appendix 1 were used, with the kinetic parameters for the latter based on the SP-PLP-EPR study by Kattner and Buback.[5] The model predictions (i.e. monomer conversion profiles and polymer MWs) are compared to the experimental work from the small-scale batch bulk and solution polymerization data discussed in the first part of this chapter.

Table 5.5: FRP reaction mechanisms used in modeling VAc and VPi polymerization kinetics.

Initiation:	$I \xrightarrow{k_d} 2fI^*$
	$I^* + M \xrightarrow{k_p} P_1$
Propagation:	$P_n + M \xrightarrow{k_p} P_{n+1}$
Transfer to Monomer:	$P_n + M \xrightarrow{k_{tr\_mon}} D_n + P_1$
Transfer to Solvent:	$P_n + S \xrightarrow{k_{tr\_sol}} D_n + P_1$
Termination (Disproportion):	$P_n + P_n \xrightarrow{k_{td}} D_n + D_m$

5.2.1 Modeling Results and Analysis: Bulk Polymerization

Table 5.6: Key notes of the model for bulk conditions analysis.

Model	
1	Fit k_t to conversion data
2	Chain length dependent termination model
3	DuPont rate coefficients

Table 5.7: Rate coefficients and other parameters used to model VAc small-scale batch polymerization (bulk).

Polymerization step	Rate Expression	Value (at 60°C)	Reference
Initiation	$k_d = 2.4478 \times 10^{14} \exp(\frac{-1.5 \times 10^4}{T})$	6.8356×10^{-6}	6
	Initiator Efficiency, f	0.7	
Propagation: Model 1 and 2	$k_p^{av} = 1.56 \times 10^7 \exp(\frac{-2.508 \times 10^3}{T})$	8.3887×10^{3}	7
Model 3	$k_p = 2.7 \times 10^8 \exp(\frac{-3.346 \times 10^3}{T})$	1.17×10^{4}	8
Chain Transfer to Monomer: Model 1 and 2	C_M	3.5×10^{-4}	*
Model 3	$k_{tr\_mon} = 2.94 \times 10^6 \exp(\frac{-4.529 \times 10^3}{T})$	3.67	9
Termination (Disp.): Model 1	Model 1: k_{td}	5.5×10^{8}	*
Model 2	$k_t^{11} = 3.24 \times 10^{10} \exp(\frac{-1.088 \times 10^3}{T})$	1.24×10^{9}	7
Model 3	$k_t = 2.7 \times 10^{10} \exp(\frac{-1.409 \times 10^3}{T})$	3.93×10^{8}	9
V67 Initiator density		1.100×10^{3}	
VAc density	9.584×10^{2} -1.3276T (°C)	8.7874×10^{2}	8
Poly(VAc) density		1.190×10^{3}	

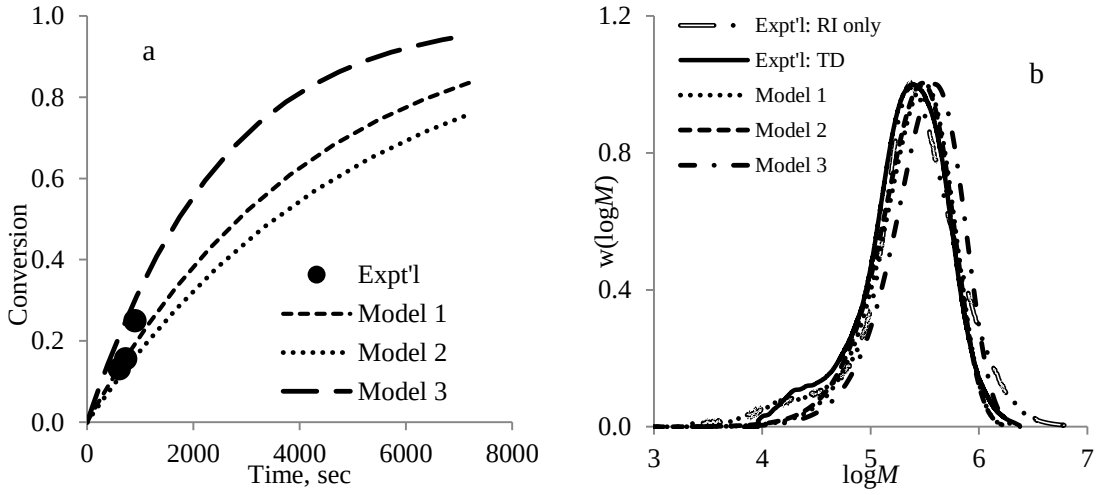

Figure 5.5: Monomer Conversion profile (left) and MMDs (right) for small-scale batch polymerization (bulk) of vinyl acetate at 60 °C.

Figure 5.5(a) show the experimental monomer conversion data compared to the simulation results (using parameters in Table 5.7) for small-scale batch polymerization (bulk) of VAc at 60 °C. As only low conversion data are available, it is difficult to evaluate the best fit. However, it can be seen that the Model 2 monomer conversion profile is close to, but slightly below the experimental data as the reaction time increases, while the Model 3 conversion profile seem to overestimate the experimental data. The experimental points were used to fit the k_t value reported for Model 1 in Table 5.7, which provides the best fit to the data. Figure 5.5 (b) compares the MMDs of the 15 minutes sample (RI and TD) to the simulated results; while the predictions from Models 1 and 2 are quite similar, the predictions from the Model 3 are shifted to higher MWs. All three predictions results in MMDs that are higher than those measured experimentally, with Models 1 and 2 providing a better estimate. The corresponding weight-average MW values are summarized in Table 5.8. It is interesting to note that while the MMDs predicted by the three models are shifted to higher positions than the experiments, the calculated MW values are lower than the value calculated from RI calibration; this difference is due to the high MW tail observed in the experimental measurement (but not seen in the MMD calculated using triple detector output). Due to the limited experimental data set, it is difficult to conclude which set of model parameters can be considered the best.

Table 5.8: Molecular weight (Mw) values obtained for experimental and simulation results for poly(VAc) prepared in 15 minutes (bulk) at 60 °C.

	Mw, $g \cdot mol^{-1}$
Model 1	310000
Model 2	297000
Model 3	379000
Expt'l: RI only	389400
Expt'l: TD	293700

5.2.3 Modeling Results and Analysis: Solution Polymerization

5.2.3.1 Vinyl acetate (VAc)

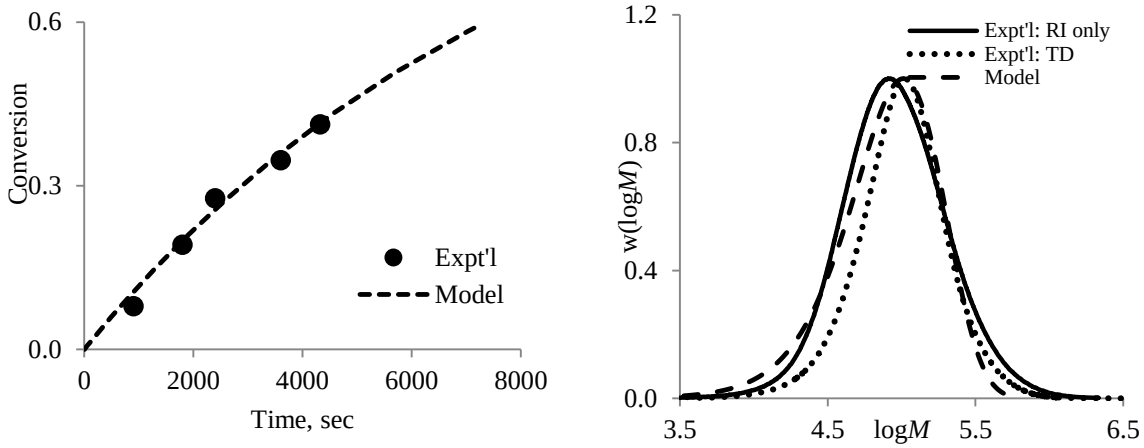

Figure 5.6: Monomer Conversion profile (left) and MMDs (right) for small-scale batch polymerization of vinyl acetate at 60 °C (solution).

Only Model 1 was used to fit the experimental data for small-scale batch polymerization of VAc in EAc (50% by volume), with Figure 5.6(a) comparing the simulation results to the experimental monomer conversion profile. In order to provide the excellent fit shown, k_t was increased from 5.5×10^8 to 2.0×10^9 $L\cdot mol^{-1}\cdot s^{-1}$, with all other rate coefficients the same as for the bulk model. Chain transfer to solvent was added to the model, with C_S set to a value of 4×10^{-4} (within the range of values reported in literature[10]) to provide the representation of the MMDs shown in Figure 5.6(b); the experimental distributions are for the final 60 min sample measured using both RI (with universal calibration) and by TD-SEC. The value of C_S was set to have the model match the peak position of the TD-SEC distribution, with the model-calculated Mw value (105000 $g\cdot mol^{-1}$) slightly lower than the experimental values of 126000 $g\cdot mol^{-1}$. The underprediction of the Mw values (for both bulk and solution) may be an indication that it is necessary to add the long-chain branching mechanism to the model. However, given the limited data set and the inability of TD-SEC to detect branching in our samples, this model extension was not attempted in this study.

5.2.3.2 Vinyl pivalate (VPi)

Table 5.9: Rate coefficients and other parameters used to model VPi small-scale batch solution polymerization.

Polymerization step	Rate Expression	Value (at 60°C)	Reference
Initiation	$k_d = 2.4478 \times 10^{14} \exp(\frac{1.5 \times 10^4}{T})$	6.8356×10^{-6}	6
	Initiator Efficiency, f	0.7	
Propagation	$k_p^{av} = 6.78 \times 10^6 \exp(\frac{-2.09 \times 10^3}{T})$	1.27×10^4	11
Chain Transfer to Monomer	C_M	4.0×10^{-4}	*
Chain Transfer to Solvent	C_M	1.0×10^{-4}	*
Termination (Disp.)	k_{td} (Model 1)	5.10×10^8	*
VPi density	8.933×10^2 -1.1116T (°C)	8.7874×10^2	11
EAc density	9.2693×10^2 -1.2719T (°C)	8.5062×10^2	12

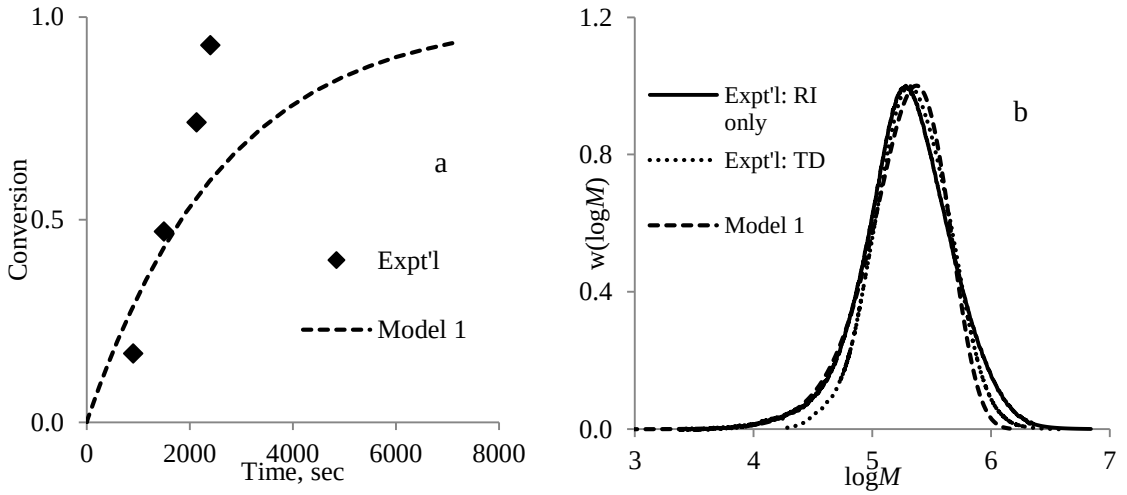

Figure 5.7: Monomer Conversion profile and MMDs for small-scale batch polymerization of vinyl pivalate at 60°C (solution).

As determined in this work, the value of k_p^{av} for VPi is significantly higher, by roughly 50%, than VAc. In addition, Kattner and Buback[5] report that k_t of VPi is lower than that of VAc by a factor of five. With rate of conversion proportional to $k_p^{av} / k_t^{0.5}$, these differences explain the much faster rate observed for VPi compared to VAc (see Figure 5.1(b) and 5.2(b)). Figure 5.7(a) compares simulation

to experimental results, with k_t adjusted to provide the best fit to the first couple of conversion data points. Table 5.9 contains the full set of kinetic coefficients used to model the VPi system. Without implementation of a gel effect correlation (decreasing k_t with increasing conversion), the model is not able to represent the acceleration in conversion observed experimentally. Using a value for C_S within the range reported in literature,[10] the model also provides a good representation of the experimental MMD, as shown in Figure 5.7(b). Once again, the model prediction of Mw (2.45×10^5 g·mol^{-1}) is below the experimentally measured values ($2.6\text{-}2.9\times10^5$ g·mol^{-1}). This comparison was done for the 25 min sample, for which the model provides a good fit to the experimental conversion.

5.3 Conclusions

Small-scale batch polymerizations have been used to compare the polymerization behavior of vinyl ester monomers (VAc, VPi and VBz) at 60 °C in both bulk and solution. The rate of monomer conversion is fastest for VPi, followed by VAc and then a very slow rate observed for VBz in both bulk and solution, an ordering that is consistent with the k_p determined by PLP-SEC. From the elution volume plots and MMDs obtained, the triple detector Viscotek SEC system is not sensitive enough to detect the level of branching for our experimental samples, as the MMDs and elution behavior were not affected by monomer conversion.

A model for batch homopolymerization (bulk and solution) has been developed using Predici, with the propagation kinetics set to our experimentally-determined values. The values of k_t were adjusted to fit the monomer conversion profiles for both bulk and solution, and transfer constants fit to represent the experimental MMDs. For VAc the k_t value required to fit the solution polymerization data is greater than that used for the bulk system. For solution polymerization of VPi, it was necessary to reduce the k_t value significantly, in agreement with a recent independent kinetic investigation. Although the data

sets obtained are not large, the kinetic models show that the experimental trends can be captured using reasonable values of the kinetic rate coefficients. With additional data, the model can be expanded to include other reaction steps such as transfer to polymer and head-to-head monomer addition.

References

1. D. Britton, F. Heatley, P.A. Lovell, *Macromolecules* **1998**, *31*, 2828.
2. A.N. Morin, C. Detrembleur, C. Jérôme, P. De Tullio, R. Poli, A. Debuigne, *Macromolecules* **2013**, *46*, 4303.
3. C. Preusser, R. A. Hutchinson, *Macromol. Symp.* **2013**, *333*, 122.
4. M. Nerkar, J. A. Ramsay, B. A. Ramsay, M. Kontopoulou, R. A. Hutchinson, *J. Polym. Environ.* **2013**, *21*, 24.
5. H. Kattner, M. Buback, *Macromol. Chem. Phys.* **2014**, *215*, 1180.
6. https://www.chemours.com/Vazo/en_US/products/grades/grade_selector.html, **2015**.
7. O. Monyatsi, A. N. Nikitin, R. A. Hutchinson, *Macromolecules* **2014**, *47*, 8145.
8. R.A Hutchinson, J. R. Richards, M. T. Aronson, *Macromolecules* **1994**, *27*, 4530.
9. C. Kiparissides, J. P. Congalidis, J. R. Richards, *Ind. Eng. Chem. Res.* **2005**, *44*, 2592.
10. I. Sakurada, Polyvinyl Alcohol Fibers, *International Fiber Science and Technology*, Series, 6, New York, **1985**.
11. O. Monyatsi, R. A. Hutchinson, accepted by *Macromol. Chem. Phy*. **September 26, 2015**.
12. http://ddbonline.ddbst.de/DIPPR105DensityCalculation/DIPPR105CalculationCGI.exe, **2015**.

Chapter 6: Conclusions and Recommendations

Free radical homopolymerization kinetic studies of vinyl ester monomers (i.e. vinyl acetate (VAc), vinyl pivalate (VPi) and vinyl benzoate (VBz)) have been conducted using various techniques over a range of operating conditions. The PLP-SEC technique has been applied to systematically investigate the propagation kinetics of VAc, VPi and VBz in the temperature range of 25 -90 °C for both bulk and solution conditions. Batch polymerizations were also conducted to further explore the polymerization kinetic behavior of these monomer systems, with this work accompanied by the development of kinetic models.

6.1 PLP-SEC studies

An extensive set of PLP-SEC experiments has been conducted for VAc, VPi and VBz bulk homopolymerizations at 25 - 90 °C and the solution polymerization of VPi and VBz at 50 °C. The propagation rate coefficient, k_p, measured for VPi and VAc increases significantly with the laser pulse repetition rate (prr), with up to 20 % k_p variation between 200 and 500 Hz prr. This behavior is attributed to the effect of head-to-head addition that occurs during vinyl ester polymerizations, with the possibility that this addition affects k_p reduced as the time between pulses decreases. In addition, the k_p value for VPi is significantly higher than VAc. The k_p values obtained for solution polymerization of VPi and VAc were similar to bulk conditions, indicating that there is no significant solvent effect with heptane and ethyl acetate. The PLP study of VBz homopolymerization was not successful, suggesting that the radical formed is stabilized, and that the polymerization behavior for this monomer is significantly different from the rest of the vinyl ester family

6.2 Small-scale batch polymerization

Small-scale batch polymerization experiments for VAc, VPi and VBz were conducted at 60 °C for both bulk and solution conditions. This experimental work was performed in order to investigate and compare the kinetic behavior of these monomer systems. It was found that the rate of conversion is faster for VPi followed by VAc and finally VBz, a pattern consistent with the k_p values determined by PLP-SEC. Kinetic models were implemented to represent the batch polymerization of VAc (bulk and solution) and VPi (solution) systems, with reasonable agreement achieved by fitting termination and transfer coefficients (kept within reasonable limits) to the limited experimental data.

6.3 Recommendations

The increase in VPi and VAc k_p values has been attributed to head-to-head addition, as the experimental observations for VAc are consistent with the simulation work conducted by Dr. A. Nikitin in Russia. This work attempted to verify head-to-head addition for VPi system, as it has not yet been reported in the literature. However, the NMR investigation summarized in Appendix 4 was inconclusive, and further work in this area needs to be done to verify the reaction, although it is expected based on the results reported for a series of vinyl esters. Further PLP studies of the propagation kinetics of the vinyl esters in solution over a broader range of temperature and repetition rates should be conducted, especially to see if the influence of prr on propagation is also observed in solution. As no structure was found in the PLP-generated poly(VBz) MMDs, it would be interesting to use the PLP-EPR techniques utilized by the Buback group to learn more about the radical structure in this system.

For further study of the batch polymerization of these monomers, it would be beneficial to run the reactions over a broader range of conditions and to higher conversions. This would be more easily achieved by following the reaction using in-situ NMR, building on the preliminary efforts made in this

study. It should be explored whether the triple detector SEC setup will be able to detect the higher levels branching expected at higher polymer conversions. This experimental work can be used to further develop and improve the kinetic models of the system, and the corresponding estimates of the kinetic rate coefficients for termination and transfer, including the incorporation of a gel-effect correlation to represent the change in k_t with conversion. With additional measurements of head-to-head defects and branching levels, the model can be expanded to include the corresponding kinetic mechanisms.

Appendices

Appendix 1: Simulation work by Dr. A. Nikitin (Ch. 3)

A1.1 The average propagation rate coefficient, k_p^{av} derivation

Consider a radical that starts growth at time 0 in one of the states. Lifetimes τ_1 and τ_2 of this radical remaining in its state without change are equal to $1/(k_{p12}[M])$ and $1/(k_{p21}[M])$, where [M] is the monomer concentration. The average time required for a radical to complete one cycle of transformation (to the opposite state and back) is $\tau_1+\tau_2 = 1/(k_{p12}[M])+1/(k_{p21}[M])$, and the number of such cycles (m_c) during time t is $m_c = t/(\tau_1+\tau_2)$. While remaining in a state, the radical grows in chain length L according to $dL/dt=k_{p11}[M]$ and $dL/dt=k_{p22}[M]$, respectively. Thus, during the average time of one cycle, chain length of the radical is increased by $k_{p11}[M]\tau_1 + k_{p22}[M]\tau_2 +2$, taking into account that in each transfer from one state to another the chain length of the radical will also be increased by 1. For m_c cycles that occur during t, the chain length of growing radical is

$$L = \left(k_{p11}[M]\tau_1 + k_{p11}[M]\tau_1 + 2\right)m_c = \frac{k_{p11}k_{p21} + 2k_{p12}k_{p21} + k_{p22}k_{p12}}{k_{p12} + k_{p21}}[M]t \qquad (A1.1)$$

As $L = k_p^{av}[M]t$ according to Equation (A1.1) we thus have the following expression for k_p^{av}:

$$k_p^{av} = \frac{k_{p11}k_{p21} + 2k_{p12}k_{p21} + k_{p22}k_{p12}}{k_{p12} + k_{p21}} \qquad (A1.2)$$

which can also be expressed by :

$$k_p^{av} = k_{p11} - \frac{k_{p11} - k_{p22} - 2k_{p21}}{1+\frac{k_{p21}}{k_{p12}}} \qquad (A1.3)$$

This expression of the average propagation rate coefficient, k_p^{av}, is valid when several transfer events between 1 and 2 states take place within t, as would be expected for polymer formation

in a continuously initiated system. Equation (A1.2) could also be obtained from the expression for average propagation coefficient, $k_p^{av\_co}$, for the terminal model of copolymerization:[1]

$$k_p^{av\_co} = \frac{r_1 f_1^2 + 2 f_1 f_2 + r_2 f_2^2}{r_1 f_1 / k_{p11} + r_2 f_2 / k_{p22}} \quad \text{(A1.4)}$$

where $r_1 = k_{p11}/k_{p12}$, $r_2 = k_{p22}/k_{p21}$, and f_1 and f_2 are the monomer mole fractions. The reactions in Scheme 3.1 are very similar to that for the terminal model, except that only one monomer is used such that $f_1 = f_2 = 1$ and equation (A1.4) can be transformed into equation (A1.2).

Some illustrative calculations can be done to investigate the effect of head-to-head propagation on overall chain-growth kinetics. If the defect insertion takes place only in 1% of propagation events (as for VAc), an average chain with length 100 will have been subjected to head-to-head propagation ($k_{p12}/k_{p11}=0.01$) and will have also had to pass through a tail-to-tail addition to regain the usual chain-end radical structure (see Scheme 3.1 (Ch.3)). It is expected that the rate of tail-to-tail (VAc adding to the inverted radical structure with coefficient k_{p21}) propagation is also not high and is close to the value for the rate of VAc addition to an ethylene radical.[2-3] It is difficult to estimate a value for the tail-to-head k_{p22} rate coefficient, which propagates the defect structure as a sequence along the chain. It is expected to be low, although this may be difficult to verify through analysis of polymer structure.

Figure A1.1 plots k_p^{av} values calculated as a function of k_{p21} by Equation A1.3 with k_{p11} fixed at 5000 $L \cdot mol^{-1} \cdot s^{-1}$ and k_{p22} fixed at a low value. The four curves are generated at k_{p12} values of 0.5, 5, 50 and 500 $L \cdot mol^{-1} \cdot s^{-1}$, corresponding to head-to-head insertions of 0.01, 0.1, 1 and 10 %, respectively. Note that according to Equation A1.1 if $k_{p22} << k_{p21}\left(2 + \frac{k_{p11}}{k_{p12}}\right)$ the value of k_{p22} does not influence on k_p^{av}

; therefore the dependencies for k_p^{av} shown for k_{p22} equal to 0 and 50 L·mol^{-1}·s^{-1} do not deviate from each other.

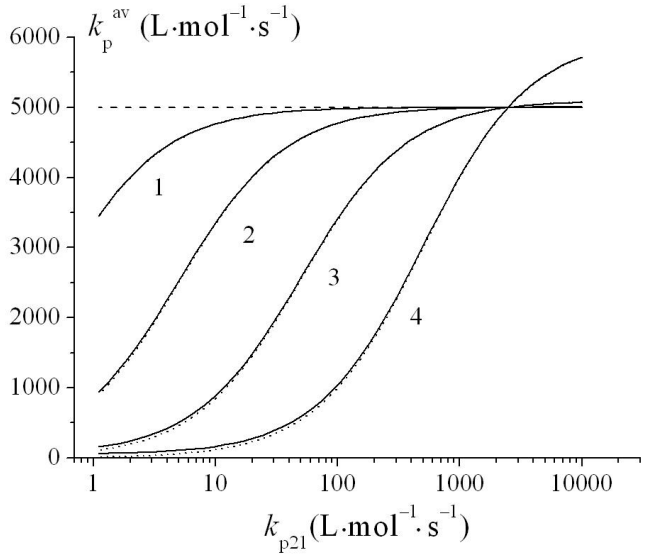

Figure A1.1: The variation in average propagation rate coefficient (k_p^{av}) with propagation rate coefficient k_{p21}, calculated for k_{p11} = 5000 L·mol^{-1}·s^{-1} (shown by horizontal dashed line) and k_{p22} = 0 (dotted curves) and 50 L·mol^{-1}·s^{-1} (solid curves): k_{p12} = 0.5 (1), 5 (2), 50 (3) and 500 L·mol^{-1}·s^{-1} (4)

The following observations can be made from the calculations:

- Even if the level of the head-to-head propagation is low, it can still cause a significant decrease in k_p^{av} compared to k_{p11}. For example for curve 1 with head-to-head level of 0.01% the k_p^{av} value deviates more than 10% from k_{p11} if k_{p21} is below 8 L·mol^{-1}·s^{-1}.
- If the level of the head-to-head propagation is about 1% as found for VAc (curve 3 in Figure 3.1), the k_p^{av} value is within 10% of k_{p11} only for values of k_{p21} > 500 L·mol^{-1}·s^{-1}.

If the level of the head-to-head propagation is 10% (as for fluorinated α–olefins) the k_p^{av} value is close to k_{p11} only for the small region of k_{p21} in which $k_{p21} = (k_{p11} - k_{p22})/2$. For the unlikely case that $k_{p21} > (k_{p11} - k_{p22})/2$ the k_p^{av} value could be markedly higher than k_{p11} (curve 4).

These calculations demonstrate the potential influence of head-to-head addition on radical polymerization kinetics. For certain monomers such as VAc, the single k_p value used widely to characterize the propagation must be considered as an averaged composite (k_p^{av}) of four propagation rate coefficients, as given by expressions (A1.2) and (A1.3). The implications of this general finding will be explored after first using the variation of k_p^{app} with prr to estimate individual rate coefficients for VAc propagation from the PLP-SEC results.

A1.2 Simulation of PLP-SEC results

To simulate the experimental results obtained at different temperatures and prr, the basic model (initiation, propagation, termination and chain transfer to monomer, with propagation modeled according to the reactions in Scheme 3.1 (Ch.3)) shown in Scheme A1.1 has been implemented in PREDICI.[4] Initiator, monomer and primary radicals are shown as I, M and R_0, respectively. Growing normal "head" radicals, inverted "tail" radicals and dead macromolecules are shown by R_i, V_i and P_i, respectively, with subscript *i* indicating the chain length of the species.

Scheme A1: Vinyl acetate polymerization mechanisms

Initiation

$$I \xrightarrow{h\nu} 2\,R_0 \quad \text{(A1.5)}$$

$$R_0 + M \xrightarrow{k_{i1}} R_1 \quad \text{(A1.6)}$$

$$R_0 + M \xrightarrow{k_{i2}} V_1 \quad \text{(A1.7)}$$

Propagation

$$R_i + M \xrightarrow{k_{p11}} R_{i+1} \quad \text{(A1.8)}$$

$$R_i + M \xrightarrow{k_{p12}} V_{i+1} \quad \text{(A1.9)}$$

$$V_i + M \xrightarrow{k_{p22}} V_{i+1} \quad \text{(A1.10)}$$

$$V_i + M \xrightarrow{k_{p21}} R_{i+1} \quad \text{(A1.11)}$$

Chain transfer to monomer

$$R_i + M \xrightarrow{k_{trM1}} P_i + R_0 \quad \text{(A1.12)}$$

$$V_i + M \xrightarrow{k_{trM2}} P_i + R_0 \quad \text{(A1.13)}$$

Termination

by disproportionation

$$R_i + R_j \xrightarrow{k_t^{i,j}} P_i + P_j \quad \text{(A1.14)}$$

$$R_i + V_j \xrightarrow{k_t^{i,j}} P_i + P_j \quad \text{(A1.15)}$$

$$V_i + V_j \xrightarrow{k_t^{i,j}} P_i + P_j \quad \text{(A1.16)}$$

The Arrhenius parameters used in the simulations are summarized in Table A1.1. Those for propagation are approximate values, with the activation energy for k_{p11} chosen to be higher than the one for k_p^{av} to describe the experimental data. For k_{p12} the values of E_a and A are chosen to satisfy two conditions: the activation energy is chosen to be about 5 kJ higher than the one for k_{p11} in accordance with ref. [5],

with the pre-exponential fixed such that $0.01k_{p11} \leq k_{p12} \leq 0.02k_{p11,}$ again in accordance with the literature evidence discussed previously. The value of k_{p22} is assumed to have the same Arrhenius parameters as for k_{p12}; as shown previously (Figure A1.1), it was found by simulation that the value of k_{p22} does not influence significantly the calculated MMDs. The activation energy for k_{p21} was estimated in order to match the observed experimental activation energy of k_p^{av} of 20 kJ·mol^{-1}.

Table A1.1: Kinetic parameters used for simulation of VAc polymerization

kinetic parameters	E_a (kJ·mol^{-1})	A (L·mol^{-1}·s^{-1})	value at 50 °C (L·mol^{-1}·s^{-1})	reference
k_{p11}	23.7	6.31×10^{7}	9400	This work
k_{p12}	28.1	3.64×10^{6}	103	This work
k_{p22}	28.1	3.64×10^{6}	103	This work
k_{p21}	16.2	9.87×10^{4}	240	This work
k_{trM1}	38.8	2.4×10^{6}	1.3	6
k_{trM2}	31.3	3.7×10^{3}	0.033	This work
$k_t^{1,1}$	9.0	3.3×10^{10}	1.15×10^{9}	7
α_1			0.57	4
α_2			0.16	4
i_c			20	4

Termination is modeled according to the composite model proposed by Smith et al.[8] It is assumed that for both radicals R_i and V_i the termination mode is disproportionation and the termination rate coefficients $k_t^{i,i}$ are identical, as expressed by:

$$k_t^{i,i} = k_t^{1,1} i^{-\alpha_1}, \; i \le i_c \tag{A1.17}$$

$$k_t^{i,i} = k_t^{1,1} i_c^{(-\alpha_1+\alpha_2)} i^{-\alpha_2}, \; i \ge i_c \tag{A1.18}$$

In this expression, i_c represents the chain length separating macromolecules with termination rate controlled by center-of-mass diffusion ($i \le i_c$) from those for which segmental reorientation controls rate ($i \ge i_c$), with the specific parameters for VAc given in Table A1.1 taken from literature.[7] The rate coefficients of cross termination are expressed using the geometric mean:

$$k_t^{i,j} = \sqrt{k_t^{i,i} k_t^{j,j}} \tag{A1.19}$$

The rate coefficient for chain transfer to monomer, k_{trM1}, for R_i is calculated from Arrhenius parameters found in literature.[9] For V_i chain transfer rate coefficient is assumed to be equal to $\frac{k_{p21}}{k_{p11}} k_{trM1}$. Rate coefficients for initiation k_{i1} and k_{i2} have been chosen to be equal k_{p11} and k_{p12}, respectively.

The model shown in Scheme A1.1 is enough to show the repetition rate dependence of k_p^{app}. Nevertheless the model is extended to account the fact that in experiments the increase of either pulse energy or initiator concentration results in disappearance of PLP structure in molar mass distributions.[10] To explain this feature it was assumed that each laser pulse creates specific radicals (Z) that behave as retarders; the concentration of these radicals are assumed to be proportional to the concentration of primary radicals produced by a pulse (ρ, in $mol \cdot L^{-1}$). Then the effect of retardation is taken into account by the following reactions:

$$R_i + Z \xrightarrow{k_z} P_i + R_0$$

$$Z + Z \xrightarrow{k_{z2}} P_0$$

with k_z =1×10^9 L·mol^{-1}·s^{-1} and k_{z2} =6×10^7 L·mol^{-1}·s^{-1}.

The model has been used to calculate MMDs at different prr for VAc polymerization at 40.5 °C (corresponding to the experiments of Junkers et al.[11]) and 50 °C, with the distributions plotted as Figure A1.2 and used to determine the values of k_p^{app}. To provide a comparison, MMDs have also been simulated assuming that VAc propagates solely through head-to-tail addition ($k_{p11} = k_p^{av}$, $k_{p12} = k_{p22} = k_{p21}$=0) with the value of k_p^{av} = 6750 L·mol^{-1}·s^{-1}; all other kinetic parameters used for this calculation were taken from Table A1.1.

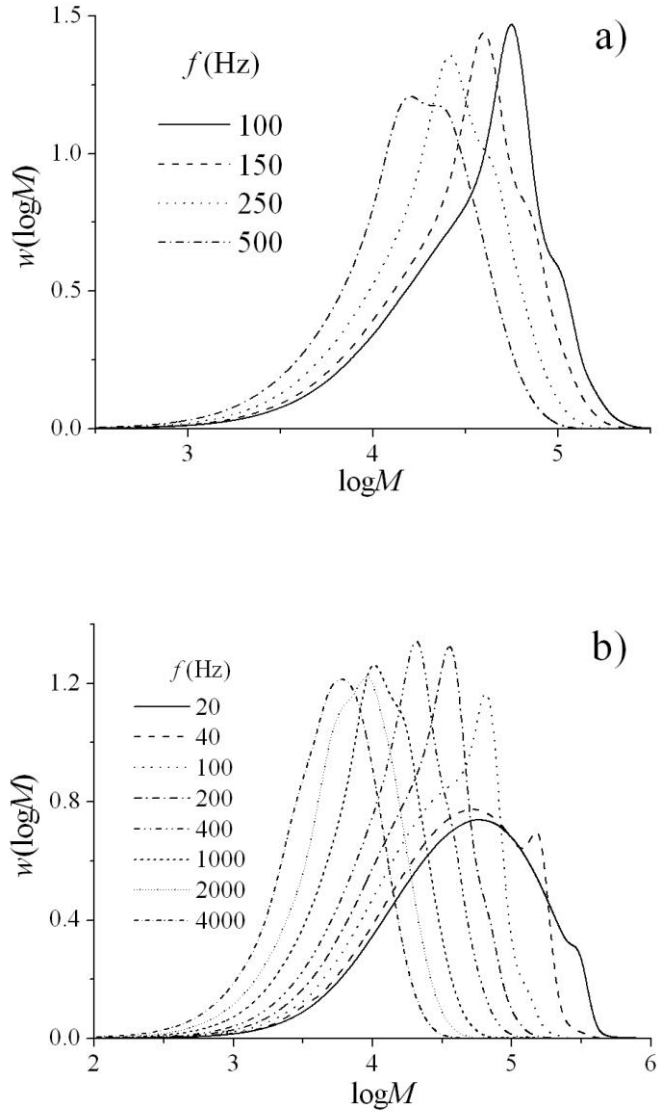

Figure A1.2. Polymer molar mass distributions simulated for vinyl acetate pulsed laser polymerization at 40.5 (a) and 50 °C (b) for different repetition rates in the presence of head-to-head addition. Calculated with σ (SEC dispersion parameter) =0.04 for $\rho = 3\times10^{-7}$ (a) and 6×10^{-7} mol·L^{-1} (b). Other kinetic parameters for calculations are given in Table A1.1.

References

1. T. Fukuda, Y. –D. Ma, H. Inagaki, *Macromolecule*s **1985**, *18*, 17.
2. S. Beuermann, M. Buback, *Prog. Polym. Sci*. **2002**, *27*, 191.
3. E. F. McCord, W. H. Shaw Jr., R. A. Hutchinson, *Macromolecules* **1997**, *30*, 246.
4. M. Wulkow, *Macromol. Theory Simul.* **1996**, *5*, 393.
5. P. E. Flory, F. S. Leutner, *J. Polym. Sci.* **1948**, *3*, 880.
6. H. de Bruyn, PhD Thesis, University of Sydney, **1999.**
7. H. Kattner, M. Buback, *Macromol. Chem. Phys.* **2014**, *215*, 1180.
8. G. B. Smith, G. T. Russell, J. P. A. Heuts, *Macromol. Theory Simul.* **2003**, *12*, 299.
9. H. de Bruyn, PhD Thesis, University of Sydney, **1999**.
10. D. R. Hensley, S. D. Goodrich, A. Y. Huckstep, H. J. Harwood, R. L. Rinaldi, *Macromolecules* **1995**, *28*, 1586.
11. T. Junkers, D. Voll, C. Barner-Kowollik, *e-Polymers* **2009**, *no 076*.

Appendix 2: Temperature Equilibration (Chapter 3)

Temperature equilibration time set- PLP procedure

The same PLP procedure described in Ch. 3 was followed. The quartz cell with bulk monomer solution was placed in the sample holder and the time taken to reach 0.5 °C below the target temperature was noted. The solution was then pulsed until the temperature increased to 0.5 °C above the target temperature and the pulsing time was also noted. The sample was then taken out of the sample holder for approximately 1 minute to cool. After returning back to the thermostatted sample holder, the sample temperature was again allowed to increase until it was -0.5 °C below the target temperature, with the time again noted. The sample solution was pulsed again to 0.5 °C above the target temperature, noting the pulsing time. The same procedure was repeated three times for 100 Hz and 500 Hz pulse repetition rates (prr) and six times for the same repetition rates. The same procedure was repeated for the same repetition rates and three times with the solution pulsed till it reached a temperature +1.5 °C above the target temperature instead. Table A2.1 shows the time taken to reach the (-0.5 °C) target temperature including cooling.

Table A2.1: Time taken to reach (49.5 °C) and the pulsing time for 100 Hz and 500 Hz repetition rate for the three-and-sixth times run.

Prr, (Hz)	100		500	
3rd -run: Monomer conversion, (%)	0.82		0.64	
	Time to reach 49.5 °C (sec)	Pulsing time (sec)	Time to reach 49.5 °C (sec)	Pulsing time (sec)
Initial	198	21	199	6
2nd + cooling	259	22	289	11
3rd + cooling	197	29	205	10
6th -run: Mon. conversion, (%)	1.74		1.39	
Initial	204	20	205	4
2nd + cooling	275	26	154	8
3rd + cooling	218	25	175	7
4th + cooling	192	23	173	12
5th + cooling	171	26	151	15
6th + cooling	201	30	138	6

Table A2.2: Time taken to reach (49.5 °C) and the pulsing time to 51.5 °C for 100 Hz and 500 Hz repetition rate for the three-times run.

Prr, (Hz)	100		500	
Mon. Conversion, (%)	1.77		1.49	
	Time to reach 49.5°C (sec)	Pulsing time (sec)	Time to reach 49.5°C (sec)	Pulsing time (sec)
Initial	226	37	162	15
2nd + cooling	151	38	137	15
3rd + cooling	185	30	102	21

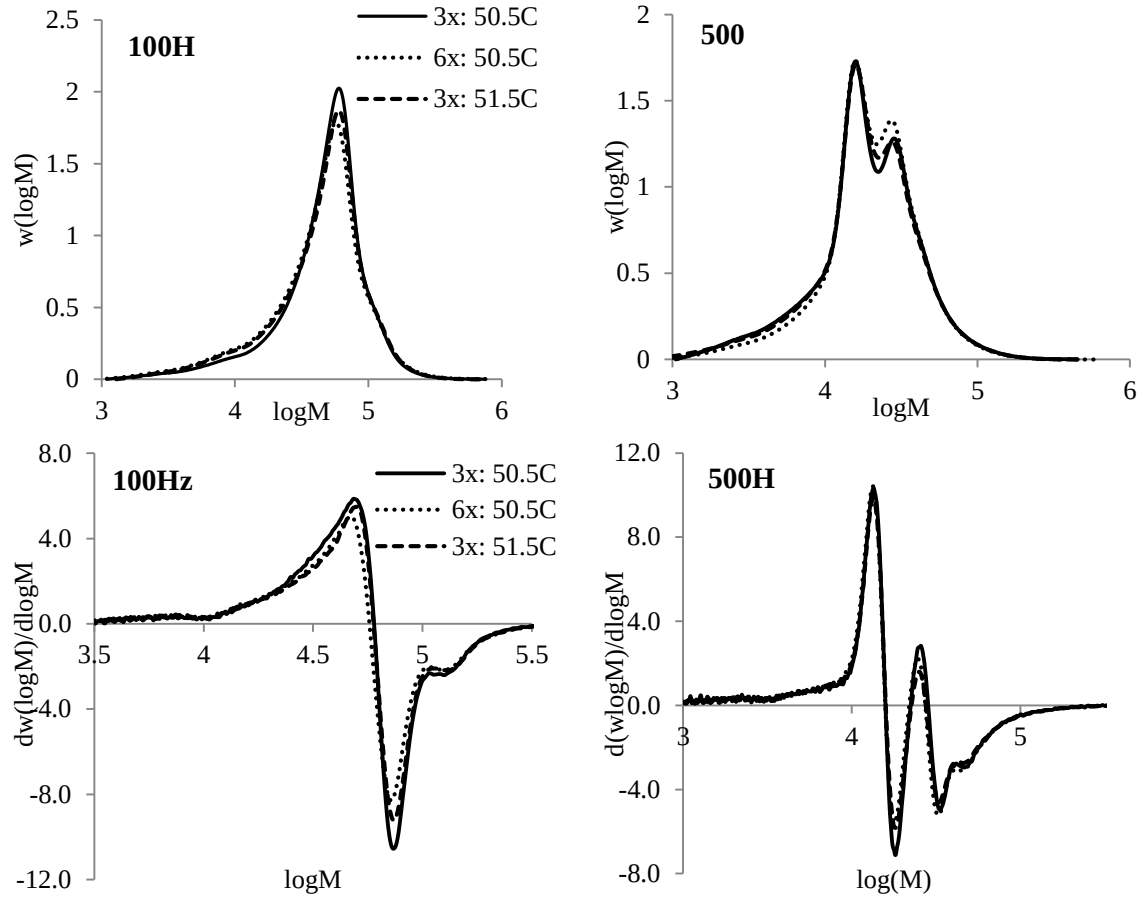

Figure A2.1: MMD and corresponding 1st derivative plots for poly(VAc) conducted at 100Hz and 500Hz pulse repetition rates and 50°C, at various pulsing runs.

Figure A2.1 shows the MMDs plots for PVAc conducted at 500 Hz and 100 Hz repetition rates, at 50 °C for different pulsing runs. For the experiments at 500 Hz a clear 2nd inflection point is observed, while for 100 Hz the 2nd inflection point is less distinct, as seen in the corresponding 1st derivative plots of the corresponding MMDs. Most importantly, the infection points occur at the same log (M) position for each run, independent of the number of heating/cooling cycles used, as summarized in Table A2.3. The maximum variation in the inflection points is only 4% at 100 Hz, while for 500 Hz the k_p values are within 2% within each other. This set of experiments proves that the difference in k_p values at 500 and 100 Hz is not caused by a higher temperature exotherm at the higher pulse repetition rate.

Table A2.3: M_{01}, M_{O2}, k_p values obtained for 100Hz and 500Hz repetition rate analyzed at 50°C using benzoin as the photo-initiator at different pulsing runs.

Prr, (Hz)	Run	M_{O1}, g·mol^{-1}	M_{O2}/M_{O1}	M_{O3}/M_{O1}	k_p (L·mol^{-1}·s^{-1})
100	3x: 50.5C	48249	2.24	-	5407
	6x: 50.5C	47065	2.27	-	5275
	3x: 51.5C	49057	2.27	-	5498
500	3x: 50.5C	13528	1.87	3.10	7580
	6x: 50.5C	13438	1.85	3.07	7530
	3x: 51.5C	13710	1.83	3.04	7683

Appendix 3: Propagation rate coefficient Variation

Outer and lower Intervals k_p values for VAc experiments at 50°C

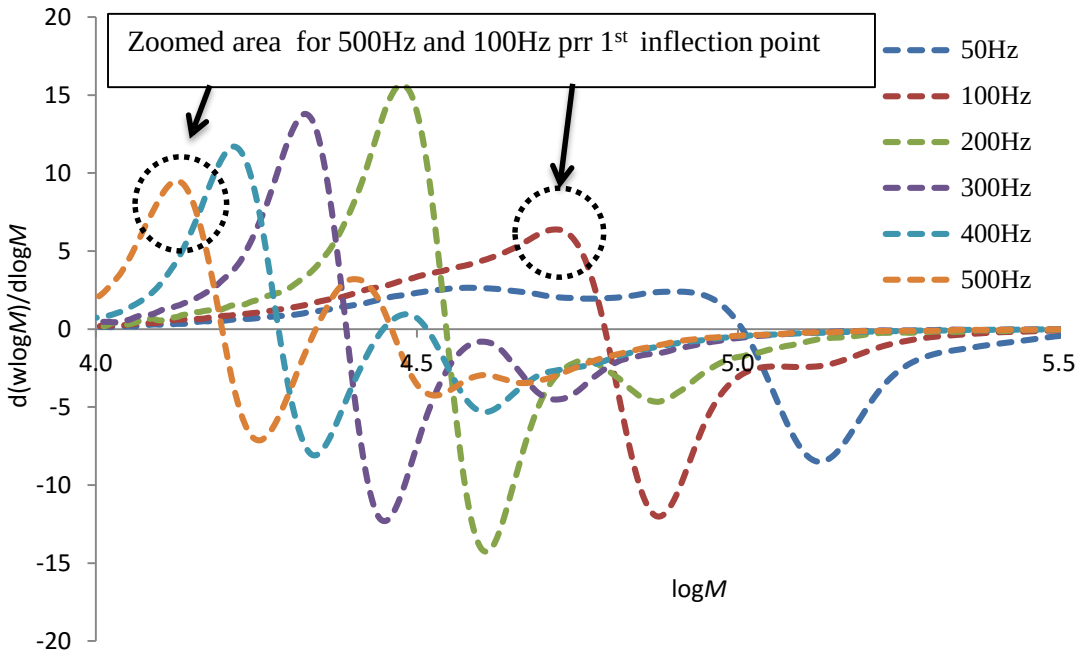

Figure A3.1: First derivative MMD plots of poly(VAc) varying pulse repetition rates (p.r.r) at 50°C with benzoin photo-initiator.

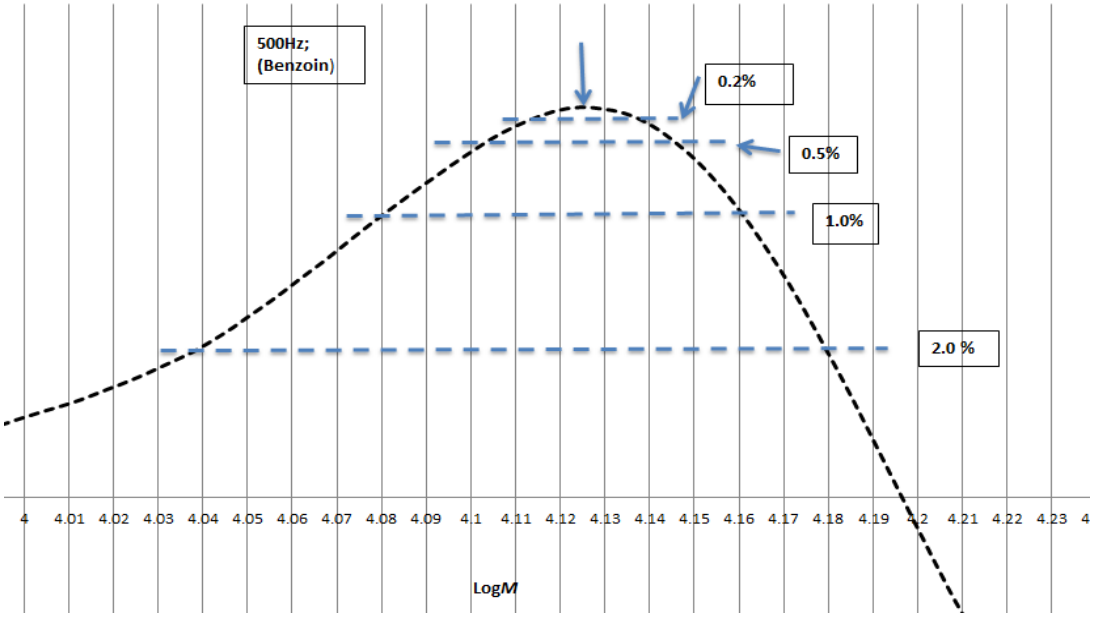

Figure A3.2: Zoomed area of first derivative MMDs plot of poly(VAc) at 50°C and 500Hz prr with benzoin photoinitiator.

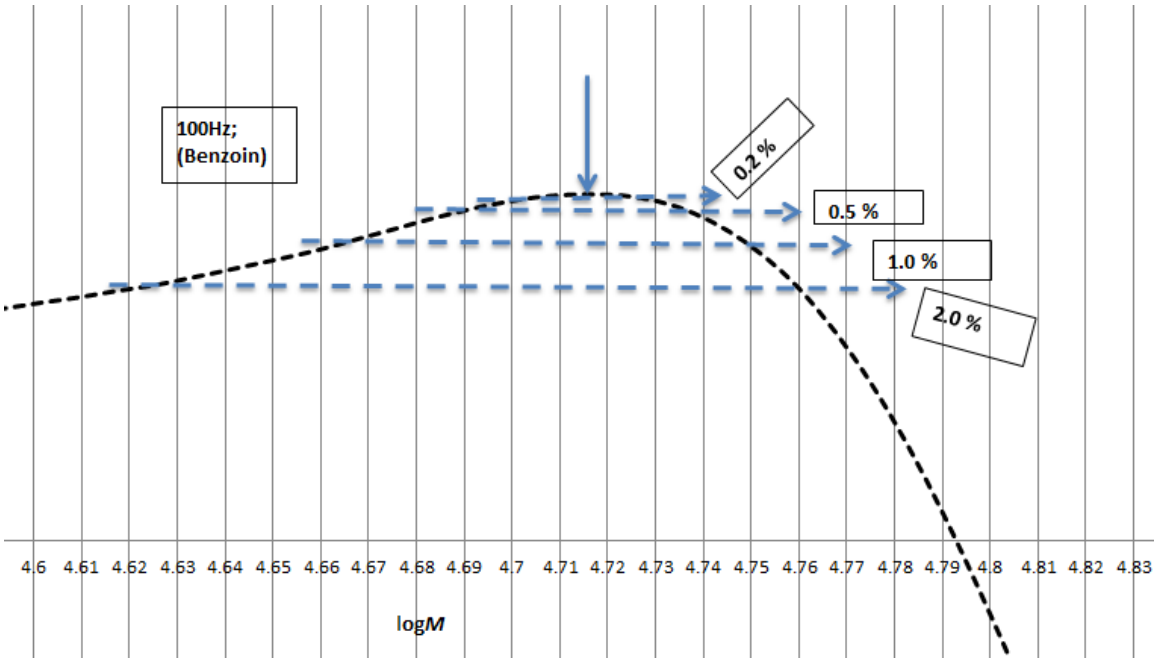

Figure A3.3: Zoomed area of first derivative MMDs plot of poly(VAc) at 50°C and 100Hz prr with benzoin photoinitiator.

Figure A3.1 shows the first derivative MMDs plots for PVAc at 50 °C and various prr with benzoin photoinitiator. Figure A3.2 and A3.3 illustrates the zoomed area of the 1st inflection point for the first derivative MMDs plot of poly(VAc) at 500 and 100 Hz prr respectively. Also shown on these plots are the range of logM values that might occur if there is difficulty in exactly determining the position of the maximum on the first directive plot. From this analysis, it can be seen that the broader peak found for the experiment run at 100 Hz can lead to more difficulty in identifying an exact position of the inflection point. For example, it can be seen from Figure A3.2 and A3.3 that the 2% bound line is relatively far from the center point for 500 Hz prr plot compared to 100 Hz due to the sharper 1st inflection point at 500 Hz.

Table A3.1: M_{01}, k_p values for the outer and lower bounds for VAc experiments at 50 °C and 100Hz prr with benzoin photoinitiator.

% from the center logM_{01}	Bound	logM_{01}	M_{01}, (g·mol^{-1})	k_p, (L·mol^{-1}·s^{-1})	k_p % dev.
0.20	Lower	4.706443	50868	5701	-2.1
	Outer	4.725306	53126	5954	2.2
0.50	Lower	4.692295	49237	5518	-5.3
	Outer	4.739454	54885	6151	5.6
1.0	Lower	4.668716	46635	5226	-10.3
	Outer	4.763033	57947	6494	11.0
2.0	Lower	4.621557	41837	4689	-19.5
	Outer	4.810192	64594	7239	24.3
	Center	4.715874	51985	5826	-

Table A3.2: M_{01}, k_p values for the outer and lower bounds for VAc experiments at 50 °C and 500 Hz prr with benzoin photoinitiator.

% from the center logM_{01}	Bound	logM_{01}	M_{01}, (g·mol^{-1})	k_p, (L·mol^{-1}·s^{-1})	k_p % dev.
0.20	Lower	4.113217	12978	7272	-1.88
	Outer	4.129703	13480	7554	1.92
0.50	Lower	4.100853	12614	7068	-4.63
	Outer	4.142067	13870	7772	4.86
1.0	Lower	4.080246	12029	6741	-9.05
	Outer	4.162675	14544	8150	9.95
2.0	Lower	4.039031	10940	6130	-17.29
	Outer	4.203889	15992	8961	20.90
	Center	4.121460	13227	7412	-

Table A3.1 and A3.2 tabulate the k_p values obtained for the outer and lower bounds at different percentages from the center, for 100 Hz and 500 Hz prr, respectively. As the deviation from the maximum increases, so does the deviation of the k_p values deviation from the best estimate. The increase in the k_p deviation for both prr is almost same as the deviation from the peak position, close to (2.0%, 5.0%, 10% and 20%) for the respective increase in the logM_{01} of (0.20%, 0.50%, 1.0% and 2.0%) from the center logM_{01}. The same scenario, but in the opposite direction, is observed for the variation in the

lower bound. The results for change by 2% of the logM_{01} yield k_p values off from the center by approximately ±20%. This sensitivity study shows the error that may arise from uncertainty in determining the exact position of the maximum point corresponding to the inflection point on the first derivative plot. Although the uncertainty is greater at 100 Hz due to the broader peaks, the relative error in k_p is similar for both repetition rates, and it is not likely that this uncertainty can lead to the systematic experimental variation in k_p observed with prr.

Appendix 4: NMR Analysis of Vinyl esters monomers

Polyvinyl esters NMR analysis:

Table A4.1: Structures and proton NMR spectrum of polyvinyl acetate and polyvinyl pivalate.

	Polyvinyl acetate[1]	Polyvinyl pivalate[2]
Reference	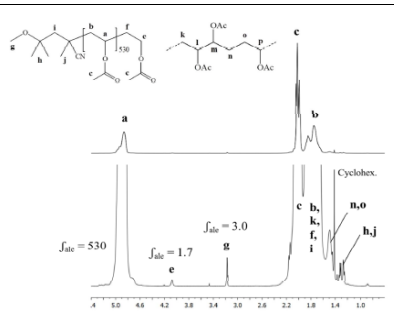	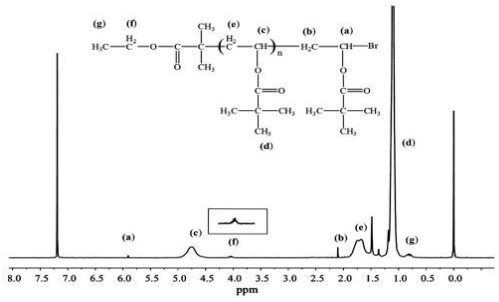
Our work	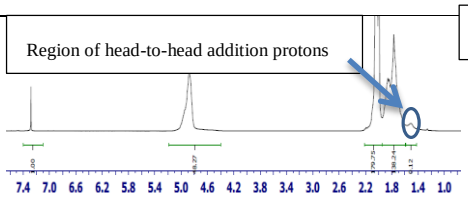	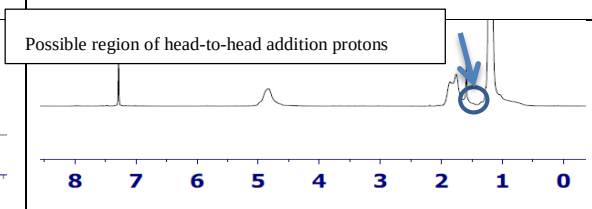

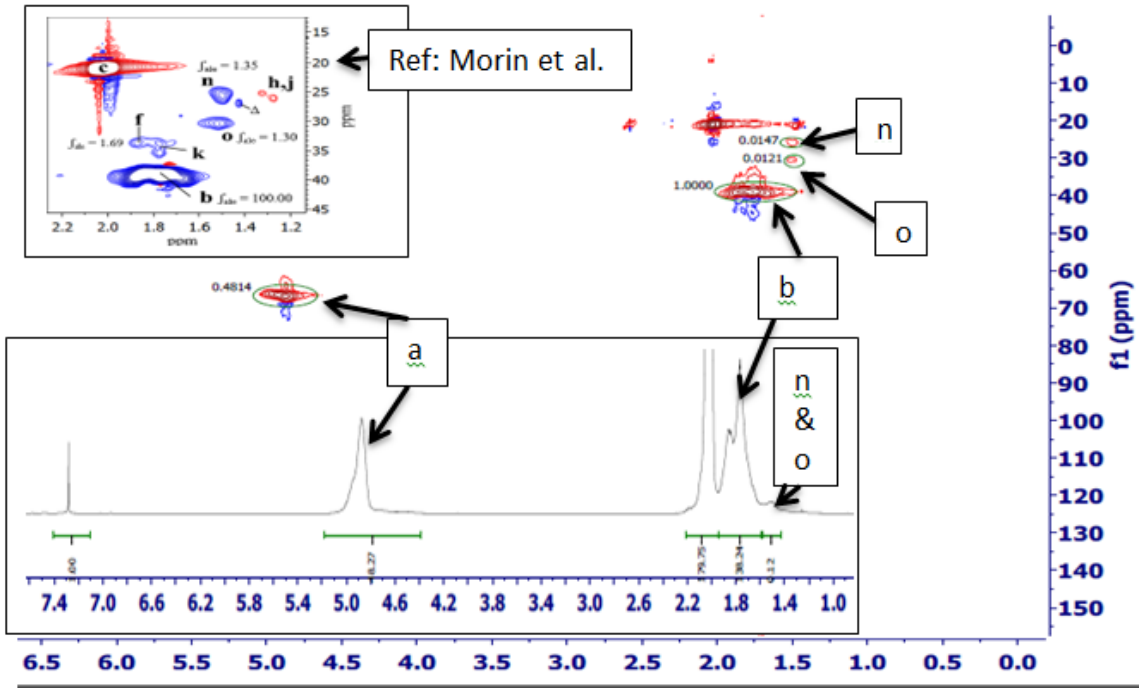

Figure A4.1: HSQC spectrum of poly(VAc) (prepared at 65°C and 100Hz pulse repetition rate) in chloroform-d solvent (with ^{1}H-NMR spectrum).

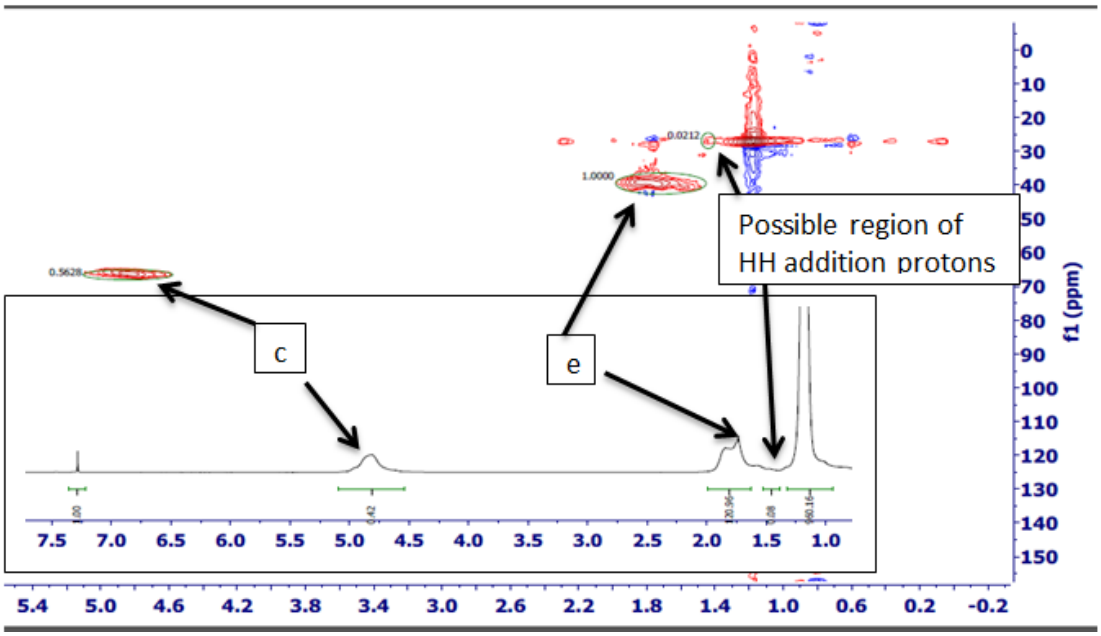

Figure A4.2: HSQC spectrum of poly(VPi) (prepared at 85°C and 100Hz pulse repetition rate) in chloroform-d solvent (with ^{1}H-NMR spectrum).

Figure A4.1 shows the HQSC spectrum of poly(VAc) prepared at 65°C and 100 Hz pulse repetition rate (prr). As illustrated in the figure, the head-to-head addition protons (n and o) can be seen in the region reported by Morin.[1] When these protons are integrated relative to proton 'b' in HQSC-NMR spectrum, the ratio estimated (i.e. 1.31 %) is also close to the value of 1.23% determined by Morin.[1] The chemical shift integration range for these protons were, (b: 1.49-2.0 ppm), (n: 1.45-1.58 ppm) and (o: 1.44-1.60 ppm). NMR analyses were conducted for several experiments conducted at different prr and temperature, with the results summarized in Table A4.2.

Table A4.2: Amount of head-to-head addition present in VAc and VPi polymerization at various temperatures.

		b and a – PVAc; c and e – PVPi		**Protons**		**% HH addition**	**Ref 3**	**Ref 2**	**Ref 4**
		b/e	a/c	n	o				
A	100Hz, 65°C	1.000	0.4814	0.0147	0.0121	1.31	1.22	1.23	-
	100Hz, 50°C	1.000		0.0082	0.0101	0.91	1.17		
	50°C (V-67 initiator)	1.000		0.0092	0.0080	0.85	1.17		
	60°C (V-67 initiator)	1.000	0.5494	0.0143	0.0116	1.26	1.20		1.73
B	100Hz, 85°C	1.000	0.5628	0.0212	-	2.08			
	100Hz, 25°C	1.000	0.5439	0.0230	-	2.49			

A. Poly(VAc) and B- poly (VPi)

From the poly(VAc) results, the integration area of protons (n and o) relative to proton (b) is:

$$= \frac{(int\ area_n + int\ area_o)/2}{int\ area_b + int\ area_n + int\ area_o} = \frac{\frac{0.0147 + 0.0121}{2}}{1.00 + 0.0147 + 0.0121} = 0.0131 = 1.31\%$$

The equation (A4.1) was developed by Flory[3] to relate the amount of head-to-head (HH) addition occurring VAc polymerization to the favorable normal addition (i.e. head-to-tail (HT)).

$$log\Delta = 1.00 - \frac{273}{T} \quad \text{(A4.1)}$$

Where Δ - ratio of the velocity constant (Activation energy) of HH to HT.

Using this equation for one of our sample (i.e. poly(VAc) at 65°C and 100Hz)

$$\Delta = \exp\left(1.00 - \left(\frac{273}{273.15 + 65}\right)\right) = 1.22\%$$

Table A4.2 shows the amount of head-to-head addition (HH) present during polymerization of VAc at different temperatures. It can be observed as the temperatures increases, the amount of HH present also slightly increases. Our experimental results for the amount of HH at 60 °C are closer to the literature

value from Flory[3] compared to the value reported by Otsu:[4] even though both results are between 1-2%, the difference is approximately 27%.

The structure of VPi is similar to that of VAc, with a *tert*-butyl group instead of the methyl group attached to the carbonyl. , Thus, we expect the NMR spectra to have similar characteristics. In particular, as the head-to-head addition (HH) protons region was found for PVAc in HSQC spectrum, we expect to have HH protons of poly(VPi) at the same region. However, as shown in Figure A4.2, there is only one proton detected in the PVPi HSQC spectrum. Although this signal has been used to estimate the level of head-to-head addition that occurs during VPi polymerization (see Table A4.2), it is uncertain whether the value can be considered reliable, due to the differences from the VAc spectrum.

References:

1. A. N. Morin, C. Detrembleur, C. Jérôme, P. De Tullio, R. Poli, A. Debuigne, *Macromolecules* **2013**, *46*, 4303.

2. M. N. Islam, Y. Haldorai, V. H. Nguyen, J.-J. Shim, *Eur. Polym. J.* **2014**, *61*, 93.

3. P. J. Flory, F. S. Leutner, *J. Polym. Sci.* **1948**, *3*, 880.

4. K. Hayashi, T. Ostu, *Makromol. Chem.* **1969**, *127*, 54.

Appendix 5: PLP-SEC Results for Vinyl acetate (VAc) (Chapter 3)

Table A5.1. Vinyl acetate (VAc) bulk homopolymerization kinetics: PLP experimental conditions and SEC results at 25.2 °C with [benzoin] =5mmol·L^{-1} and laser energy of 4.0 mJ per pulse.

Pulse Repetition Rate (Hz)	Initiator	Pulsed Time (s)	Conversion %	SEC Result		
				RI		
				M_1 (g·mol^{-1})	M_2/M_1	k_p from M_1 (L·mol^{-1}·s^{-1})
100	Benzoin	48	0.280	29303	2.00	3166
200	Benzoin	24	0.280	15912	1.91	3439
300	Benzoin	19	0.285	11098	1.91	3597
400	Benzoin	17	0.250	8587	1.96	3711
500	Benzoin	14	0.220	6816	2.01	3682

Table A5.2. Vinyl acetate (VAc) bulk homopolymerization kinetics: PLP experimental conditions and SEC results at 30 °C with [benzoin] =5mmol·L^{-1}, [DMPA] = 5mmol·L^{-1} and [DCP] = 90mmol·L^{-1} and laser energy of 5.3 mJ per pulse.

Pulse Repetition Rate (Hz)	Initiator	Pulsed Time (s)	Conversion %	SEC Result		
				RI		
				M_1 ($g \cdot mol^{-1}$)	M_2/M_1	k_p from M_1 ($L \cdot mol^{-1} \cdot s^{-1}$)
100	Benzoin	64	0.50	33863	2.06	3684
	Benzoin	18	0.42	33084	1.72	3600
	DMPA	33	0.20	31588	2.13	3437
	DCP	27	2.40	32077	1.92	3490
200	Benzoin	35	0.70	18366	1.92	3996
	DMPA	24	0.60	17859	1.96	3886
300	Benzoin	19	0.29	11098	1.91	3597
400	Benzoin	17	0.25	8587	1.96	3711
	DMPA	13	0.6	9240	2.03	4021
500	Benzoin	17	0.6	7551	2.02	4108
	DMPA	13	0.4	7365	2.04	4007
	DCP	18	2.6	7790	2.00	4238

Table A5.3. Vinyl acetate (VAc) bulk homopolymerization kinetics: PLP experimental conditions and SEC results at 40 °C with [benzoin] =5mmol·L^{-1} and laser energy of 3.5 mJ per pulse.

Pulse Repetition Rate (Hz)	Initiator	Pulsed Time (s)	Conversion %	SEC Result		
				RI		
				M_1 (g·mol^{-1})	M_2/M_1	k_p from M_1 (L·mol^{-1}·s^{-1})
100	Benzoin	50	1.80	42207	2.12	4660
200	Benzoin	23	0.4	42289	2.00	4669
300	Benzoin	29	0.92	24295	1.96	5365
400	Benzoin	29	0.94	17030	1.85	5641
500	Benzoin	21	1.10	13071	1.93	5773

Table A5.4. Methyl methacrylate (MMA) bulk homopolymerization kinetics: PLP experimental conditions and SEC results at 50 °C with [DMPA] =5mmol·L^{-1} and laser energy of 3.7 mJ per pulse.

Pulse Repetition Rate (Hz)	Initiator	Pulsed Time (s)	Conversion %	SEC Result
				RI

				M_1 ($g \cdot mol^{-1}$)	M_2/M_1	$k_{p,cop}$ from M_1 ($L \cdot mol^{-1} \cdot s^{-1}$)
20	DMPA	66	0.5	29793	2.05	656
50	DMPA	52	0.4	12915	1.92	711
75	DMPA	34	0.4	8015	2.06	662
100	DMPA	22	0.5	6280	2.10	691
150	DMPA	17	0.4	4246	1.93	701
200	DMPA	19	0.8	3102	2.07	683
300	DMPA	15	0.5	1963	2.25	648

Table A5.5. Vinyl acetate (VAc) bulk homopolymerization kinetics: PLP experimental conditions and SEC results at 50 °C with [benzoin] =5mmol·L^{-1}, [DMPA] = 5mmol·L^{-1} and [DCP] = 90mmol·L^{-1} and laser energy of 3.7 mJ per pulse.

Pulse Repetition Rate (Hz)	Initiator	Pulsed Time (s)	Conversion %	SEC Result						
				RI			LS			$k_{p,LS}/k_{p,RI}$
				M_1	M_2/M_1		M_1	M_2/M_1		

				($g \cdot mol^{-1}$)		k_p from M_1 ($L \cdot mol^{-1} \cdot s^{-1}$)	($g \cdot mol^{-1}$)		k_p from M_1 ($L \cdot mol^{-1} \cdot s^{-1}$)	
100	Benzoin	12	0.9	51985	2.22	5826	52498	-	5883	1.01
	Benzoin	72	0.8	48249	2.24	5407	56330	1.69	6313	1.17
	Benzoin	150	1.7	47065	2.27	5275	55320	1.71	6200	1.18
	Benzoin	105	1.8	49057	2.27	5498	59460	1.69	6664	1.21
200	Benzoin	20	0.3	29942	1.75	6711	26517	1.54	5944	0.89
	DMPA	16	0.4	26943	2.00	6039	28115	1.55	6302	1.04
	DMPA			26076	2.15	5845				
	DCP	23	1.2	30171	1.94	6762	34883	-	7819	1.16
	DCP	17	1.4	29268	2.02	6560	25684	-	5757	0.88
300	Benzoin	19	0.7	21316	1.83	7167	20214	1.50	6796	0.95
	DMPA	11	0.3	19848	1.83	6673				
	DCP	15	1.5	20420	1.90	6866				

400	Benzoin	12	0.9	16320	1.85	7316	13794	1.81	6183	0.85
	DMPA	11	0.7	15596	1.86	6992				
	DCP	22	0.7	16893	2.29	7562				
500	Benzoin	10	0.4	13227	1.91	7412				
	Benzoin	27	0.6	13528	1.87	7580	12980	1.82	7273	0.96
	Benzoin	52	1.4	13438	1.85	7530	14580	1.71	8170	1.08
	Benzoin	51	1.5	13710	1.83	7683				
	DMPA	10	0.5	12965	1.82	7265	12366	1.93	6929	0.95
	DCP	10	1.6	13495	1.84	7573				

Table A5.6. Vinyl acetate (VAc) bulk homopolymerization kinetics: PLP experimental conditions and SEC results at 60 °C with [benzoin] =5mmol·L^{-1} and laser energy of 3.5 mJ per pulse.

Pulse Repetition Rate (Hz)	Initiator	Pulsed Time (s)	Conversion %	SEC Result		
				RI		
				M_1 ($g \cdot mol^{-1}$)	M_2/M_1	k_p from M_1 ($L \cdot mol^{-1} \cdot s^{-1}$)
100	Benzoin	29	1.0	64202	2.18	7305
200	Benzoin	25	1.3	36287	2.06	8257
300	Benzoin	22	1.3	25577	1.98	8730
400	Benzoin	19	1.3	20434	1.86	9300
500	Benzoin	16	1.7	17267	1.83	9823

Table A5.7. Vinyl acetate (VAc) bulk homopolymerization kinetics: PLP experimental conditions and SEC results at 65 °C with [benzoin] =5mmol·L^{-1} and laser energy of 4.3 mJ per pulse.

Pulse Repetition Rate (Hz)	Initiator	Pulsed Time (s)	Conversion %	SEC Result						
				RI			LS			$k_{p,cop,LS}/k_{p,cop,RI}$
				M_1 ($g\cdot mol^{-1}$)	M_2/M_1	$k_{p,cop}$ from M_1 ($L\cdot mol^{-1}\cdot s^{-1}$)	M_1 ($g\cdot mol^{-1}$)	M_2/M_1	$k_{p,cop}$ from M_1 ($L\cdot mol^{-1}\cdot s^{-1}$)	
100	Benzoin	33	0.51	69811	1.85	8004	76300	2.18	8748	1.09
200	Benzoin	30	1.21	36945	2.07	8472	35170	2.13	8065	0.95
300	Benzoin	19	0.93	27181	2.00	9349	27360	1.91	9411	1.01
400	Benzoin	16	0.54	21352	1.93	9792	19750	1.72	9058	0.92
500	Benzoin	13	0.71	17895	1.70	10258	19040	1.70	10915	1.06

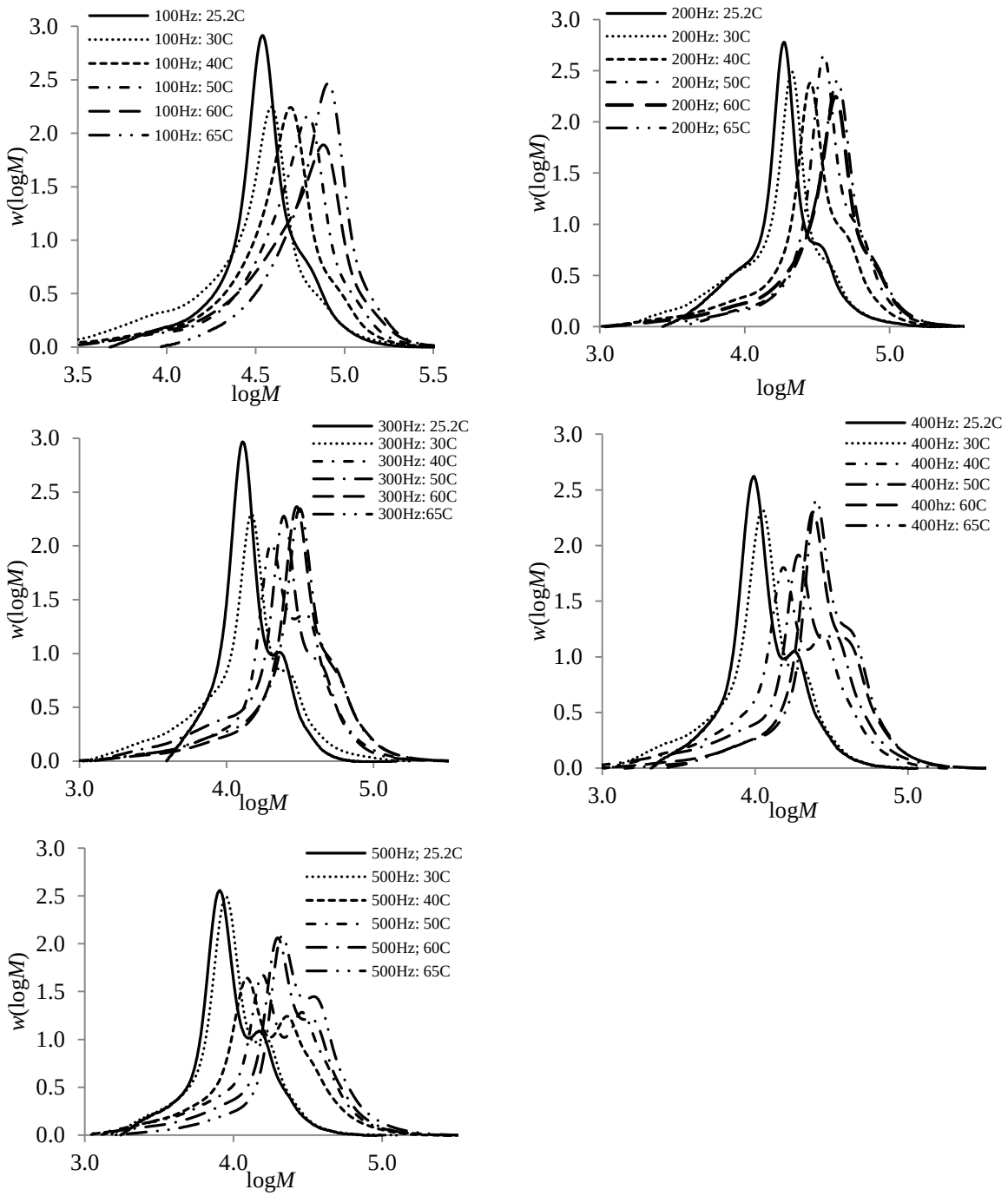

Figure A5.1. MMDs plots for poly(VAc) produced by PLP at various pulse repetition rates and temperature with benzoin photoinitiator.

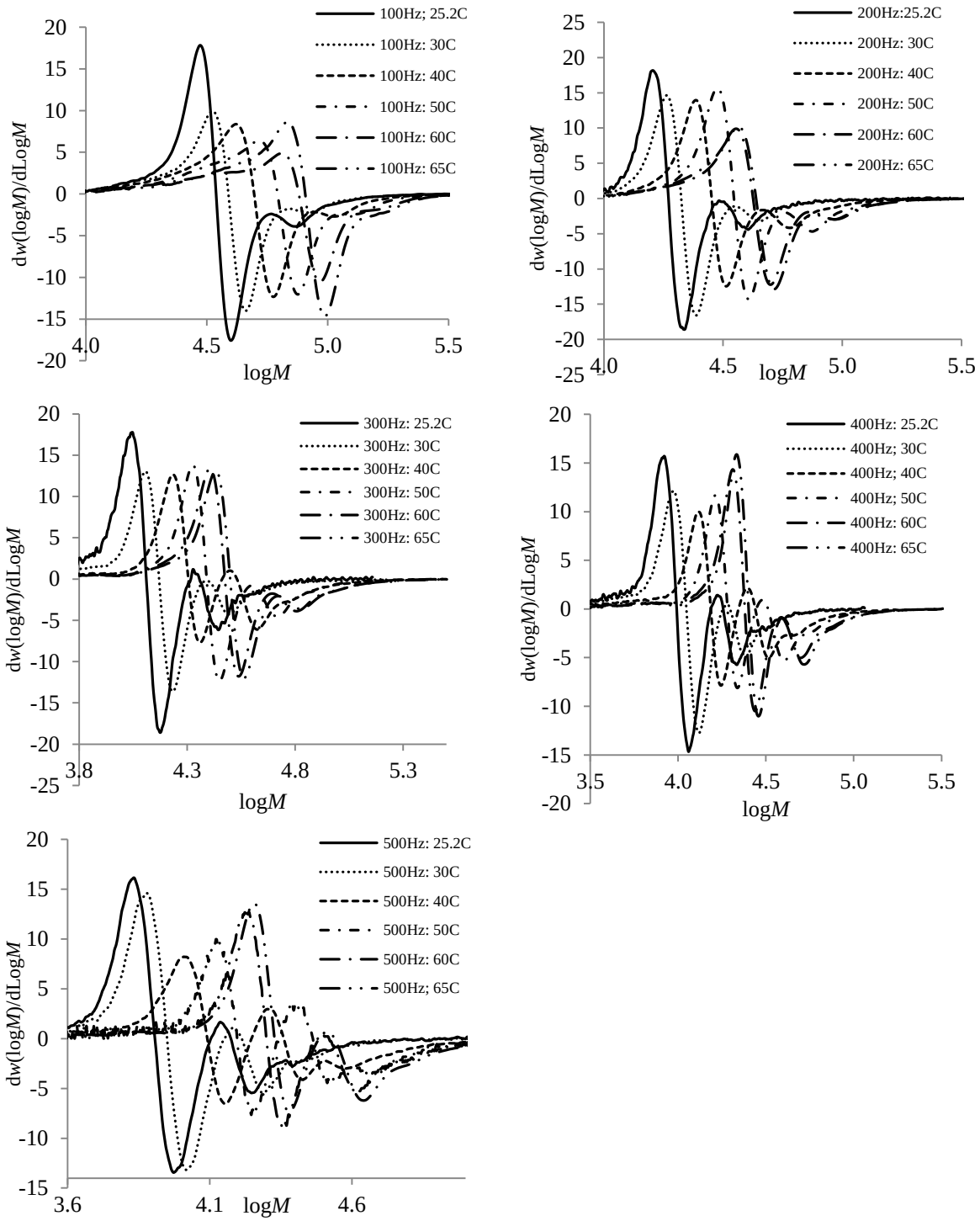

Figure A5.2. MMDs first-derivative plots for poly(VAc) produced by PLP at various pulse repetition rates and temperature with benzoin photoinitiator.

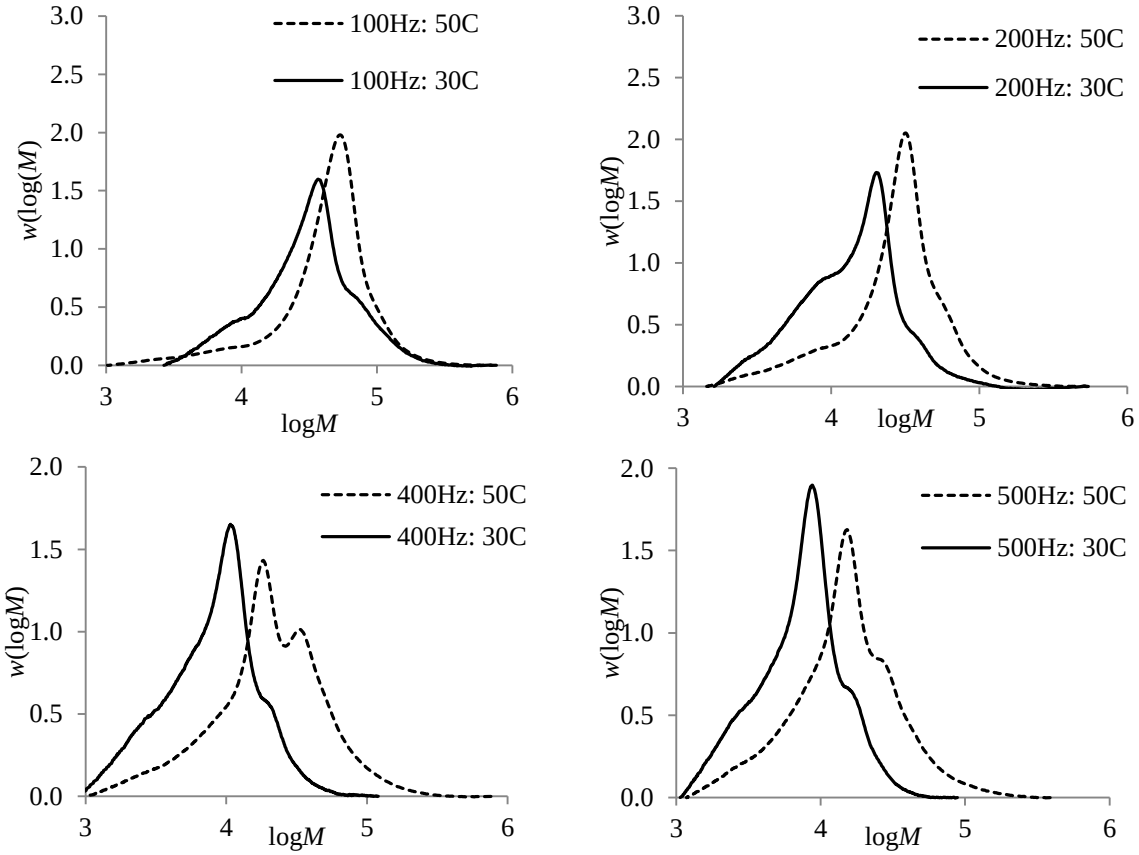

Figure A5.3. MMDs plots for poly(VAc) produced by PLP at various pulse repetition rates and temperature with DMPA photoinitiator.

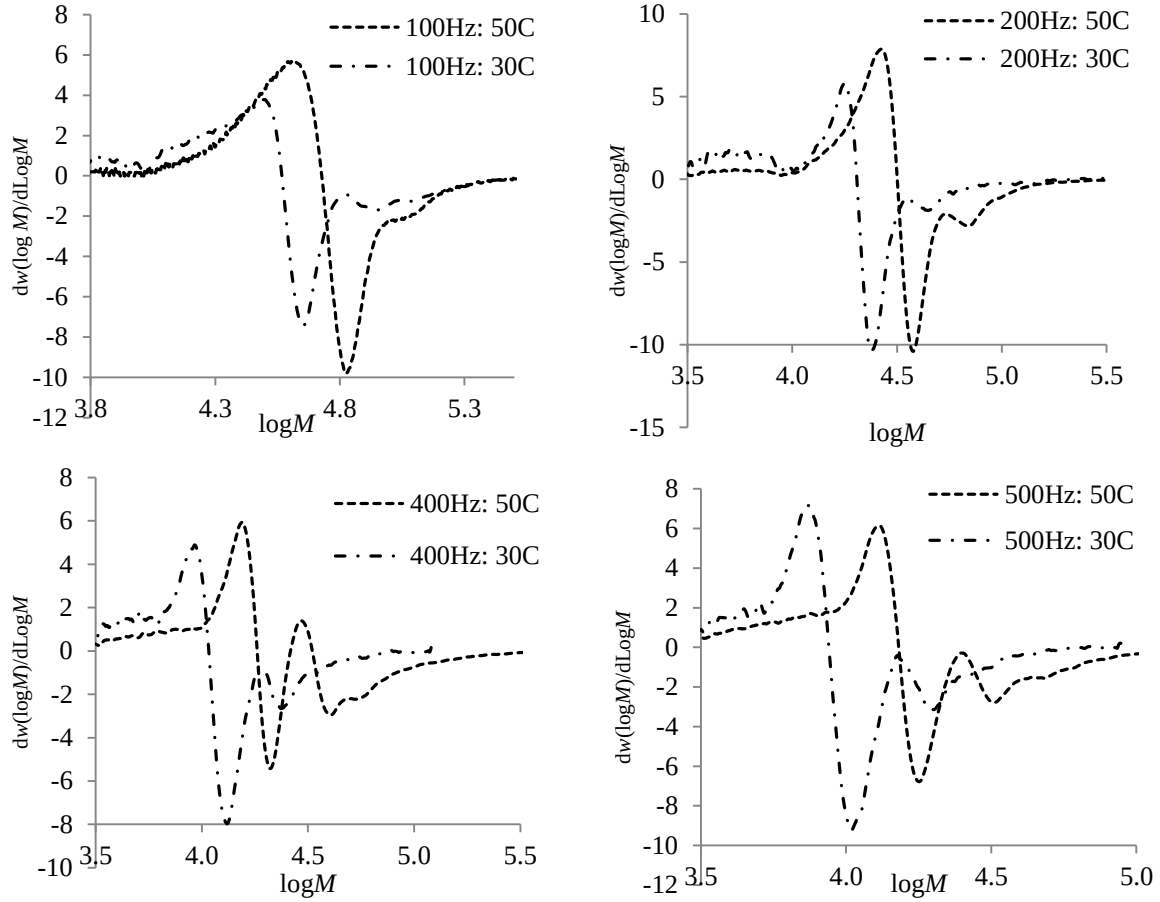

Figure A5.4. MMDs first-derivative plots for poly(VAc) produced by PLP at various pulse repetition rates and temperature with DMPA photoinitiator.

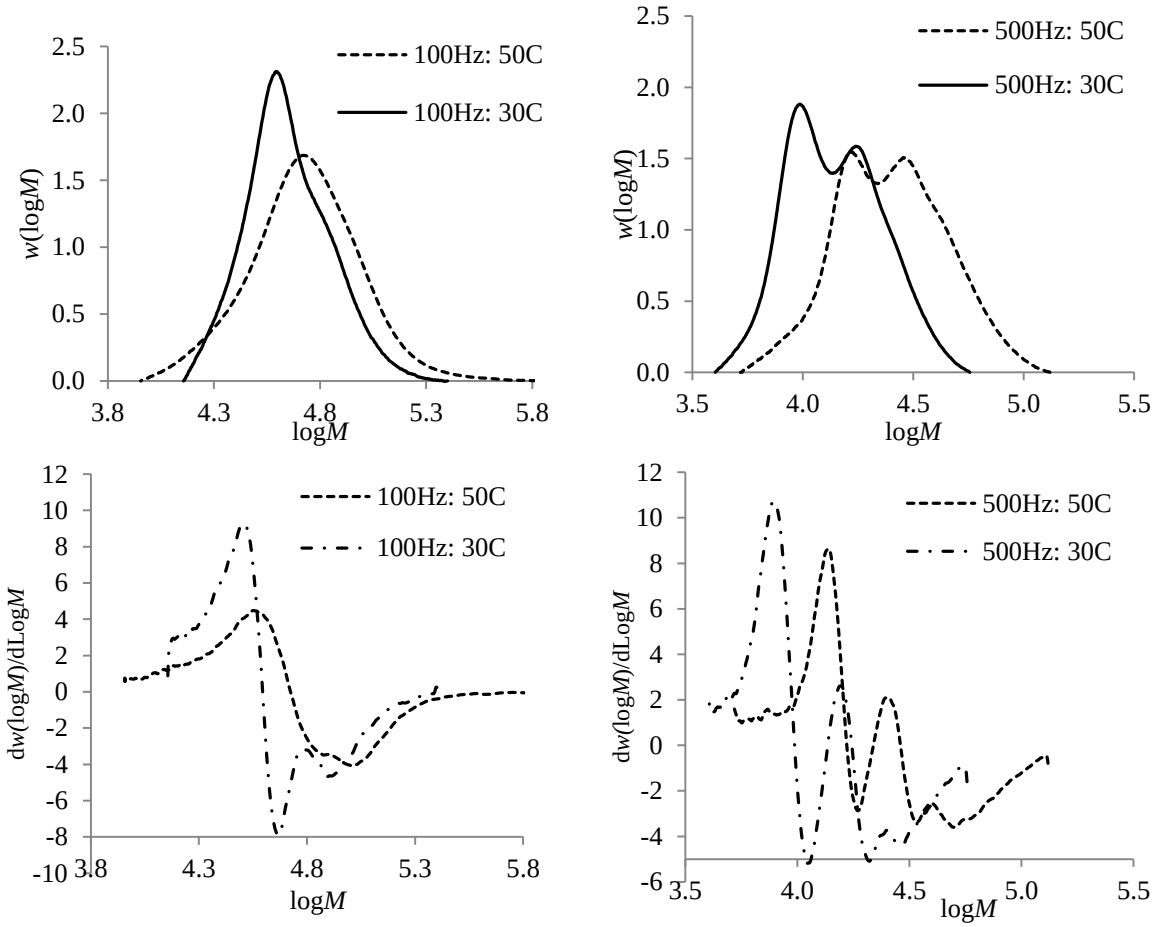

Figure A5.5. MMDs and corresponding first-derivative plots for poly(VAc) produced by PLP at various pulse repetition rate and temperature with DCP photoinitiator.

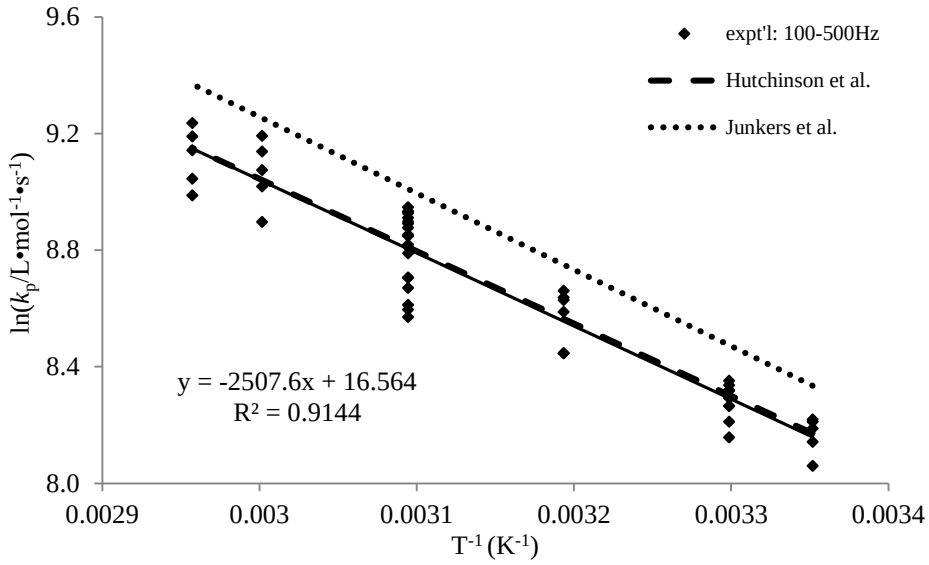

Figure A5.6. A comparison of VAc apparent propagation rate coefficients obtained from all experiments conducted at 100 to 500 Hz and best Arrhenius fit (line) to predictions from Arrhenius fits taken from literature

Appendix 6: PLP-SEC Results for Vinyl pivalate (VPi) and Vinyl benzoate (VBz) (Chapter 4)

Determination of VPi density

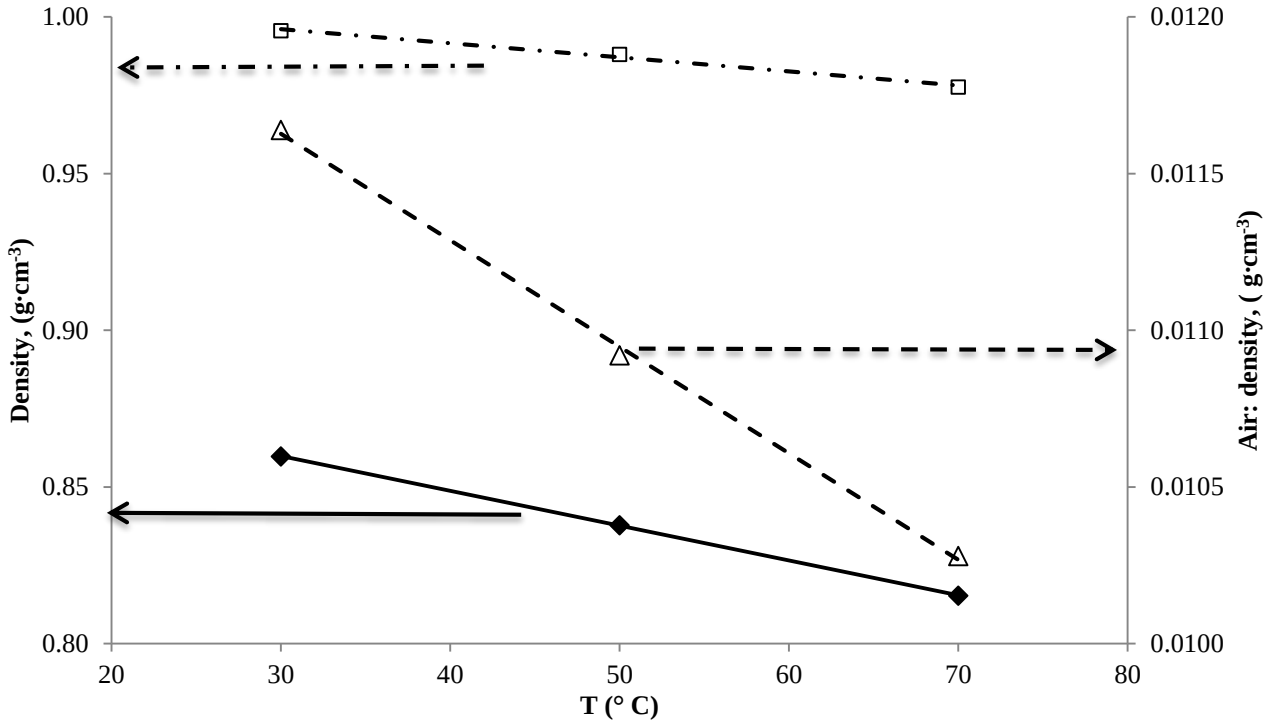

Figure A6.1: Density vs. Temperature graph for air (Δ), water (□) and VPi (♦).

SEC Calibration Parameters for PVPi

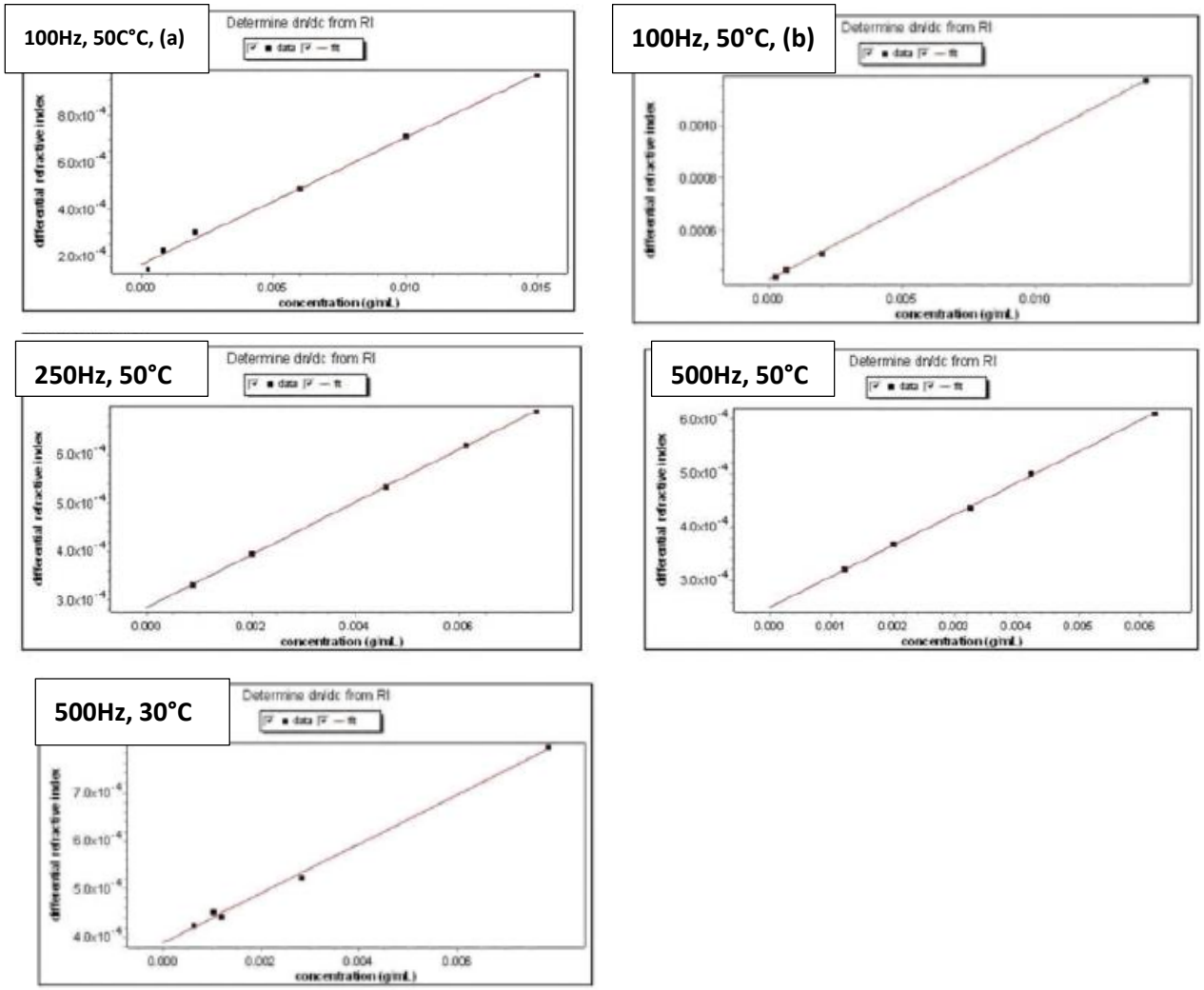

Figure A6.2. Determination of the d*n*/d*c* value for poly(VPi) in THF at 35 °C.

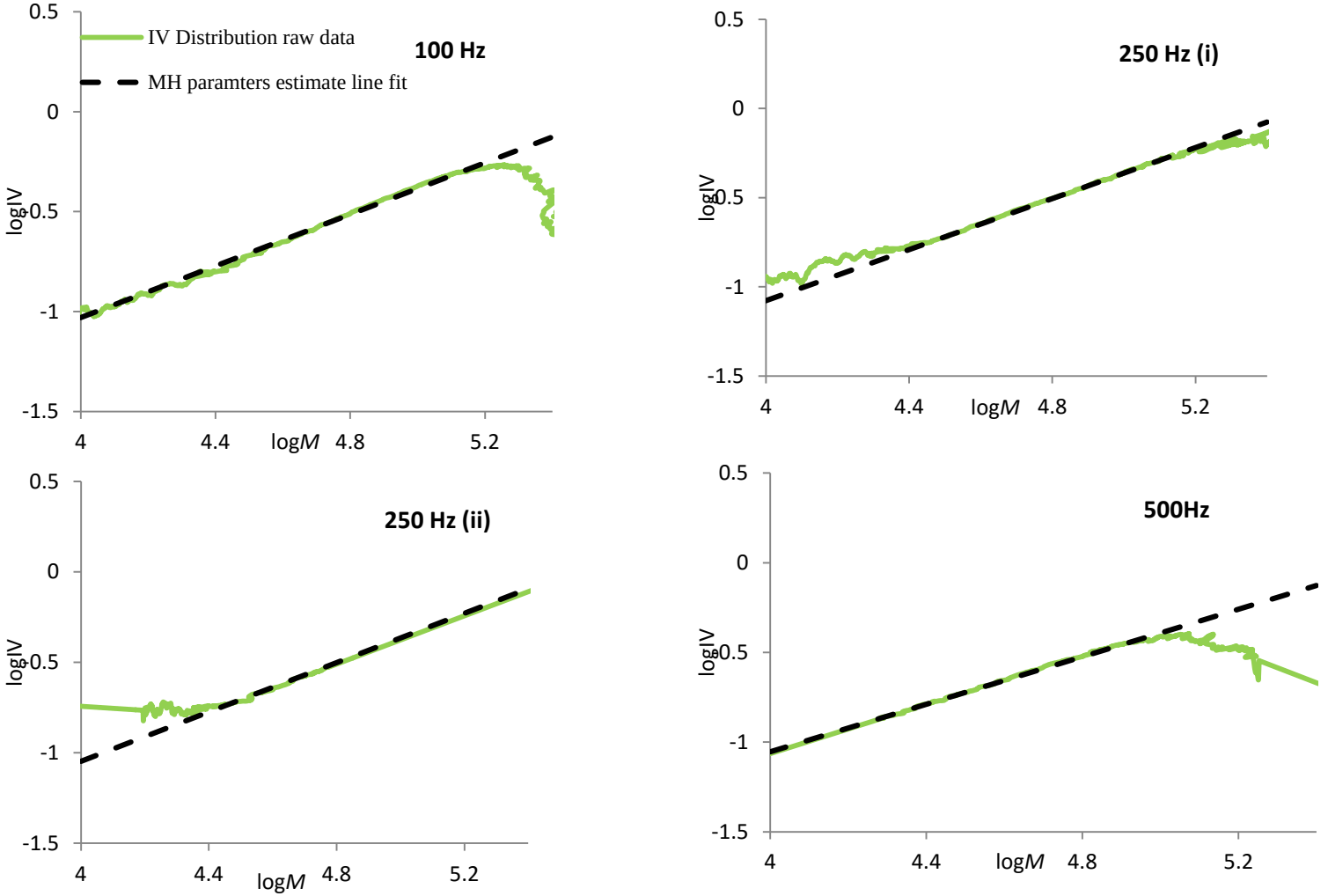

Figure A6.3. log*IV* vs. log*M* for PVPi samples prepared by PLP and used to estimate Mark-Houwink parameters from TD-SEC.

SEC Calibration Parameters for PVBz

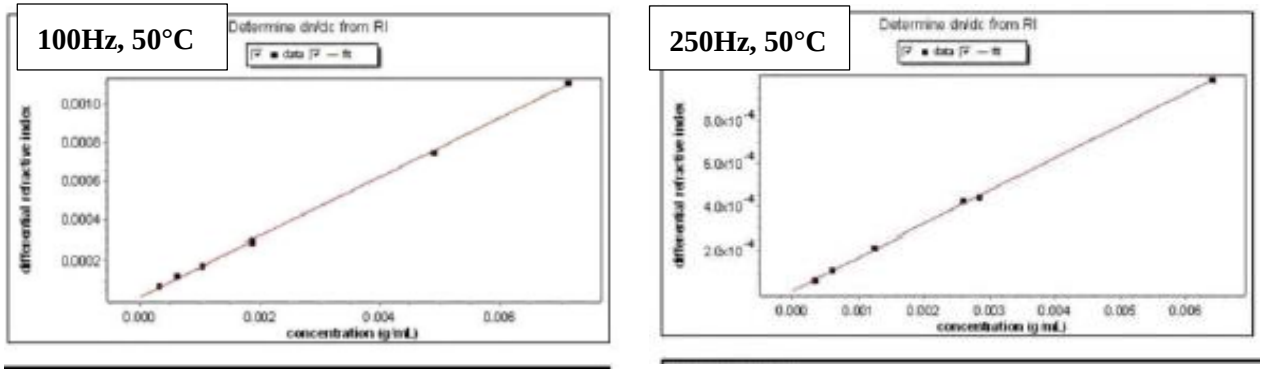

Figure A6.4. Determination of the d*n*/d*c* value for poly(VBz) in THF at 35 °C.

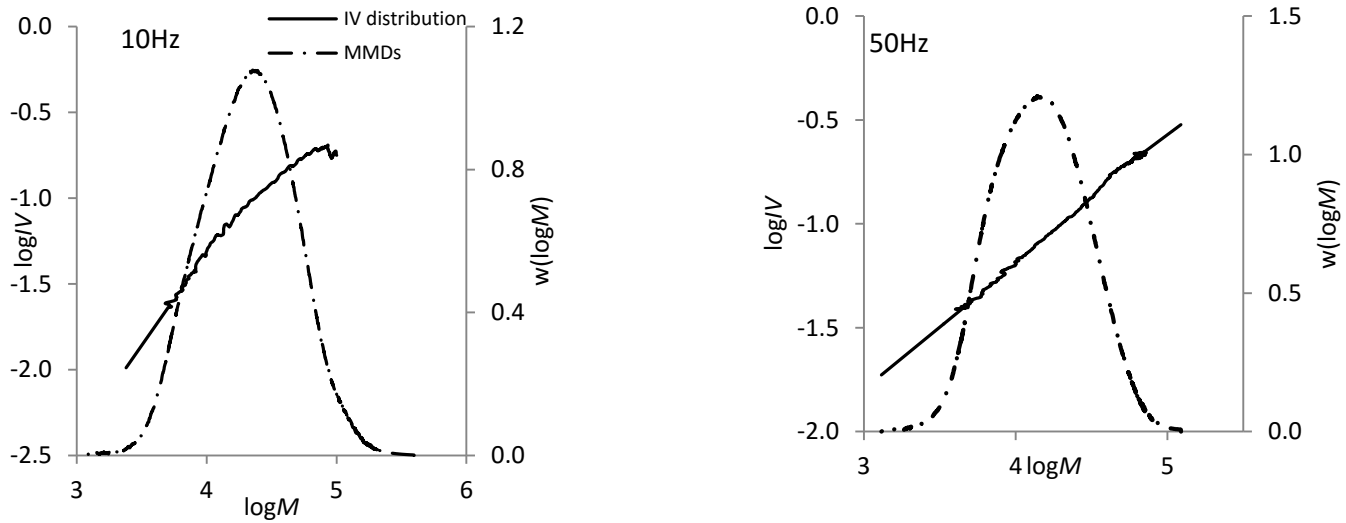

Figure A6.5. logIV vs. logM for PVBz samples prepared by PLP and used to estimate Mark-Houwink parameters from TD-SEC (top),. and global fit performed to estimate MH parameters (bottom).

Table A6.1. The *d*n/*d*c values determined for polyvinyl pivalate (PVPi) samples prepared by PLP at various pulse repetition rate and temperatures, as indicated.

Pulse repetition rate, (Hz)	Temperature (°C)	R^2	*d*n/*d*c, (mL·g^{-1})
100Hz	50	0.9952	0.0546 ± 0.0017
100Hz	50	0.9998	0.0537 ± 0.0004
250Hz	50	0.9997	0.0544 ± 0.0004
500Hz	30	0.9966	0.0512 ± 0.0015
500Hz	50	0.9996	0.0580 ±0.0006
Average			0.054

Table A6.2. d*n*/d*c* values obtained for pVBz prepared at 100 and 250Hz pulse repetition rate and 50°C with [benzoin]=5mmol·L^{-1}

Pulse repetition rate, Hz	**R^2**	**d*n*/d*c***, mL·g^{-1}
100	0.999209	0.1528 ± 0.0019
250	0.999474	0.1526 ± 0.0016
Average (Global fit)		0.1527

Table A6.3. MH parameters used to interpret PLP-SEC results and determine k_p for VBz experiments

Prr (Hz)	*K* (dL·g^{-1}) × 10^{-4}	*a*	$[\eta]=K^*(MW)^{a^{**}}$
10	1.37	0.651	0.247
50	1.70	0.645	0.285
Average (Global fit)	1.53	0.648	0.265

**calculated for equivalent MW of 10^5 Da

Detailed Results from PLP study of Vinyl Pivalate

Table A6.4. Vinyl pivalate (VPi) bulk homopolymerization kinetics: PLP experimental conditions and SEC results at 25°C with [benzoin] =5mmol·L^{-1} and laser energy of 4.0 mJ per pulse.

Pulse Repetition Rate (Hz)	Initiator	Pulsed Time (s)	Conversion %	SEC Result		
				RI		
				M_1 ($g \cdot mol^{-1}$)	M_2/M_1	k_p from M_1 ($L \cdot mol^{-1} \cdot s^{-1}$)
100	Benzoin	27	0.34	42400	2.20	4899
200	Benzoin	22	0.35	24230	1.81	5599
300	Benzoin	26	0.63	16864	1.91	5845
400	Benzoin	17	0.36	12939	1.90	5980
500	Benzoin	18	0.54	10211	2.01	5898

Table A6.5. Vinyl pivalate (VPi) bulk homopolymerization kinetics: PLP experimental conditions and SEC results at 30 °C with [benzoin] =5mmol·L^{-1} and laser energy of 4.84 mJ per pulse.

Pulse Repetition Rate (Hz)	Initiator	Pulsed Time (s)	Conversion %	SEC Result		
				RI		
				M_1 ($g \cdot mol^{-1}$)	M_2/M_1	k_p from M_1 ($L \cdot mol^{-1} \cdot s^{-1}$)
100	Benzoin	30	0.21	45180	-	5253
100	Benzoin	37	0.29	38512	-	4478
200	Benzoin	24	0.39	29652	1.81	6896
300	Benzoin	23	0.26	20015	1.78	6982
400	Benzoin	18	0.35	15177	1.95	7059
500	Benzoin	16	0.68	13267	1.97	7713

Table A6.6. Vinyl pivalate (VPi) bulk homopolymerization kinetics: PLP experimental conditions and SEC results at 40 °C with [benzoin] =5mmol·L^{-1} and laser energy of 3.72 mJ per pulse.

Pulse Repetition Rate (Hz)	Initiator	Pulsed Time (s)	Conversion %	SEC Result						
				RI			LS			$k_{p,LS}/k_{p,RI}$
				M_1 (g·mol^{-1})	M_2/M_1	k_p from M_1 (L·mol^{-1}·s^{-1})	M_1 (g·mol^{-1})	M_2/M_1	k_p from M_1 (L·mol^{-1}·s^{-1})	
100	Benzoin	27	0.98	53442	-	6274	57590	-	6784	1.08
100	Benzoin	40	1.12	50008	-	5891	58300	1.91	6868	1.17
200	Benzoin	18	0.68	31740	2.01	7478				
300	Benzoin	17	0.90	23085	1.79	8158				
400	Benzoin	14	0.75	18400	1.74	8670				
500	Benzoin	12	0.54	14672	1.89	8642				

Table A6.7. Vinyl pivalate (VPi) bulk homopolymerization kinetics: PLP experimental conditions and SEC results at 50 °C with [benzoin] =5mmol·L^{-1} and laser energy of 3.7-3.84 mJ per pulse.

Pulse Repetition Rate (Hz)	Initiator	Pulsed Time (s)	Conversion %	SEC Result						
				RI			LS			$k_{p,LS}/k_{p,RI}$
				M_1 (g·mol^{-1})	M_2/M_1	k_p from M_1 (L·mol^{-1}·s^{-1})	M_1 (g·mol^{-1})	M_2/M_1	k_p from M_1 (L·mol^{-1}·s^{-1})	
100	Benzoin	37	1.07	69122	2.11	8250	-	-	-	-
100	Benzoin	26	0.84	72586	-	8664	72720	1.82	8680	1.00
100	Benzoin	27	1.34	75213	-	8977	-	-	-	-
200	Benzoin	31	1.47	39141	2.06	9344	-	-	-	-
200	Benzoin	16	0.72	40063	2.17	9564	47990	1.82	11456	1.20
300	Benzoin	33	2.12	28736	1.94	10290	-	-	-	-
300	Benzoin	16	0.96	30101	1.96	10779	29020	1.89	10392	0.96
400	Benzoin	26	1,43	22049	1.91	10527	-	-	-	-
400	Benzoin	15	0.88	24110	1.77	11511	23330	1.83	11139	0.97
500	Benzoin	28	2.08	18205	1.90	10865	-	-	-	-
500	Benzoin	13	0.77	19874	1.82	11861	20850	1.78	12443	1.05

Table A6.8. Vinyl pivalate (VPi) bulk homopolymerization kinetics: PLP experimental conditions and SEC results at 70 °C with [benzoin] =5mmol·L^{-1} and laser energy of 3.72- 4.68 mJ per pulse.

Pulse Repetition Rate (Hz)	Initiator	Pulsed Time (s)	Conversion %	SEC Result						
				RI			LS			$k_{p,cop,LS}/k_{p,cop,RI}$
				M_1 (g·mol^{-1})	M_2/M_1	$k_{p,cop}$ from M_1 (L·mol^{-1}·s^{-1})	M_1 (g·mol^{-1})	M_2/M_1	$k_{p,cop}$ from M_1 (L·mol^{-1}·s^{-1})	
100	Benzoin	20	0.81	84569	-	10369	-	-	-	-
100	Benzoin	32	1.02	87219	-	10694	103200	-	12653	1.18
200	Benzoin	14	1.05	54158	2.21	13280	61690	1.86	15128	1.14
300	Benzoin	16	1.98	41029	2.06	15092	44970	1.87	16541	1.10
400	Benzoin	12	1.40	32227	1.99	15805	36480	1.96	17891	1.13
500	Benzoin	12	1.02	27722	1.83	16995	33650	1.70	20629	1.21

Table A6.9. Vinyl pivalate (VPi) bulk homopolymerization kinetics: PLP experimental conditions and SEC results at 85 °C with [benzoin] =5mmol·L^{-1} and laser energy of 2.56 - 4.84 mJ per pulse.

Pulse Repetition Rate (Hz)	Initiator	Pulsed Time (s)	Conversion %	SEC Result						
				RI			LS			$k_{p,cop,LS}/k_{p,cop,RI}$
				M_1 (g·mol^{-1})	M_2/M_1	$k_{p,cop}$ from M_1 (L·mol^{-1}·s^{-1})	M_1 (g·mol^{-1})	M_2/M_1	$k_{p,cop}$ from M_1 (L·mol^{-1}·s^{-1})	
100	Benzoin	23	1.09	89352	-	11184	115000	-	14394	-
100	Benzoin	25	1.68	94784	-	11864	113300	-	14181	1.20
200	Benzoin	17	1.33	68847	-	17234	79820	1.97	19981	1.16
300	Benzoin	16	2.22	49023	2.16	18408	57430	1.92	21565	1.17
400	Benzoin	17	2.84	40382	2.06	20218	43970	1.97	22014	1.09
500	Benzoin	10	0.81	35617	1.98	22290	34510	1.94	21597	0.97

Table A6.10. VAc and VPi solvent (heptane and ethyl acetate (EAc)) homo-polymerization kinetics: SEC results at 50°C with [benzoin] = 5mmol·L^{-1}

	Solvent	Prr, Hz	M_1, g·mol^{-1}	M_2/M_1	k_{psol}, L·mol^{-1}·s^{-1}	k_{pbulk}, L·mol^{-1}·s^{-1}	$k_{pheptane}/k_{pEAc}$	k_{psol}/k_{pbulk}	k_{psol}/k_{pref}
VAc	Heptane	200	19168	1.94	8593	6711 [1]	1.26	1.28	
		200	17348	1.76	7777	6711	1.14	1.16	
		300	12897	1.93	8672	7167	-	1.21	
		400	9836	2.02	8818	7316	-	1.21	
		500	7838	1.98	8784	7412	1.24	1.19	
		500	7519	2.07	8427	7412	1.19	1.14	
	EAc	200	15195	1.90	6812	6711		1.02	
		500	6318	2.01	7080	7412		0.96	
VPi	Heptane	200	22068	1.97	10536	9344	1.22	1.13	1.56
		200	21815	2.08	10416	9344	1.20	1.11	1.54
		300	15742	1.96	11274	10290	-	1.13	1.67
		400	12310	1.84	11754	10527	-	1.10	1.74
		500	9559	1.95	11410	10865	1.30	1.05	1.69
		500	9269	2.04	11063	10865	1.27	1.02	1.64
	EAc	200	18062	1.86	8623	9344		0.92	1.28
		500	7308	2.01	8723	10865		0.80	1.29
Ref[2]					6748				

[1] O. Monyatsi, A. N. Nikitin, R. A. Hutchinson, *Macromolecules* **2014**, *47*, 8145

[2] N. Kubota, A. Kajiwara, P. B. Zetterlund, M. Kamachi, J. Treurnicht, M. P. Tonge, R. G. Gilbert, B. Yamada, *Macromol. Chem. Phys.* **2007**, *208*, 2403.

PLP-SEC MMDs for VPi (bulk) experiments

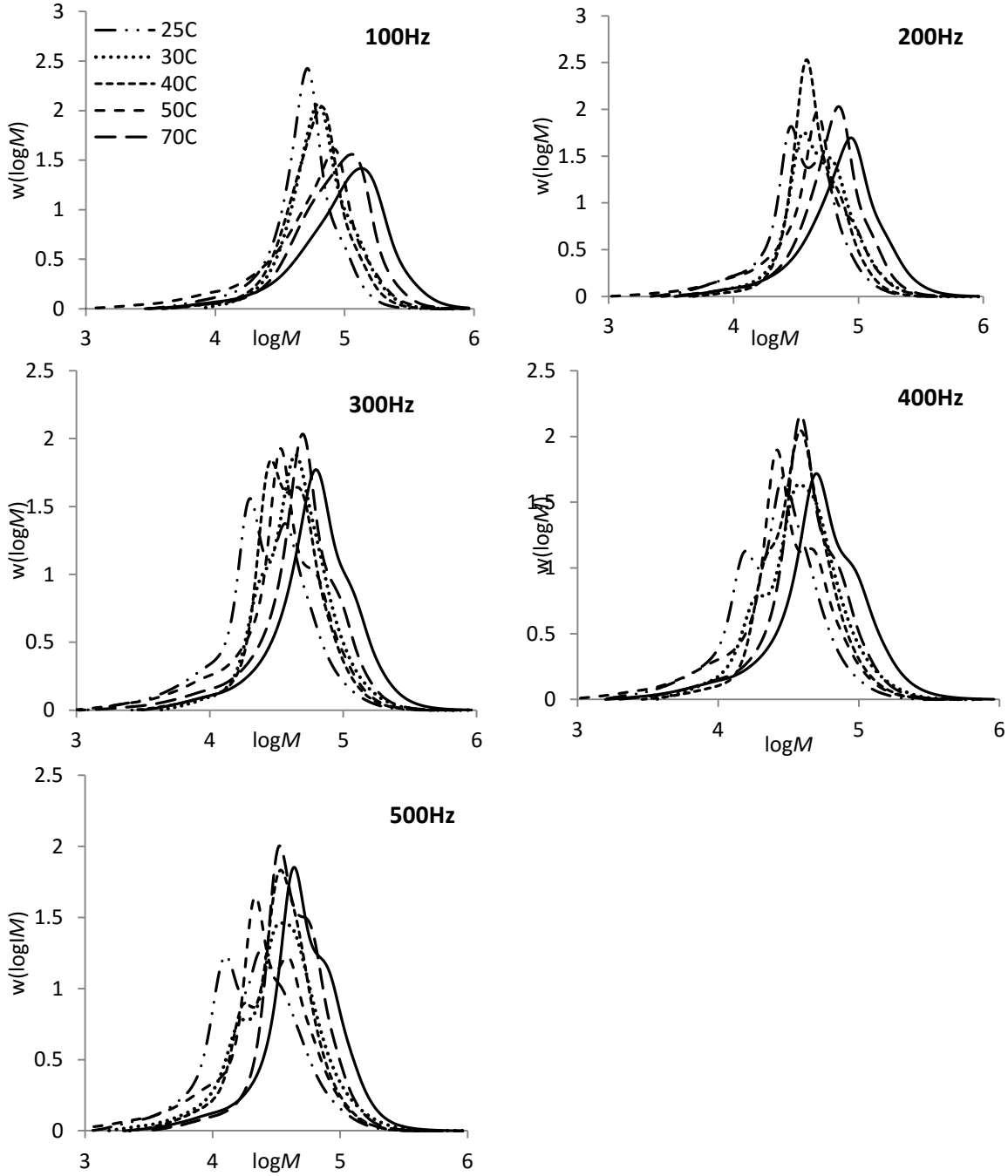

Figure A6.6. MMDs plots for poly(VPi) produced by PLP at constant pulse repetition rates and varying temperature with benzoin photoinitiator.

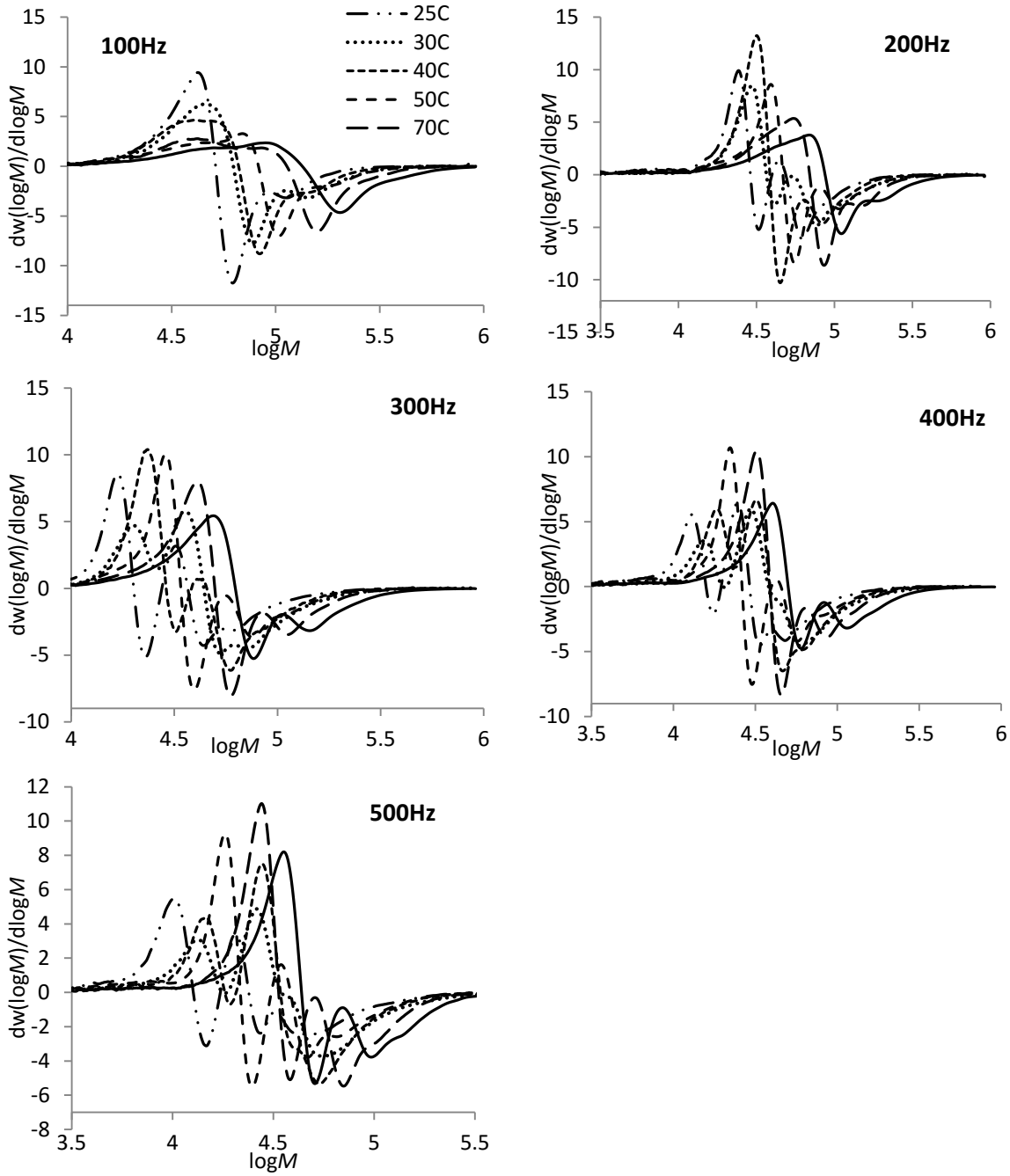

Figure A6.7. MMDs first-derivative plots for poly(VPi) produced by PLP at constant pulse repetition rates and varying temperature with benzoin photoinitiator.

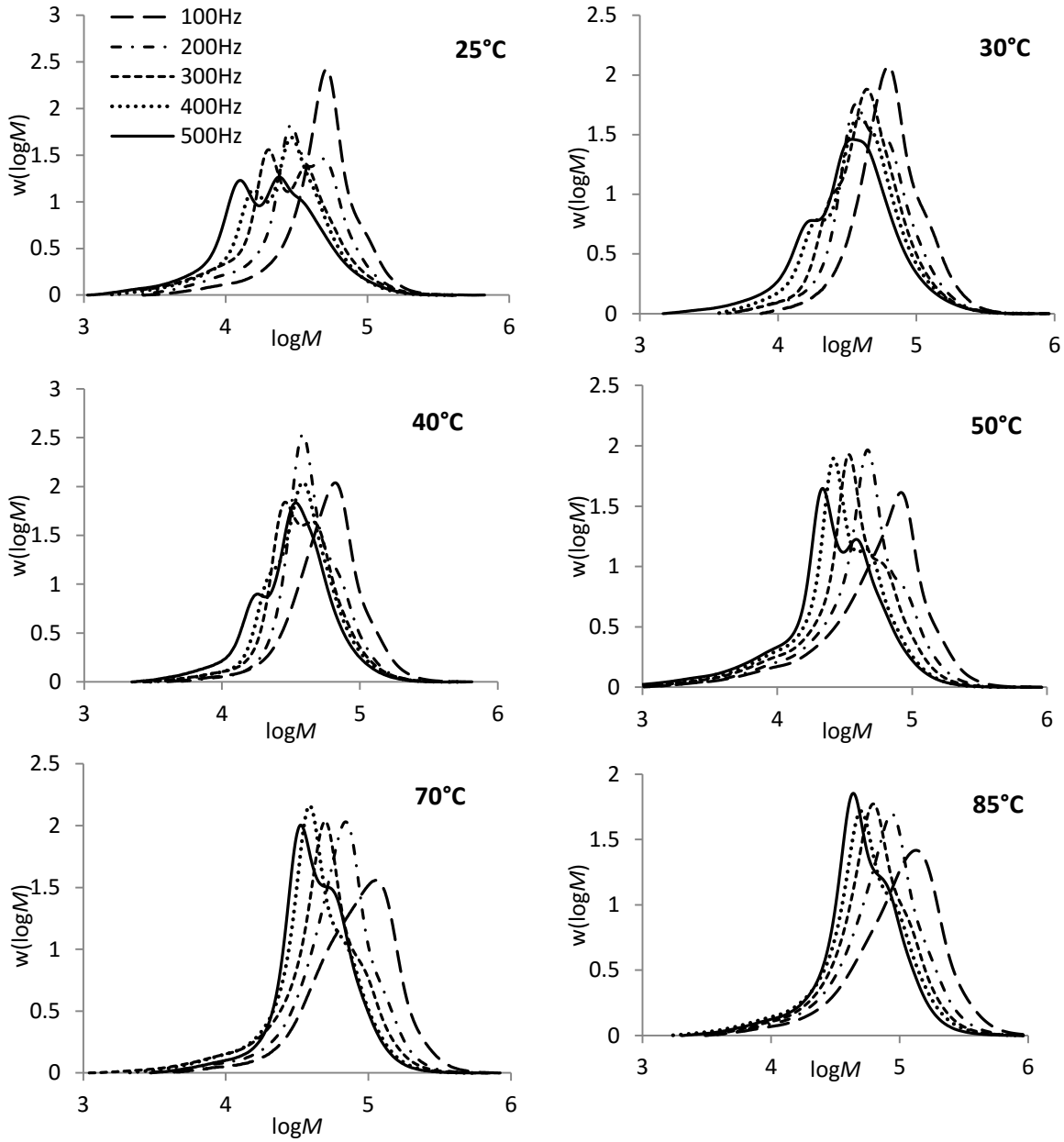

Figure A6.8. MMDs plots for poly(VPi) produced by PLP at constant temperature and varying pulse repetition rates with benzoin photoinitiator.

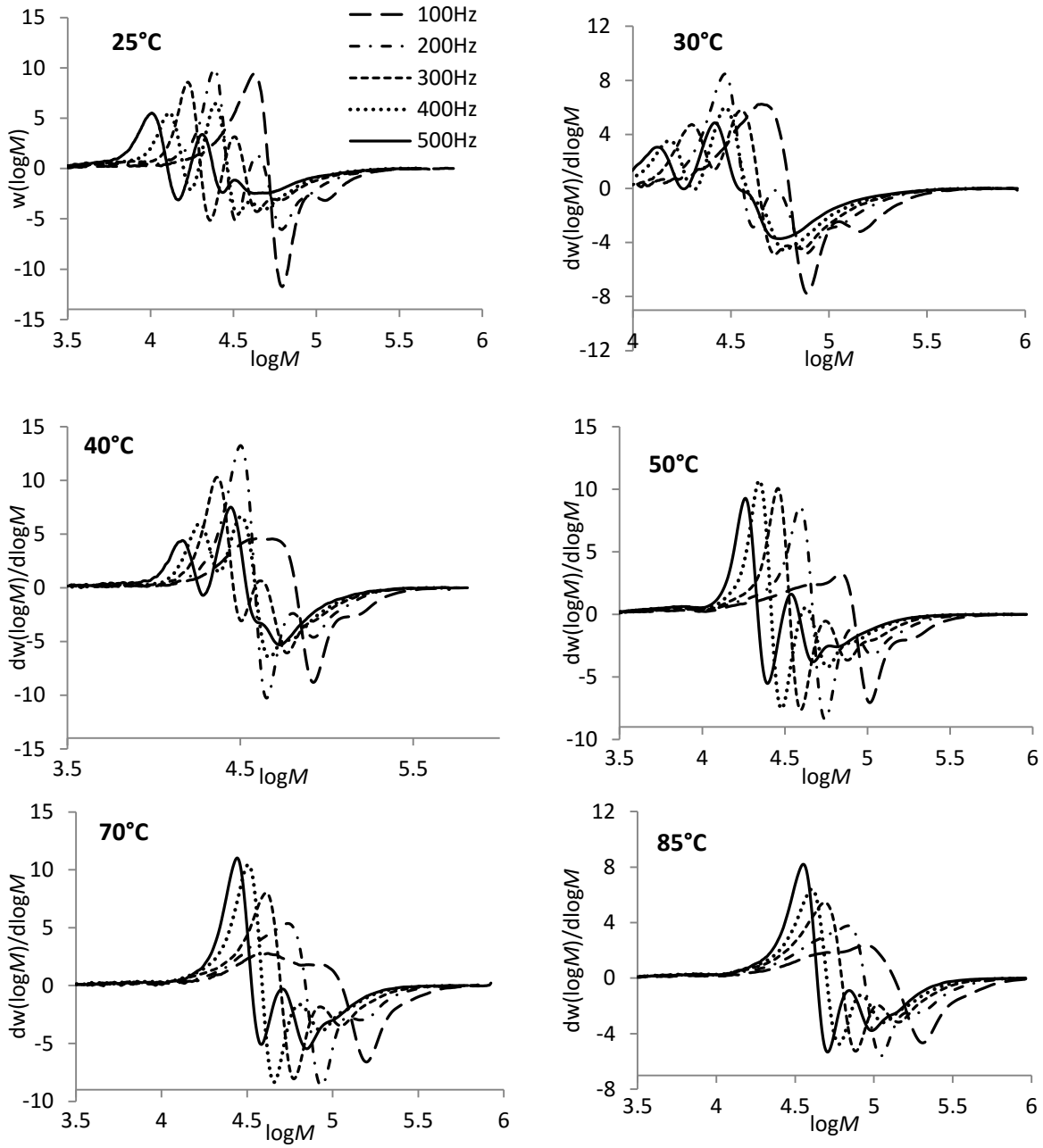

Figure A6.9. MMDs first-derivative plots for poly(VPi) produced by PLP at constant temperature and varying pulse repetition rates with benzoin photoinitiator.

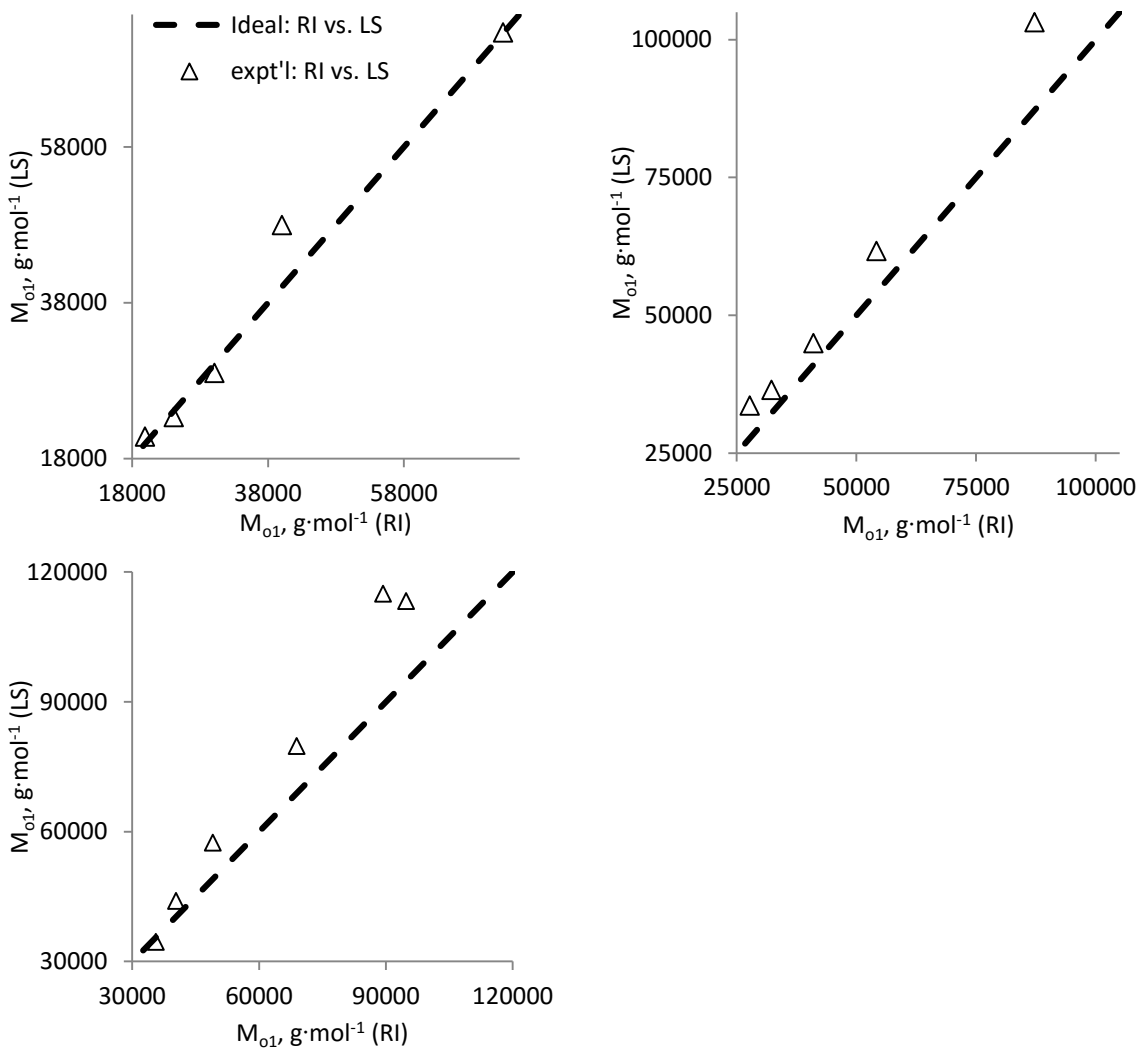

Figure A6.10. A comparison of inflection points determined by RI and LS detectors for PVPi produced by PLP at 50 (top left), 70 (top right) and 85 (bottom left) °C.

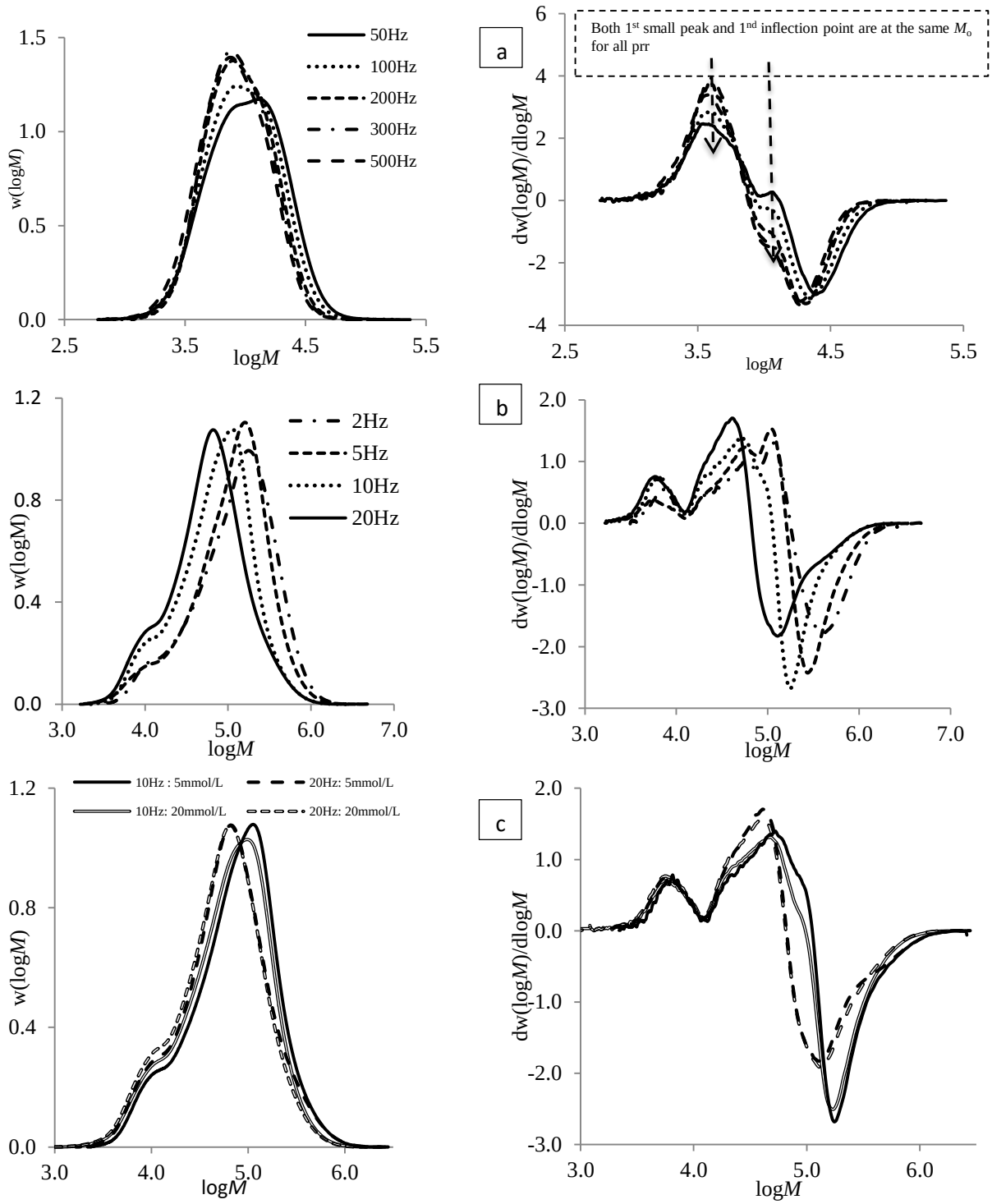

Figure A6.11. MMDs (left) and corresponding first derivative plots (right) for poly(VBz) produced by PLP: at 50 °C with [Benzoin] =5mmol·L^{-1} and varying prr (a), at 90 °C with [Benzoin] =5mmol·L^{-1} and varying prr (b), at 50 °C and 10–20 Hz with varying [Benzoin] (c).

PLP-SEC MMDs of VAc and VPi experiments in heptane and ethyl acetate (EAc)

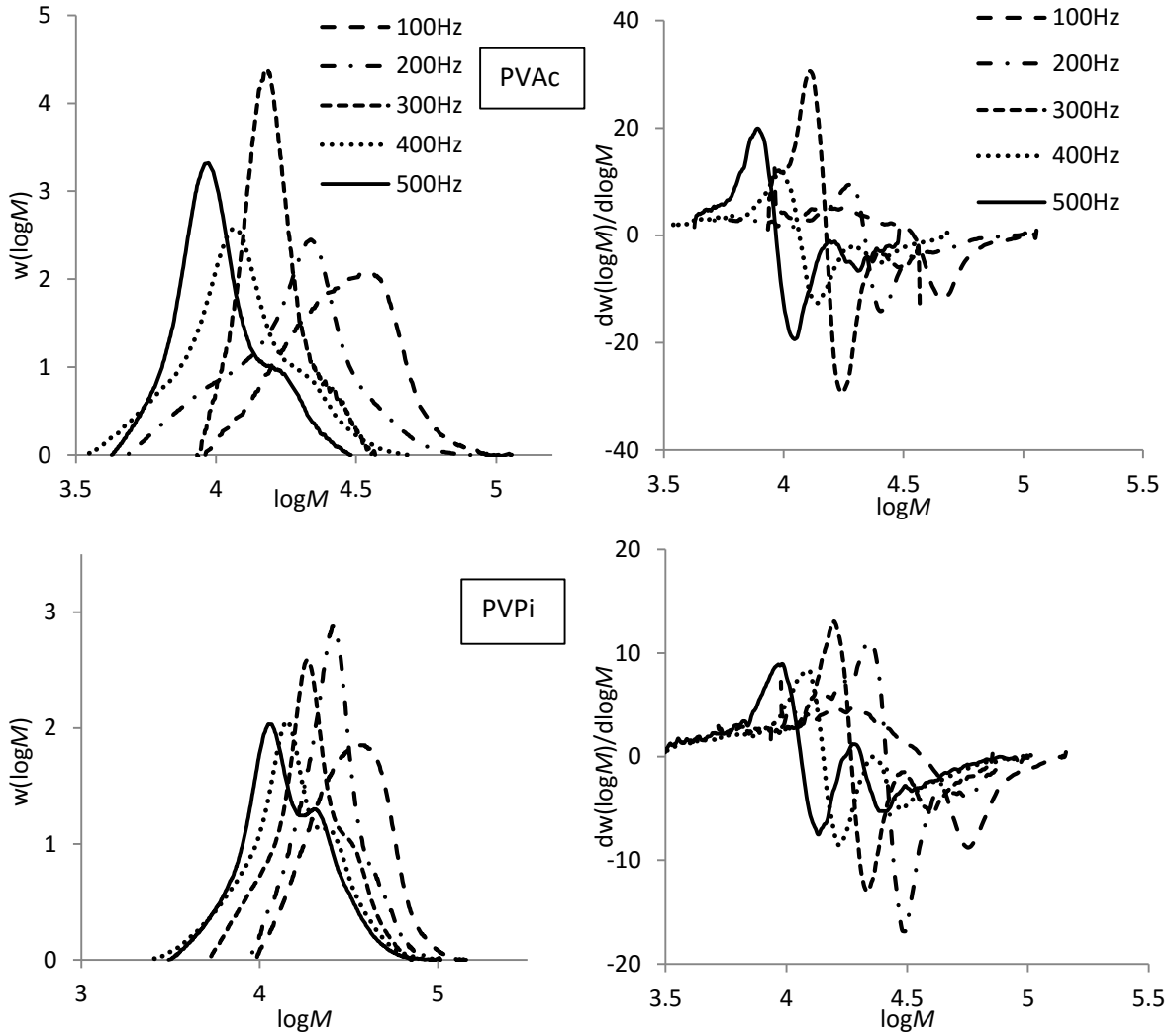

Figure A6.12. MMDs and corresponding first derivative plots for PVAc (top) and PVPi (bottom) prepared by PLP at 50°C and 100-500Hz pulse repetition rates, in heptane with benzoin photoinitiator.

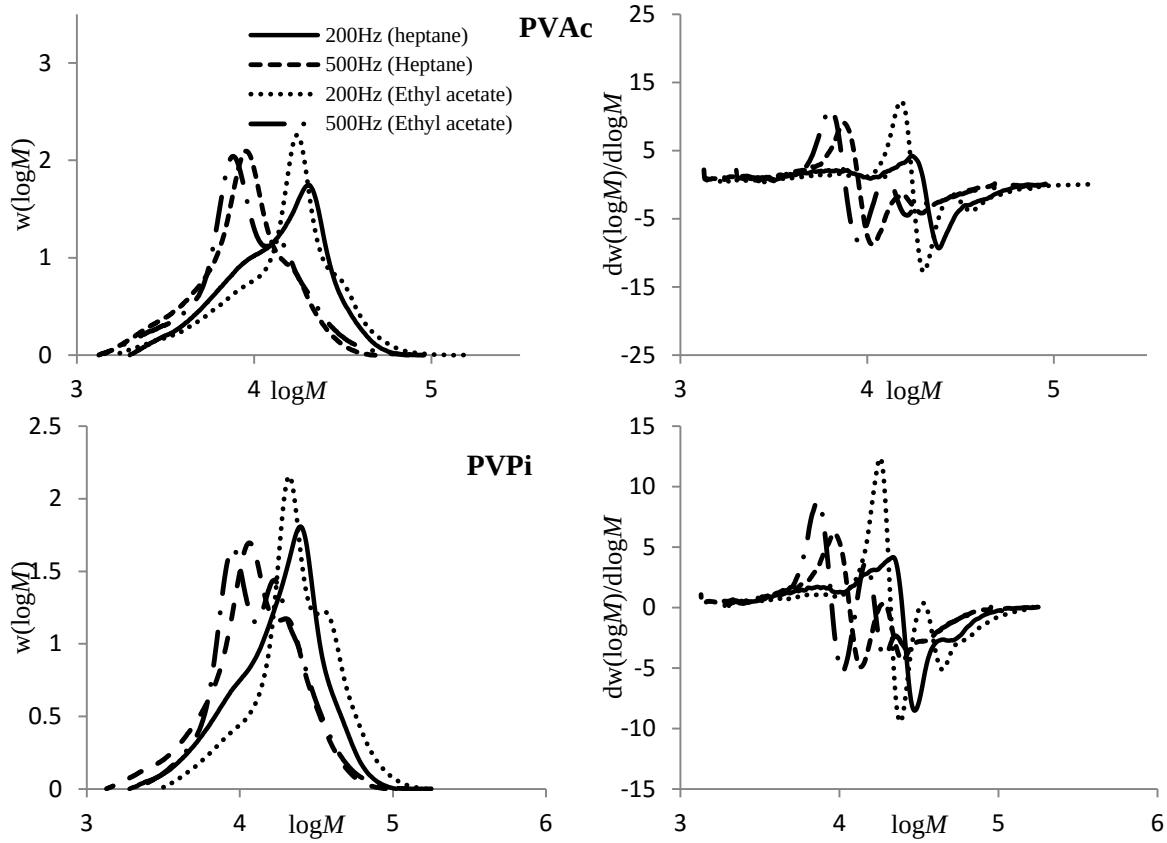

Figure A6.13. MMDs and corresponding first derivative plots for PVAc (top) and PVPi (bottom) prepared by PLP at 50°C, and 200 and 500Hz pulse repetition rates (prr), in heptane (2nd trial) and ethyl acetate (EAc) with benzoin photoinitiator.

Appendix 7: Small-scale batch polymerization Results for Vinyl esters (VPi and VBz)

A7.1: VPi Experiments

Table A7.1: Operating conditions and SEC results for polyvinyl pivalate prepared using small-scale batch polymerization method using 1.0 wt%V67 initiator in 50 vol% ethyl acetate (EAc) solvent.

Sample #	Reaction time (minutes)	Monomer Conversion, %	Mw	PDI
PVPi_9	15	17	277000	1.643
PVPi_10	25	47	276000	1.664
PVPi_11	35.5	74	230500	1.568
PVPi_12	40	93	265700	1.591

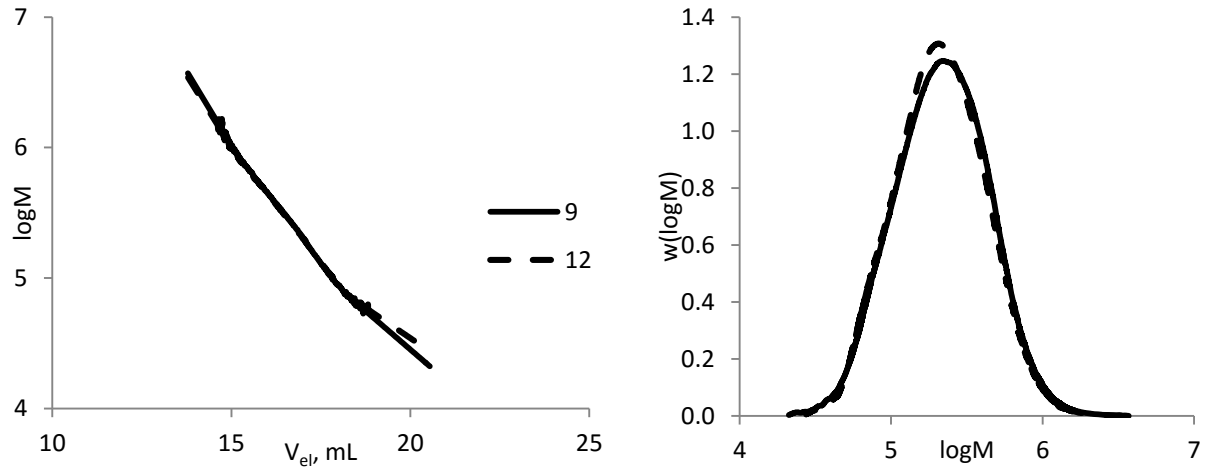

Figure A7.1: SEC results for polyvinyl pivalate prepared at 60°C prepared via small-scale polymerization (solution) technique: log*M*-elution volume (left) and MMDs (right) plots.

Table A7.2: Operating conditions and SEC results for polyvinyl pivalate prepared using small-scale batch polymerization and in-situ NMR methods using V67 initiator.

Sample #	Initiator wt. %	Solvent used	Solvent wt. %	Reaction time (minutes)	Monomer Conversion, %	Mw	PDI
PVPi_NMR	0.3	$CDCl_3$	70	120	85	19600	1.932
PVPi_bulk	1.0	N/A	0	8	42	328600	6.658
PVPi_06	2.0	EAc	50	40	65	149900	1.828
PVPi_12	1.0	EAc	50	40	93	265700	1.591

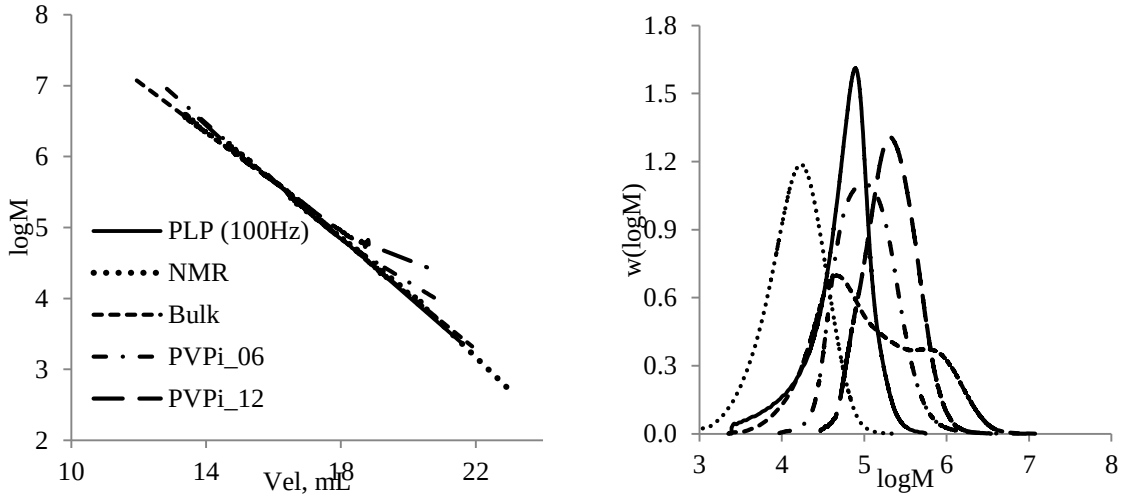

Figure A7.2: SEC results for polyvinyl pivalate prepared at 60°C prepared via small-scale polymerization (both bulk and solution) and In-Situ NMR technique: log*M*-elution volume (left) and MMDs (right) plots.

A7.2: VBz Experiments

Table A7.3: Operating conditions and SEC results for polyvinyl benzoate prepared using small-scale batch polymerization method using 1.0 wt% V67 initiator and 50 vol% ethyl acetate (EAc) solvent.

Sample #	Reaction time (minutes)	Monomer Conversion, %	Mw	PDI
PVBz_1	15	1.34	73000	1.664
PVBz_2	30	2.96	62800	1.952
PVBz_3	40	3.43	78400	1.701
PVBz_4	60	4.30	78200	1.733

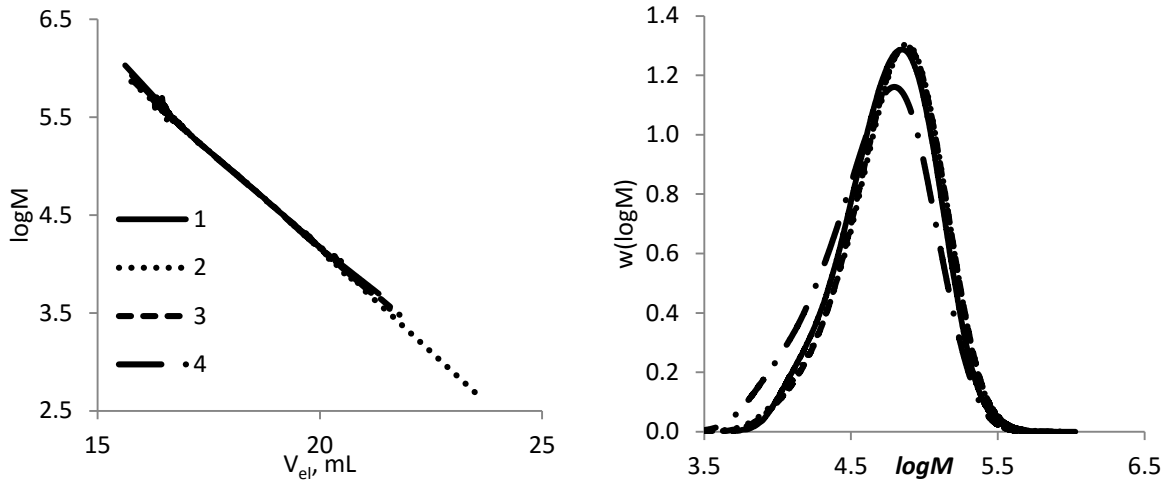

Figure A7.3: SEC results for polyvinyl benzoate prepared at 60°C prepared via small-scale polymerization (solution) technique: logM-elution volume (left) and MMDs (right) plots

Table 7.5: Operating conditions and SEC results for polyvinyl benzoate prepared using small-scale batch polymerization method using V67 initiator.

Sample #	Initiator wt. %	Solvent used	Solvent wt. %	Reaction time (minutes)	Monomer Conversion, %	Mw	PDI
PLP(10 Hz)		N/A	0	0.4			
PVBz_3	1.0	EAc	0	40	3.43	78400	1.701
PVBz_8	1.0	N/A	50	15		97700	1.591
PVBz_9	2.0	EAc	50	40	11.00	59700	1.754

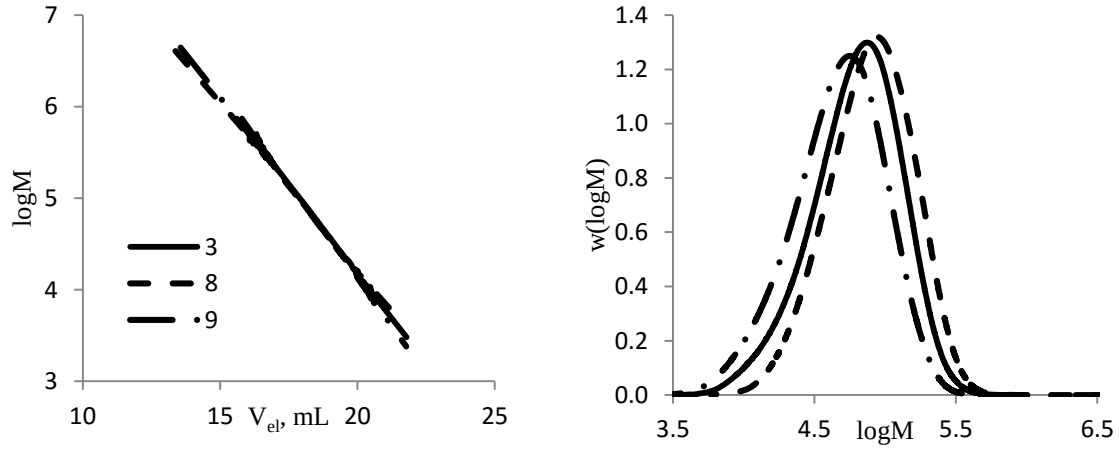

Figure A7.4: SEC results for polyvinyl benzaote prepared at 60°C prepared via small-scale polymerization (both bulk and solution) technique: log*M*-elution volume (left) and MMDs (right) plots.

NMR Experiments: VAc vs. VPi

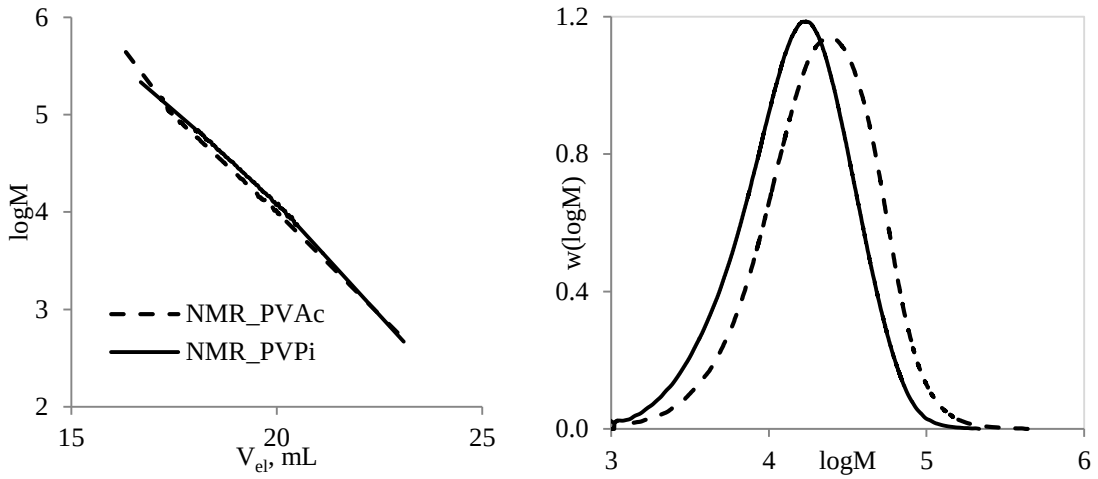

Figure A7.5: SEC results for polyvinyl acetate and polyvinyl pivalate prepared at 60°C via In-Situ NMR technique: log*M*-elution volume (left) and MMDs (right) plots.